The Emergence of Trait Anxiety during the First Year of Life in Rhesus Monkeys, and Its

Associations with Developing Anxiety-Related Neural Circuitry

By

Rachel Puralewski

A dissertation submitted in partial fulfillment of

The requirements for the degree of

Doctor of Philosophy

(Neuroscience)

At the

UNIVERSITY OF WISCONSIN-MADISON

2023

Abstract

When extreme, trait anxiety responses are indicative of later psychopathology

development. Trait anxiety emerges in early childhood, likely dependent on postnatal

maturation of neural systems that facilitate adaptive threat responses. In this

Dissertation, we examine how dynamic functional organization of prefrontal-amygdala

circuits during early-life contributes to development of threat-related anxiety responses.

Using a nonhuman primate model, we longitudinally characterized 35 rhesus monkeys

(24F/11M) from birth through the 1st-year of life, testing each subject at 5 ages (~1.5, 6,

12, 24 & 52 weeks) with the No-Eye-Contact condition (NEC) of the Human-Intruder-

Paradigm accompanied by ^{18}flurodeoxyglucose-Positron Emission Tomography (^{18}FDG-

PET). In parallel, one week following each NEC with ^{18}FDG-PET scan, monkeys also

underwent resting-state fMRI for seed-based connectivity analyses. With focus on the

development of extended amygdala-prefrontal circuitry in relation to preadolescent

monkey Anxious Temperament (AT), we characterized the developmental trajectories of

threat-related metabolism and resting-state fMRI connectivity in four regions of interest:

dorsal amygdala(dA), bed nucleus of the stria terminalis(BST), posterior orbital frontal

cortex(pOFC), and dorsal lateral prefrontal cortex(dlPFC). LME analyses demonstrate a

general increase in trait-like adaptive threat-related responses as infant monkeys

develop, manifesting as within-subject increases in AT from birth to one year. NEC-

related metabolism of dA, BST, pOFC, and dlPFC show distinct developmental

trajectories, suggesting a shift from relatively equivalent limbic-prefrontal engagement to

greater prefrontal engagement during NEC by 1 year. Across this period of significant

development, we find associations between BST NEC-related brain metabolism with AT, and age-interactions for pOFC and dlPFC metabolism when predicting AT. Parallel studies demonstrated increased fMRI functional connectivity across development between the dA and regions of the anxiety-related circuit (BST, pOFC, dlPFC). dA-BST and dA-pOFC functional connectivity both demonstrated age-related interactions in relation to AT. Together these data implicate a role of the extended amygdala in the expression of AT across the first year of life, while prefrontal regions show associations with AT later, at 1 year of age. These data provide a developmental framework for understanding risk to develop stress-related psychopathology at behavioral and neural levels in earliest stages of life, and for conceptualizing early-life, neuroscientifically informed, interventions aimed at decreasing risk for stress-related psychopathology.

Table of Contents

Chapter 1

Introduction and Overall Aims

<u>Introduction</u>

Significance & Impact

      Anxiety Disorders (ADs) are the most prevalent mental illnesses worldwide, estimated to affect 301 million individuals globally, of which 58 million are children or adolescents (Global Burden of Disease Collaborative Network, 2019). These rates are rising, exacerbated in part by the COVID-19 pandemic, with ADs increasing 26% just in the year 2020 alone (Mental Health and Substance Use,WHO Headquarters, 2022). In addition to the suffering of individual patients, these disorders carry a large burden on society. When extreme, these disorders become debilitating and interfere with an individual's capability to achieve goals, care for themselves and others, and live their life to its fullest potential. The current first-line treatments for ADs include Cognitive Behavioral Therapy (CBT) and psycho-pharmaceutical medications, including selective serotonin reuptake inhibitors (SSRIs) and benzodiazepines. While helpful for many individuals suffering from ADs, these medications are found to be effective in only ~50% of patients (Kodal et al., 2018). CBT appears to be slightly more effective as a treatment for ADs (~60% effective in long-term outcomes of youth patients with AD (Kodal et al., 2018), especially when used in combination with medication (Wehry et al., 2015). Thus, for many patients, current treatments are either ineffective or their effectiveness wanes with time. This highlights the need for continued research focused on an understanding of the neural circuit alterations underlying ADs, especially in youth during which anxiety disorders tend to emerge. Such a mechanistic understanding has the potential to lead to

the development of novel therapeutic strategies for the treatment of these debilitating

disorders.

Characteristics of Anxiety Disorders

It is important to note that ADs typically emerge early in life and are the most

common psychiatric disorder affecting youth and adults (Fox & Kalin, 2014; Kessler et

al., 2005). It is estimated that approximately 20% of adolescents suffer from ADs

(Kagan & Snidman, 1999; Rapee et al., 2023). In general, AD symptoms include chronic

states of worry and fearfulness, physiological symptoms associated with increased

arousal, and avoidance behaviors (Walter et al., 2020). Typically, in individuals with

ADs, anxiety related symptoms follow a chronic and recurrent course across the

lifespan (Fox & Kalin, 2014). Additionally, it is important to note that ADs are highly

comorbid with depression and substance abuse (Walter et al., 2020). In children, ADs

frequently go unnoticed and/or untreated, which can result in significant impairments in

social and emotional development and further facilitate the emergence of depression

and substance use.

Prior to the onset and diagnosis of an AD many children exhibit extreme

behavioral inhibition, which is a temperamental trait characterized by marked shyness

and avoidance behaviors when confronted with potentially threatening situations, such

as exposure to strangers or novelty (Kagan et al., 1987, 1989). It is estimated that

approximately 40-50% of children with extreme behavioral inhibition will later develop a

clinically significant anxiety disorder (Chavira et al., 2002; Jacqueline A Clauss &

Blackford, 2012). To better understand the trajectories of at-risk anxiety phenotypes and the underlying development of neural circuit alterations that confer risk of developing ADs, we are particularly focused on the earliest antecedents of anxiety. This work has the potential to identify early-life brain alterations that could be targeted during early development to increase resilience in at-risk individuals. Early-life interventions provide the opportunity not only to treat current anxiety symptoms and reduce suffering, but to potentially alter the long-term debilitating course of these disorders.

Brief Overview of Literature Supporting Experimental Rationale

Use of Nonhuman Primates to Model Adaptive and Pathological Childhood Anxiety

The use of nonhuman primates (NHPs, specifically the rhesus macaque, *macaca mulatta*) to study human psychopathology is crucial for translational models of psychiatric illnesses such as ADs. The recent evolutionary divergence of NHPs and humans begets a number of similarities that make monkeys an especially useful model for studying neural circuits as they relate to psycho-social behavioral phenotypes. NHPs and humans share similar emotional and behavioral expressions, especially in the context of social interactions and early rearing patterns (HARLOW & ZIMMERMANN, 1959; van der Horst et al., 2008). Furthermore, they also share many similarities in brain structure and function, and in brain development (Kim et al., 2020; Scott et al., 2016). One important similarity with respect to the translational utility of the NHP model is the significant complexity of the prefrontal cortex (PFC, in rhesus monkeys, along with its protracted development (Donahue et al., 2018; Petrides et al., 2012). The PFC is
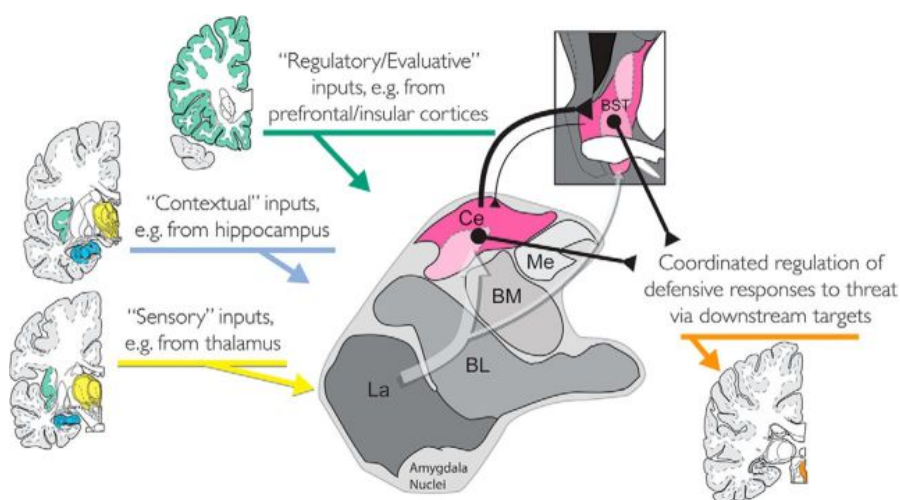
particularly relevant in the study of psychopathology, as it 1) plays a key role in executive function, motivational states, regulation of emotion and reward responses, as well as in planning and choice-making (Kenwood et al., 2022; Teffer & Semendeferi, 2012), and 2) is densely interconnected with limbic structures (i.e. the amygdala and anterior hippocampus) that are highly relevant to emotional expression and survival. The additional complexity of brain structure, its function, and its maturation make NHPs a highly translatable animal model for the study of the neural underpinnings of ADs, and other multifaceted emotional and behavioral disorders.

To model ADs in both children and young NHPs, researchers have focused on using paradigms that elicit behavioral inhibition (BI). BI is a trait-like feature that characterizes young children's responses to potentially threatening stimuli, such as exposure to unfamiliar adults and novel objects or scenarios. When stable and extreme, BI is a risk for the later development of psychopathology such as ADs (especially Social AD), depression, and comorbid substance abuse (Biederman et al., 1993; Henderson et al., 2015; Kagan & Snidman, 1999). In children, BI is characterized by observing how the subject responds to the intrusion of a stranger. BI can be modelled in NHPs using the Human Intruder Paradigm (HIP), a behavioral test designed to elicit species-typical responses across several threat-related contexts: separation from their conspecifics and brief isolation (*the Alone condition*), a potential indirect threat (*the No-Eye-Contact condition*), or a direct threat (*the Stare condition*) (N H Kalin & Shelton, 1989; Ned H Kalin et al., 1991). In particular, the No Eye Contact (NEC) condition entails a novel intruder presenting their profile as an indirect threat, which elicits anxiety-related

behaviors analogous to those observed in young children with extreme BI. During NEC, monkeys respond by reducing their vocalizations and inhibiting their locomotor activity, frequently resulting in freezing behavior. While this response is adaptive, functioning to protect from potential predation, it can also be maladaptive when extreme or expressed in inappropriate contexts. In addition to the behavioral responses that are similar in young monkeys and children, both species activate the pituitary-adrenal system in response to threat, resulting in the release of the stress-related hormone cortisol. Our work has built on the concept of BI by adding a physiological measure of stress reactivity, plasma cortisol concentration, to the traditional behavior measures (Fox et al., 2008). Termed anxious temperament (AT), this phenotype is comprised of three measures: 1) duration of threat-induced freezing, 2) threat-related reductions of vocalization, and 3) threat-related increases in cortisol. Studies from our laboratory demonstrate that this composite AT measure is a better predictor of anxiety-related alterations in brain function (Shackman et al., 2013) and in regional differences of anxiety-related transcript expression (Kovner et al., 2019) than its independent components. Given its relevance as a trait-like measure of anxiety and its predictive power for exploring individual differences in underlying neural circuitry in NHPs, we are especially interested in how the expression of AT emerges during the infant period and its temporal dynamics during early-life development.

Associations of Limbic and Prefrontal Regions with Expression of Anxiety Responses

Individual differences in the expression of anxiety are partially explained by functional and structural differences in limbic and prefrontal regions (Kenwood et al., 2022; Roozendaal et al., 2009). There is a substantial body of work implicating the importance of the amygdala in the processing of anxiety and fear (J A Clauss et al., 2015). The amygdala can be subdivided into many nuclei that may play distinct or coordinated roles in the expression of anxiety; of particular interest in anxiety processing are the central amygdala (Ce) and the basolateral complex, which in primates comprises the basal, accessory basal, and lateral nuclei (BLA) (Janak & Tye, 2015). The BLA receives and processes sensory input from thalamic, cortical and prefrontal regions. The posterior orbital frontal cortex (pOFC/OPro) is one of the most densely interconnected (*see figure 1.2)* with the BLA (Kenwood et al., 2022), and is hypothesized to play a regulatory role in the expression of trait-like anxiety characteristics (Kenwood et al., 2023). The Ce is thought to carry out additional processing of the BLA's output and regulate other downstream anxiety-related regions such as the bed nucleus of the stria terminalis (BST), hypothalamus, or periaqueductal gray (SAH et al., 2003; Tovote et al., 2015). Due to its structural and functional associations with the Ce, and

Figure 1.1 – Visual of extended amygdala anatomy, cortical input and outputs, image recreated from (Shackman & Fox, 2019)

due to it sharing many of the Ce's downstream targets, the BST (*see figure 1.1)* is

considered to be a part of the "extended amygdala" (Alheid & Heimer, 1988; Cassell et

al., 1999; Fox, Oler, Tromp, et al., 2015). In recent years, numerous studies have been

published indicating that neural function in many of these regions is highly associated

with levels of AT. In a sample of 592 rhesus macaques that underwent 30-minutes of N

EC in conjunction with μPET imaging of regional brain metabolism, it was demonstrated

that increased metabolism in the Ce, BST, and pOFC was associated with higher levels

of AT across individuals (Fox, Oler, Shackman, et al., 2015). This implicates a

hyperreactive response of the extended amygdala, and some of its prefrontal inputs,

during exposure to the threatening stimuli. These data suggest potential alterations

throughout anxiety-related neural circuitry during stress exposure, highlighting the

importance of a circuit-wide approach for the identification of perturbations that result in

expression of extreme AT.

   To understand the role of prefrontal regions in the regulation of amygdala function

and expression of anxiety, studies use Magnetic Resonance Imaging (MRI) to explore

individual differences in prefrontal-amygdala structural and functional connectivity.

Studies using Diffusion Tensor Imaging (DTI) to assess white matter integrity of

structural connections throughout the brain have implicated the Uncinate Fasciculus

(UF), a white matter bundle with dense connections between the pOFC and the BLA, as

having reduced white matter integrity in monkeys with extreme AT and in young children

with ADs (Tromp, Fox, et al., 2019; Tromp, Williams, et al., 2019). Functional MRI

(fMRI) studies have implicated the dorsal lateral prefrontal cortex (dlPFC) as having
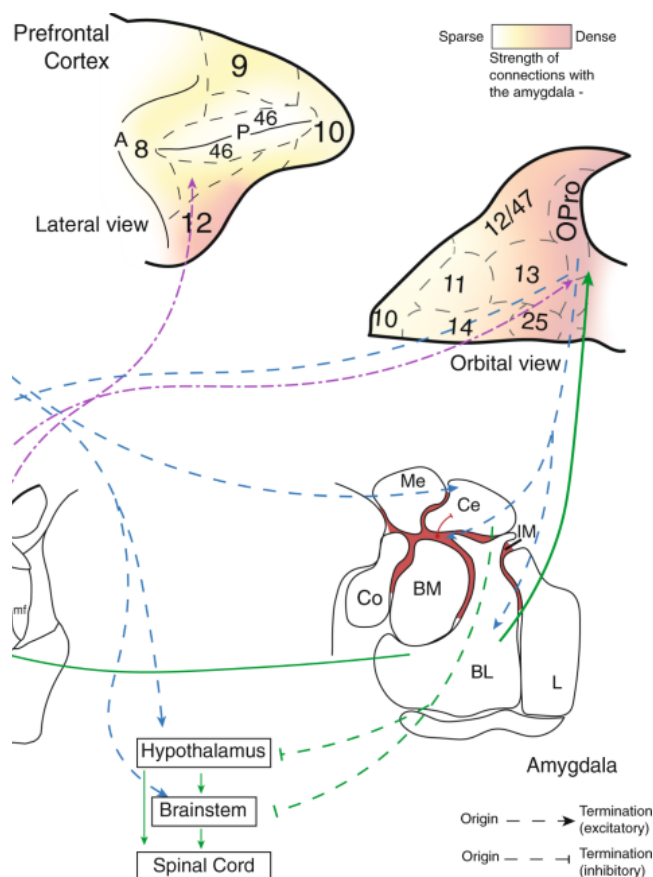
Figure 1.2 – visualization of connections between prefrontal cortex (PFC) and amygdala, modified from (Kenwood et. al, 2022)

reduced functional connectivity with the Ce in both human and NHP individuals with high levels of anxiety (Birn et al., 2014a). Both of these imaging approaches indicate a potential disruption to effective prefrontal regulation of the amygdala in the pathological expression of anxiety.

In addition to these imaging studies that highlight associations between brain function/structure and threat-related responses, we have also used mechanistic approaches to demonstrate the causal links between cortical and subcortical regions and the expression of AT. Studies in our laboratory using chemogenetic approaches, such as DREADDs, to modulate amygdala function have demonstrated a mechanistic role of amygdala activity in mediating adaptive and maladaptive anxiety (Mueller et al., 2023; Roseboom et al., 2021). Additionally, selective excitotoxic lesions of the Ce as well as large cautery/aspiration lesions of the OFC both resulted in decreased freezing behavior during NEC (Fox et al., 2010; Ned H Kalin et al., 2004, 2007). Strip lesions of the pOFC, intended to specifically disrupt the UF, also results in decreased freezing behaviors (Kenwood et al., 2023) along with decreased metabolism in the BST and

cortisol levels in response to NEC. These chemogenetic and lesion studies emphasize the significant roles of both amygdala and prefrontal regions in the expression of threat-related anxiety. Taken together with the neuroimaging data reviewed above, this suggest significant roles of both subcortical and cortical components of the anxiety-network, each of which seem to contribute towards expression of anxiety-related responses.

Postnatal Development and its Implications in Anxiety

While AT and its brain signatures appear to be trait-like and heritable (Fox et al., 2008; Fox, Oler, Shackman, et al., 2015), mature responses to threat are not immediately present at birth. Previous work has demonstrated that NHPs begin to exhibit mature anxiety regulation strategies at around 2-4 months of age (N H Kalin & Shelton, 1989). This time period roughly translates to ages 9-12 months in children, which generally corresponds to when they begin showing signatures of stranger anxiety (Brooker et al., 2013; Jacqueline A Clauss & Blackford, 2012; Rheingold & Eckerman, 1973). Other distress-related responses, such as the separation response that occurs due to disruption of attachment bonds between infant and caregiver, are evident almost immediately after birth. This delay in mature anxiety regulation strategies occurs, in part, due to the postnatal structural and functional development of the circuitry mediating anxiety.

Generally, the brain undergoes a hierarchical development, with the brain regions contributing towards the most basic functions developing first, followed by regions involved in more regulatory or executive function (Barrett, 2012; Keller et al.,

2023). On a molecular level, this is described by the developmental phases of neuronal migration, proliferation, and differentiation which contribute towards gyrification of the cortex and lamination (Jiang & Nardelli, 2016). The organizational development of discrete regions is followed by a protracted development of brain-wide circuitry that integrates function of distinct regions and facilitates more complex brain processes that require coordination of various neural systems. This corresponds with the developmental phases of synaptic overproduction and pruning, and of myelination in major projections connecting distal brain areas, which continues into adolescence (Teffer & Semendeferi, 2012). Importantly, the ongoing processes of synaptic pruning are especially influenced by external factors, allowing for adaptive development of neural processes most valuable to each individual. Much of subcortical brain structure and function is already organized at birth (Makropoulos et al., 2016), with newborns being able to express basic responses to their environment and novelty. Meanwhile, the PFC, which is the major center of higher order executive function and decision making, takes the longest to develop, continuing well into adolescence and adulthood (Kolk & Rakic, 2022; Petrides et al., 2012; Teffer & Semendeferi, 2012). This delayed development of regulatory systems may be influenced by environmental factors, which have the potential to alter maturation of adaptive neural circuitry (Tsujimoto, 2008). Given the importance of prefrontal regions in the expression of anxiety, how these regions associate with AT across development is of particular interest when it comes to enhancing our understanding of how these anxiety-related systems mature.

In the early life postnatal period, while these multitude of neural systems are experiencing their ongoing development, an infant relies on its caregiver to protect it from potential threats and provide the nurturing required for appropriate maturation of circuits with more protracted development. This close mother-infant bond means that during early life and development, an infant's experiences and learning are heavily facilitated by their caregiver (Hansen, 1966; Hinde & Spencer-Booth, 1967). Once the neural circuits that facilitate an infant's independence have matured, they can better protect themselves and independently regulate their own behavior and emotions. This crucial period of development from birth to 1-1.5 year in NHPs (~4-5 years in children) is of particular interest when considering ADs. It is around this time, in children, when trait-like BI can be identified. By examining the period of immediate postnatal development, we can explore the earliest antecedents of pathological anxiety and expand our understandings of the earliest anxiety phenotypes. The following Chapters aim to describe the developmental trajectories of the Anxious Temperament phenotype, resting-state amygdala connectivity, and threat-related brain metabolism, finishing with an exploration of relations between AT and brain function during this important developmental period. More specifically, we explore how amygdala and prefrontal components of anxiety-related neural circuitry play a role in the expression of anxiety during the earliest or later phases of postnatal development.

Specific Aims

Aim 1: *Over the course of the first year of NHP life, investigate the trajectories of threat-related responses as they relate to the development of anxious temperament.* Threat-related responses in early life represent the earliest expressions of anxiety. Adaptive threat responses, while inherent to all species, are not immediately present after birth. Infant primates are immature in their perception of the world around them and their ability to respond behaviorally is limited. In contrast, attachment responses emerge early and during the first few months are predominant. Attachment related responses function to ensure close proximity to a caregiver for nurturance and protection. Using the No Eye Contact paradigm, which consists of separation from mother (or cage mate) and exposure to a potential threat, at 5 timepoints across the first year of life, we will characterize the trajectories of threat-related responses during early-life development. These data will be essential to our understanding of how the individual differences in the development of anxiety-related circuits is associated with later manifestation of psychopathology. Based on early-life development literature, and prior work examining behavior early in primate life, *we predict that adaptive threat-related responses will emerge by 3 months of age, reaching a mature-like and stable response by 1 year of age.*

Aim 2: *Characterize the developmental patterns of regional brain metabolism in response to threat exposure across the first year of life.* We seek an understanding of how threat-provoked brain responses develop during this period. During threat

processing and stress responses, brain regions that are more active and contribute to behavioral and physiological anxiety responses take up additional glucose to fuel necessary neural processes. [18]Fluorodeoxyglucose-Positron Emission Tomography uses a radioactively labelled glucose analog, taken up during each 30 minutes of NEC to image relative activation levels in the brain. Given the immaturity of important anxiety-related circuits at birth (especially those involving the PFC), stress responses may be partially influenced by ongoing postnatal developmental processes. How brain metabolism during experience of threat changes during this period has not been clearly defined. We aim to explore the development of metabolic changes in anxiety-related regions during exposure to NEC across 5 timepoints during the first year of NHP life. We hypothesize that *metabolism in prefrontal brain regions (dlPFC, pOFC) during NEC will increase across the first year of life, as these regulatory regions mature and infants develop the capacity to more adaptively regulate their emotional responses.* In contrast, we hypothesize that *metabolism in the extended amygdala (dorsal Amygdala, BST) will not increase across development, as these regions may be more mature at birth and the influences of developing prefrontal cortical regions may provide a buffer on the threat-related activation of these regions.*

Aim 3: *Describe the developmental trajectories of anxiety-related regions with fMRI-based connectivity measures at rest.* To support our investigation into the early-life risk for anxiety-related disorders, this aim focuses on the developmental trajectories of the neural circuitry underlying adaptive and maladaptive responses to threat. Resting-state

brain activation patterns may reflect stable set points of baseline connectivity between nodes/regions of important anxiety regulating networks. The integration of complex networks throughout the brain is an important process during development. In adults, the prefrontal-amygdala circuitry has been identified to be involved in adaptive and maladaptive anxiety responses. The dorsal amygdala is of particular interest because the central nucleus within this region is a component of the extended amygdala along with the BST. Based on our work in more mature animals, we conceptualize the extended amygdala to be a core component of the neural circuitry underlying anxiety. The early life developmental characteristics of the primate anxiety circuit remain relatively unexplored; and because of the known role of the central nucleus of the amygdala, the purpose of this aim is to characterize the development of dorsal amygdala functional connectivity with other components of the anxiety-related network over the first year of life. Resting-state functional MRI allows for an understanding of the correlated fluctuations between brain regions and will be used in this study to characterize developmental changes of anxiety-related neural circuitry within subjects. We examine the development of this circuit across 5 timepoints during the first year of primate life, and hypothesize that *the connectivity between the dorsal amygdala and prefrontal regions, such as the dlPFC and pOFC, will strengthen across the first 3 months of life, a time at which young monkeys have the capacity to adaptively regulate their threat related responses.* Meanwhile, we predict that *the connectivity within the extended amygdala (i.e. between dorsal Amygdala and BST), will be present throughout early life and will not demonstrate age-related changes across development.*

Aim 4: *Characterize how individual differences in extended amygdala and prefrontal brain function relate to individual differences in trait anxiety across the early life developmental period.* **<u>Aim4a</u>**: Our laboratory has demonstrated in preadolescent monkeys that threat-induced metabolism in the extended amygdala (Ce, BST) and prefrontal cortical (pOFC) components of anxiety-related neural circuitry predict individual differences in AT. Given this, along with data supporting the delayed maturation of the prefrontal regions, we hypothesize that *threat-related metabolism in the extended amygdala (BST, Ce) across the first year of life will be associated with AT, while metabolism in prefrontal cortical regulatory regions (i.e., dlPFC, pOFC) will not predict individual differences in AT until the end of the first year of life.*

  <u>Aim4b</u>: Resting-state functional connectivity provides a measure of unperturbed brain network dynamics which allows for the opportunity to examine relations with individual differences in trait-like anxiety. Prior work from our laboratory has shown that in young children with ADs, as well as in preadolescent primates with high levels of AT, there is reduced functional connectivity between the dlPFC and the Ce of the amygdala. Additionally, we have found that individual differences in Ce-BST connectivity are also associated with AT. Based on this, and the different developmental trajectories of extended amygdala and prefrontal cortex development, we predict that *at younger ages the connectivity between Ce-BST and its associations with AT will be apparent, whereas it won't be until near the end of the first year of development when significant relations between Ce-dlPFC and Ce-pOFC connectivity and AT emerge.*

Chapter 2

The Development of Trait Anxiety During the First Year of Nonhuman Primate Life

Introduction:

An Illustrative Scenario:

Imagine a young child, with typical health and development for their age, whose parents leave them for some time in a form of child care. When a young child is put into this particular situation it presents multiple stimuli that can trigger anxiety responses. One source of stress for the child is the separation from their parents, whom they know to care for them and protect them from harm. Another source of stress in this situation is the presence of strangers who are unfamiliar to the child, and therefore have the potential to present a threat. At five years old, a child may be distressed by their caregiver's absence, but is also vigilant to strangers in their environment. During initial interactions, before gaining sufficient information to determine if any strangers pose potential threats, a five-year-old likely experiences anxiety due to the uncertainty of this situation. A strategy used by children to avoid being noticed by strangers is to become quiet and still. After some time, and perhaps some friendly interactions with any alternative caregivers present, the child may relax and return to usual activities.

In contrast, if the child were much younger, such as a three-month-old infant, their responses to this same situation would be quite different. A baby has a more basic awareness of their surroundings and situation, and may not recognize the presence of strangers in their environment or fully conceptualize their potential to be threatened by them. However, a baby is still intensely distressed by the separation from their parents, which presents as increased agitation and typically loud crying. Attenuation of this distress requires the alternative caregiver present in this situation to soothe the infant,

reassure them of their safety, and provide for their needs during the absence of their parent. If the baby continues to feel insecure, unsafe, or that their needs aren't met, they will continue to signal distress by crying. In this situation, the presence of strangers does not stimulate similar responses to what's observed in older children. Instead of inhibited movements and noises, babies seem to respond with the opposite approach, increasing their movements and making more and louder noises.

The above scenarios illustrate the typical innate responses observed in young humans experiencing common, mild childhood stressors. Threat-responses are essential for survival across the lifespan, and must develop early in life to ensure safety during the especially vulnerable periods of postnatal development. When presented with uncertainty and potential danger, a 5-year-old can respond adaptively with appropriate behaviors. Their responses are basic, but require both: recognition of environmental threat and sufficient motor control to facilitate inhibition (Fox & Kalin, 2014). As children develop through preadolescence, their responses to potential threats become more heterogeneous and sophisticated as their nervous systems become more interconnected. While additional experiences facilitate improvement of threat recognition and efficiency of stress regulation strategies (Britton et al., 2011; Herzberg & Gunnar, 2020), the initial adaptive responses themselves appear innate and trait-like (N H Kalin, 1993; Malik & Marwaha, 2023).

This childhood emergence of threat responding ensures that juveniles have innate and reflexive protective responses as they gain independence. However, in earliest infancy these adaptive threat responses are not as clearly present. This is likely

due to a newborn baby's nervous system being too underdeveloped to support recognition of threats in their proximity and/or mobilize effective behavioral responses. Given its physical vulnerability, a baby's best source of protection is its caregiver. This is consistent with crying as a predominant distress-related response, as it serves to facilitate retrieval by a caregiver who can provide protection and safety. The aim of the work presented in this chapter is to use our NHP developmental model to longitudinally characterize the development of adaptive anxiety-related threat responses during the earliest postnatal period, from birth to 1 year of life.

Characterizing Adaptive Threat Responses in Nonhuman Primates using the Human Intruder Paradigm

The Human Intruder Paradigm (HIP) was developed by Dr. Ned Kalin in 1989 to elicit and characterize context-specific behavioral responses in an NHP model (rhesus macaques) that are analogous to the typical threat-related responses present in children(N H Kalin & Shelton, 1989). The HIP (briefly introduced in Chapter 1) has three distinct contexts, which are designed to trigger distinct, adaptive, behavioral responses in preadolescent and adult monkeys. The first context is an Alone (A) condition, where a monkey is isolated in a novel testing environment, typically eliciting a separation-related response. Young NHPs respond to separation by increasing their locomotor activity and coo vocalizations as a means to facilitate maternal retrieval and/or reunion with conspecifics (Seay et al., 1962; B. Zhang et al., 2012). A similar behavioral response is also observed in young children. During infancy and toddlerhood, crying and distress

are common and developmentally appropriate when separations from caregivers occur (Bowlby, 2008). The second context is the No Eye Contact (NEC) condition, where an indirect threat is presented in the form of an unfamiliar intruder entering the room and presenting their profile to the monkey. Young monkeys respond to this potential threat by inhibiting their movements and vocalizations while remaining vigilant and focused on the intruder, termed freezing(N H Kalin & Shelton, 1989). This response serves to avoid detection from a potential predator and is analogous to that observed in some human children, who, to varying degrees, also become quiet and less active when in the presence of strangers. The final context is the Stare condition (S), where the intruder returns to the testing room and faces the monkey, making direct eye contact. Monkeys respond to this direct threat with aggressive or submissive behaviors, as they actively cope with the direct threat of a potential predator.

The responses during the NEC condition have been of particular interest in the investigation of pathological anxiety, as extreme behavioral inhibition in children is somewhat predictive of later development of AD psychopathology (Biederman et al., 1993; Henderson et al., 2015; Luis-Joaquin et al., 2020). Additionally, there has also been evidence of differences in the reactivity of the HPA-axis between children with high BI compared to low BI, as demonstrated by higher levels of circulating cortisol in children with extreme BI (Kagan et al., 1987) both during and following responses to stressful situations. This evidence further supports the hypothesis that individual differences in the underlying physiological systems regulating stress responses are altered in those with pathological anxiety. Given its relevance to the stress response,

and potential for being a marker of pathological anxiety, our characterization of NEC-related responses in primates includes an examination of post-NEC levels of circulating cortisol.

While the HIP has been used extensively in investigations of preadolescent monkey expression of anxiety, it has been used less to probe infant expression of anxiety-related responses, where the development of relevant anxiety neural circuitry is still ongoing. The threat-related response of an infant monkey during NEC is complicated by their inherent vulnerability and elevated distress due to separation from their mother. Similar to human infants, monkey infants are reliant on their caregivers for protection, and in any stressful situation during infancy, separation-related behaviors are the predominant response. Generally, attachment distress decreases with maturation (B. Zhang et al., 2012). This is typically seen in children around 4-5 years of age, and around 6 months to 1 year of age in rhesus monkeys (Battaglia, 2015). An improved characterization of how NEC-related responses change during early development will inform our understanding of the early life transition from the predominant attachment distress to trait-like behavioral inhibition.

Evidence for Emergence of Adaptive Threat-Related Responses

Since the creation of the HIP, our laboratory has conducted only a couple investigations into infant NHP responses to potential threats. Distinct separation and threat-related responses have been characterized (N H Kalin & Shelton, 1989) using the HIP in monkeys as young as 6 months. When placed alone in a testing cage, monkeys

at this age show separation-related behaviors as displayed by increases in coo-calls. When subsequently presented with the profile of an intruder (NEC), or eye contact (Stare, ST), these monkeys displayed freezing and barking behaviors, respectively. These observations suggest that as early as 6 months old, NHPs are able to mount appropriate behavioral responses in the presence of different threats. When testing the behavioral responses to distinct threat conditions at even earlier timepoints (0-2, 2-4, 4-7 weeks), distinct conditional responses were not observed across conditions (Ned H Kalin et al., 1991). Instead, infant monkeys showed a variety of undifferentiated behavioral responses regardless of condition. Freezing and barking behaviors were not specific to threatening conditions, showing similar expression levels across all HIP conditions. Once monkeys reached 9-12 weeks of age, they had developed specific expression of freezing in the NEC, and barking in ST. This cross-sectional study highlights a delayed emergence of threat-related behaviors after birth in primates, with attachment distress potentially playing a more significant role in infant responses to the HIP. This crucial early postnatal period where a monkey expresses predominantly separation-related behaviors has not been as well characterized.

Early work in NHPs by Harry Harlow, and others, effectively demonstrated the significance of the infant development period in primates. The early life mother-infant relationship in primates and humans is critical not only for physical maturation and safety, but also for the development of healthy social behaviors, cognition, and emotion regulation (Harlow & Suomi, 1971; HARLOW & ZIMMERMANN, 1959; Seay et al., 1962). For NHPs in both naturalistic and laboratory environments, the relationship

during this period is dominated by close mother-to-infant contact (Hansen, 1966; Hinde & Spencer-Booth, 1967). In addition to this, it has been demonstrated that close contact and relationships between infants and their mothers also have profound effects beyond an infant's physical health and development (Seay et al., 1962). When disrupted, or when other early life experience is interfered with, primates can develop severe emotional and behavioral effects, especially in relation to attachment and separation (Harlow & Suomi, 1971). During this sensitive period, HPA-axis development is ongoing as well. There is evidence that HPA-axis reactivity to stress in infant primates (as measured through blood or salivary cortisol measures) is also limited (Jansen et al., 2010), and infants may be reliant on their caregivers' proximity for effective stress-hormone cortisol responses in the presence of potential threats (Gunnar et al., 2015; Santiago et al., 2017). This work provides context for how early-life mother-infant attachment may contribute to increased separation distress during experiences of various potential threats.

While the work reviewed above provides compelling evidence suggesting a delayed maturation of adaptive threat-related responses during primate infancy, there have been no studies characterizing these changes in a longitudinal manner, with repeated testing across the developmental period within subjects. This work aims to fill this knowledge gap by following a cohort of 35 monkeys that undergo repeated behavioral testing with NEC, alongside parallel testing of brain function with FDG-PET and fMRI. This experimental design allows for the examination, on a group level, of differences in the magnitude of behaviors with maturation, as well as assessment of the

stability within-individuals across developmental trajectories. The brain imaging performed in parallel adds further enhancement to our dataset, by allowing for investigation into how the within-subject differences in brain function during this period may be contributing to the emergence of mature adaptive anxiety-related responses. This work is important as a better characterization of these early life responses will provide insights into the earliest manifestations of trait-like behavioral features that are relevant to the later development of psychopathology. Here, we explore changes in stress-related responses over the first year of life using a longitudinal approach to assessing threat-related anxiety of NHPs during experience of NEC.

Aim of Chapter 2: *Over the course of the first year of NHP life, investigate the trajectories of threat-related responses as they relate to the development of anxious temperament.* Using the No Eye Contact paradigm, which consists of separation from the mother and exposure to a potential threat, at 5 timepoints across the first year of life, we will characterize the trajectories of threat-related responses during early life development. Based on early life development literature, and the prior work in the Kalin lab examining behavior early in primate life, *we predict that adaptive threat-related responses will emerge by 3 months of age, and that individual differences in Anxious Temperament will be relatively stable over the first year of life.*

Methods:

Study Design and Cohort Description

The study cohort consisted of 35 NHPs (*Macaca mulatta,* 24 female and 11 male, NHPs). These monkeys were followed longitudinally during their first year of life, each tested five times with anxiety behavioral assessment and functional brain imaging between the ages of 1 week and 1 year (*see figure 2.1*, timeline). Infant monkeys were housed with their birth mothers until 26 weeks, at which point they were weaned and pair-housed with a similarly aged peer from the same cohort. Monkeys were observed during their initial meeting and interaction at weaning, to ensure compatibility and safety for paired monkeys. All monkeys were cared for in standard housing facilities at the Wisconsin National Primate Research Center in accordance with Institutional Animal Care and Use Committee protocols, including maintenance of a 12-hour on/12-hour off light schedule, regular feeding, and age-appropriate enrichment. All behavioral and imaging data were collected during the 'lights-on' period. Monkeys in this cohort were followed until euthanasia at 1.5 years of age, when brains were harvested, and blood and cerebrospinal fluid (CSF) samples were collected.

Monkeys were each tested at five ages (~1.5, 6, 12, 24, and 52 weeks) with 30 minutes of the No-Eye-Contact (NEC) condition of the Human Intruder Paradigm (HIP) in conjunction with ^{18}Fluorodeoxyglucose-Positron Emission Tomography (^{18}FDG-PET, exact protocol to be detailed in Chapter 3). At each age, monkeys were first separated from their caregiver or cage-mate and injected with ^{18}FDG. At the early time points the young study subjects were housed with and still clinging to their mothers on the day of

testing, therefore the mothers were removed from their home cage and anesthetized with Ketamine (15 mg/kg, IM). The infants were then wrapped in a towel to keep warm and transported by hand to the procedure room. Using a tabletop restraint or manual restraint, a catheter was placed, with preference given to the saphenous vein, for intravenous [18]FDG delivery. Monkeys were then placed into a novel cage in an unfamiliar room. During the first 3 timepoints, a heating pad covered by a blanket was placed on the bottom of the cage to ensure maintenance of infants' body temperature during caregiver separation. A camera was positioned opposite the testing cage, to capture behavior and vocalization sounds during the behavioral paradigm.

Description of Human Intruder Paradigm (with focus on the No Eye Contact Portion)

Assessment of anxiety-related behavioral and neuroendocrine responses was performed through use of the NEC portion of the HIP. In this version of NEC, the monkey is placed into the novel testing environment (inner dimensions of cage: 71 cm x 76 cm x 78cm) and left alone for a few moments to acclimate. *This experience of isolation is a significant stressor to an infant monkey, and produces a separation response characterized by production of vocalizations and movements intended to reunite the infant with its caregiver.* An unfamiliar intruder (a human with whom the monkey has little or no other contact) enters the room. The same "strange" intruder was used for all 35 monkeys at all 5 ages. This intruder stood opposite the testing cage in view of the subject, approximately 2.5 meters from the front of the cage, with their profile facing the monkey for 30 minutes. *This presents a potential threat to the monkey,*

typically triggering behavioral inhibition in adolescent NHPs as observed through

suppression of vocalizations and movements, along with elevated levels of circulating

cortisol in the blood (N H Kalin & Shelton, 1989). Vocalizations and movement

behaviors during NEC were scored using The Observer XT from Noldus (Zimmerman et

al., 2009). Movements were scored as mutually exclusive duration behaviors that fell

into one of the following categories: Locomotion (LO), Stereotypical Locomotion

(LOST), Freezing (fully inhibited, FF), Hypervigilance (partially inhibited, HV), Immature

movements (OM), Falling Down (FA) or idle (IN). Other movement scores that had very

low (or no) levels of expression included Huddle (HU), Lying Down (LY), and Resting

(RE). Vocalizations were scored by vocalization type and frequency of occurrence.

Vocalization types of infants included: Cooing (VV), Shrieking (SH), Coo-Shrieking (CS),

Barking (BA), or undefined vocal (OV). See Appendix A.1 for detailed descriptions of

each behavior type.

After 30 minutes of NEC, the monkeys were removed from the testing cage,

weighed, and anesthetized with ketamine (15 mg/kg, IM) under supervision of veterinary

staff. During anesthesia, blood pressure, heart rate, and body temperature vitals were

constantly monitored to ensure subject safety (details of anesthesia and vital monitoring

can be found in Chapter 3 with detailed [18]FDG-PET scanning procedure). Once asleep,

blood was drawn and spun down to separate out plasma. Samples were frozen at -80

degrees Celsius until hormone assay was performed. Plasma was tested for the stress

hormone, cortisol, using an ELISA assay (Lewis & Elder, 1985), run in duplicate, and

averaged across replicates. After having their blood drawn, monkeys were placed in a

PET scanner for visualization of brain function during NEC (detailed methods in Chapter 3). Following the PET scan, monkeys were monitored while anesthesia effects wore off and then were reunited with their mother or their cage-mate (mother: T1-4; peer: T5).

Data Description and Statistical Analyses

Behavioral data was scored by four trained observers with high reliability between scorers (>90% agreement in each behavior category). Behavioral data was collected in six bins of five minutes each, and an average score of duration or frequency per 5-minute bin was computed. Vocalization frequency data was square-root transformed, and movement duration data was $\log_{10}$ transformed, as is typical in the literature for this type of behavioral data (Fox et al., 2008; N H Kalin et al., 2001; N H Kalin & Shelton, 1989) to ensure normal distribution of data. The transformed data was then used in following computational manipulations or statistical analyses.

To account for diurnal cortisol rhythm, we computed residuals from models associating cortisol blood levels and time of day (TOD) the samples were collected. At younger ages, some monkeys needed multiple draws to collect enough blood for hormone assays. In such cases, the last time of draw was used as collection TOD for computation of residuals. There was relatively little variability in TOD for blood collection; blood for all subjects at each age was collected between 8 AM-1 PM, with the average collection time being 10:05 AM +/- 52 min (SD)/8 min 47 sec (SEM). These residuals were used as the cortisol values for all subsequent manipulations or statistical analyses.

All statistical analyses were conducted in R. Associations between timepoints were examined using Pearson correlations, and p-values determined with individual pairwise t-tests. For Anxious Temperament (AT) scores, transformed cortisol, freezing duration, and cooing frequency were first z-scored across all timepoints. Because coo vocalizations typically decrease with increased anxiety, the inverse of cooing was used to calculate AT as follows: cooing was subtracted from freezing added to cortisol, and the sum of the z-scores was divided by 3 (the AT composite is an "average" of the 3 variable components, (FF – VV + Cort)/3). We also conducted Intraclass Correlation (ICC) analyses to evaluate the stability of measurements within subjects, across the developmental timepoints. For our ICCs, we chose average two-way mixed effects models for consistency (ICC(3,k)). ICCs were conducted across all timepoints, as well as on truncated datasets including only the final 3 timepoints. This allows us to examine how the stability of measures may differ across the whole sample when compared to the stability within the later, more "mature", developmental timepoints.

Individual developmental trajectories for the variables of interest (behavioral, neuroendocrine, AT composite) were determined using within-subject linear mixed-effects models (Bates et al., 2015) while controlling for possible effects of gestation length and sex, and included a random intercept to account for magnitude differences across subjects. Logarithmic growth patterns with increasing age were tested within the linear model framework by using $\log_{10}$ transformed age values. Linear, quadratic, & cubic shapes for the age-associated changes were also tested, as well as an *a priori* model testing each timepoint as a distinct variable. To determine which developmental

growth shape best fit the data, we compared Akaike Information Criteria (AIC) and Bayesian Information Criteria (BIC) values for each model using the lowest (>2) AIC/BIC value as indicating a model with the best fit. Models including random slopes, in addition to a random intercept, were also tested. We did not find that the inclusion of random slopes (for any variable of interest), improved the fit of the model (did not lower AIC/BIC values), nor was the random slope variable found to be significant within the best fit model as determined by AIC/BIC values. Therefore, we concluded that any differences between subjects for our variables of interest were restricted to differences in magnitude, and not differences in the rate of change across the developmental time period. We used the Bonferroni method for multiple comparison correction, to adjust our p-value threshold of significance. With 4 variables of interest, our adjusted p-value for developmental trajectories was $p=0.0125$. All of our developmental trajectories passed this threshold of significance and can be interpreted as highly significant. With 10 between-timepoint pairwise comparisons, our adjusted threshold for significance is $p<0.005$. We still report correlations with a $p<0.1$ as trending, but these findings should be interpreted cautiously.
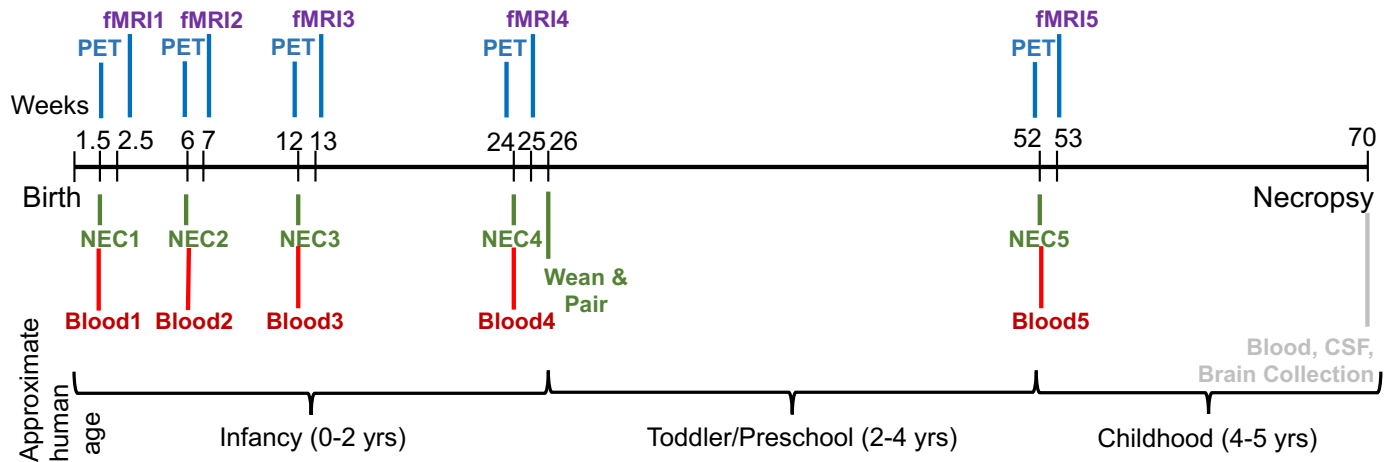
Results:

Figure 2.1 – full timeline of longitudinal testing, timepoints of behavioral testing are bolded in green

		Linear	Logarithmic	Quadratic	Cubic	*a priori*
Cortisol	AIC	1460.354	1444.176	1448.238	1423.23	1419.39
	BIC	1479.343	1463.165	1470.391	1448.548	1447.873
Cooing	AIC	803.2591	883.7663	797.8121	763.8706	767.2101
	BIC	822.2478	902.755	819.9656	789.1889	795.6932
Freezing	AIC	225.3075	306.0589	192.3938	168.8011	171.9208
	BIC	244.2962	325.0476	214.5473	194.1194	200.4038
AT	AIC	215.8534	286.2451	214.4199	212.9107	213.4057
	BIC	234.8421	305.2451	236.5734	238.229	241.8887

Table 2A – AIC and BIC Values for each shape tested for age-associated changes. Lowest BIC values (highlighted in yellow) indicated best fit, and informed choice for description of age-related changes

	Cortisol	Cooing	Freezing	AT
ICC(3,k)	.74	.626	.669	.44
P value	0.000000011	0.000031	0.0000031	0.0099

Table 2B – ICC(3,k) performance of measures across all timepoints, with corresponding p values

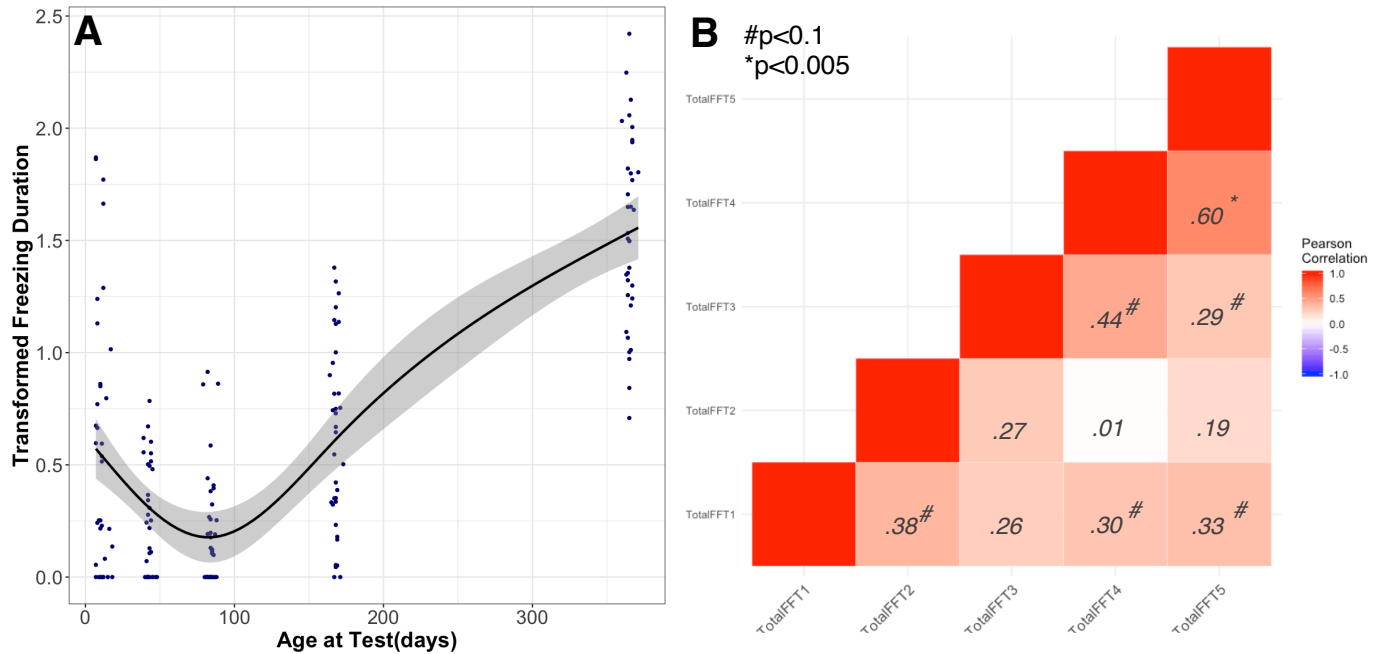Longitudinal emergence of freezing in response to potential threat exposure

Figure 2.2 – A) within-subject developmental trajectory of freezing (p<2.2x10⁻¹⁶), illustrating best fit of cubic age-related changes B) pairwise correlations between freezing expression across timepoints

Over the first year of life, infant monkeys demonstrate a dramatic 5X increase in freezing behavior (T1 raw average: 60s -> T5 raw average: 313s). The best fit for the age-related changes within-subject in freezing expression was cubic (*See Table 2A)*, such that individuals showed a decrease in freezing between 1.5 weeks and 12 weeks, followed by an increase from 12 weeks to 24 weeks, and a final, more gradual, increase from 24 weeks to 1 year (p<2.2x10⁻¹⁶, *see Figure 2.2 A*). We found that inclusion of random effects due to age did not improve the performance of our model, indicating that between subject differences were restricted to magnitude, and not differences in age-related slopes. Regarding stability of individual differences, ICC(3,k) for freezing across all 5 timepoints was "good" (*See Table 2B*, .67, p<0.0000032). Regression analyses assessing the stability of individual differences across timepoints revealed moderate

correlations (Rs ranging from .27-.60, *see figure 2.2B*). It is noteworthy that the two-week time point is moderately predictive of individual differences in freezing behavior at 1 year (r=.33, p=0.05). Additionally, the correlation between 24 weeks and 1 year (r = .60, p<0.000132) is higher than the other pairwise comparisons.

Changes to separation-induced vocalizations during postnatal development
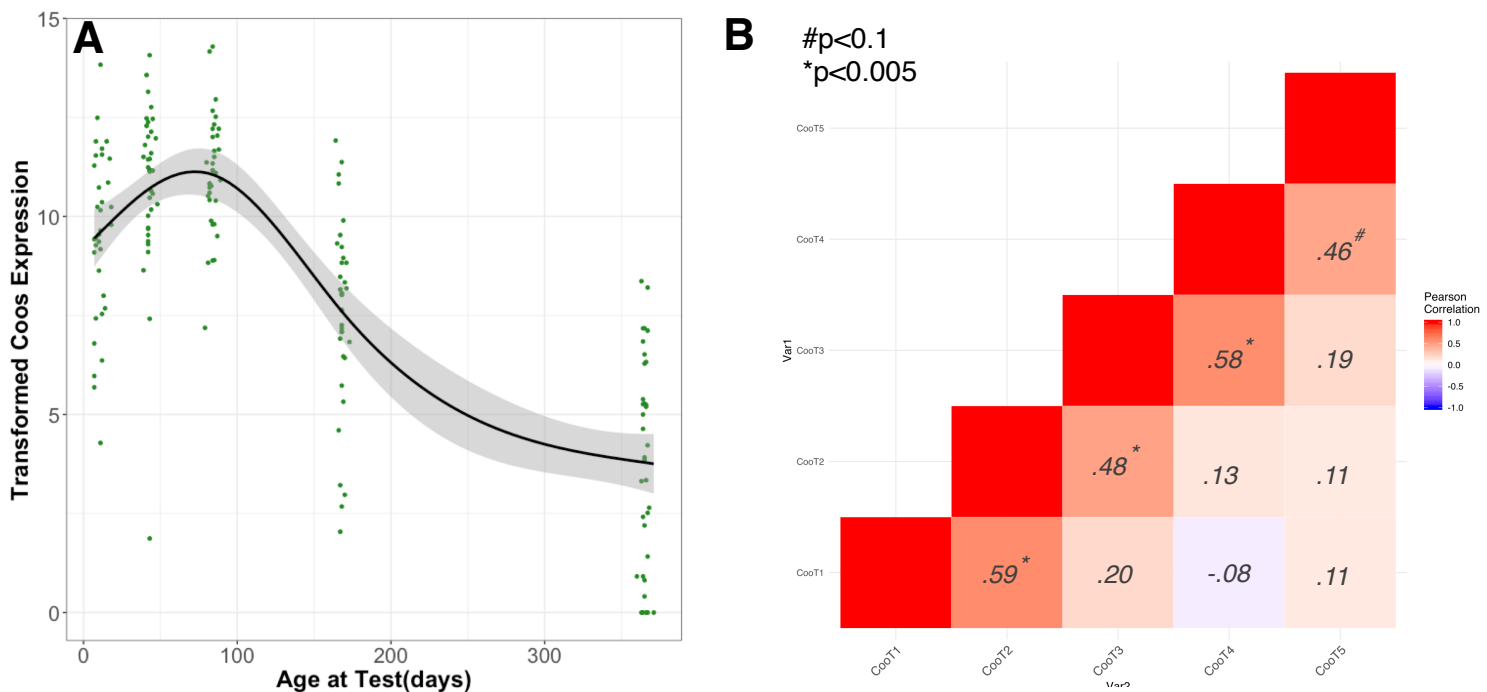

Figure 2.3 – A) developmental trajectory of within-subject changes in cooing (p<2x10^-16), depicting cubic age-related change; B) pairwise correlations examining individual differences in cooing across timepoints

During the first year of life, we observed a dramatic 4.75X decrease in vocalization frequency (T1 raw average: 568.86 -> T5 raw average: 127.54). The best fit for the age-related changes of within-subject of cooing frequency was cubic (*See table 2A)*, with individuals showing an initial increase from birth to 12 weeks, followed by a steep decrease between 12 weeks to 24 weeks, and a final more gradual decrease from 24 weeks to 1 year (p<2x10^-16, *See figure 2.3A*). Including age as a random effect

did not improve the performance of our model. ICC(3,k) for cooing across all 5 timepoints was considered "good" (see *table 2B*, .63, p<0.000032), indicating stability of individual differences across this developmental period. Regression analyses assessing the stability of individual differences across adjacent timepoints revealed moderate to strong correlations (*r*'s ranging from .46-.59, *see figure 2.3B*). Regression analyses did not identify any significant relationships amongst nonadjacent timepoints.

Longitudinal changes in circulating cortisol during experience of mild threat
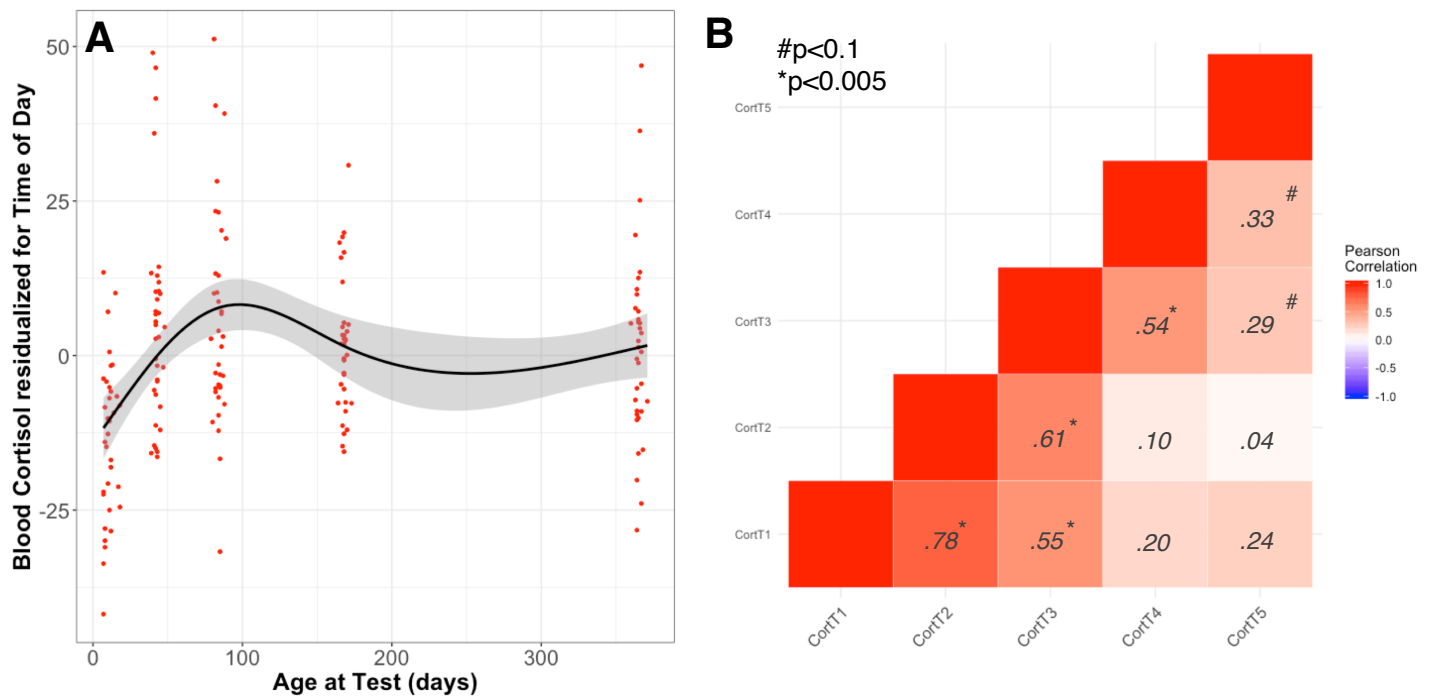

Figure 2.4 – A) developmental trajectory of within-subject changes to cortisol (p<0.00000000155), depicted with the best fit cubic age-related change B) pairwise correlations examining cortisol expression across timepoints

We observed a 1.3X increase in blood cortisol levels following 30 minutes of NEC (T1: 47.53, T5: 62.35) during the first year of NHP life. The best fit for the age-related changes within-subject of cortisol was cubic (See *Table 2A*), with individuals showing an initial increase from 1.5-12 weeks, switching to a decrease from 12-24

weeks, and finishing with a final increase from 24 weeks to 1 year (*See figure 2.4A,*

p<0.00000000155). Accounting for between subject differences of the age-related

slopes (inclusion of age as random effect) did not improve model performance. The

performance of ICC(3,k) for post-NEC blood cortisol was considered "good," almost

reaching "excellent" (.74, p<0.000000011, *see Table 2B*). Regression analyses

assessing the stability of individual differences across adjacent timepoints revealed

moderate to strong correlations (*r*'s: .33 - .78, *see figure 2.4B*), with the strongest

associations being between the cortisol levels at T1 and T2 (*r* = .78, p<0.0000000476,

see figure 2.4B). While not as strong, there were moderate associations between the

latter two timepoints (*r* = .33, p<0.054, *see figure 2.4B*)

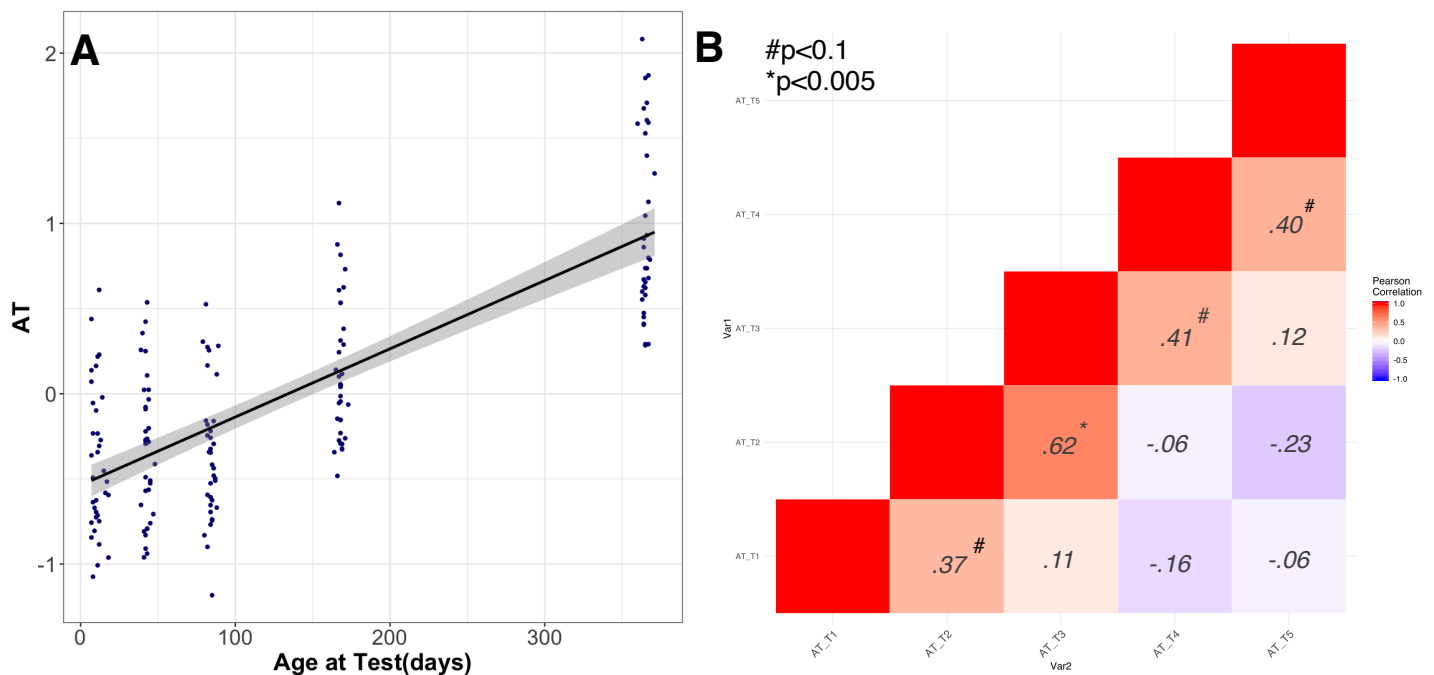Emergence of Anxious Temperament across first year of development

Figure 2.5 – A) within -subject developmental trajectory of Anxious Temperament (p<2x10^{-16}), with linear age-related change; B) pairwise correlations of AT across timepoints.

From 1.5 weeks of age to 1 year, we observed a ~2.5X increase in AT with the best fit for age-related changes as linear (See *Table 2A*), predicting a significant increase from birth to one year (p<2x10^{-16}, *see figure 2.5A*). Regarding the stability of AT within-subjects, ICC(3,k) performance was considered "moderate" (.44, p<0.0099, see *Table 2B*) across all five timepoints. Regression analyses assessing the stability of individual differences across adjacent timepoints demonstrate moderate correlations (*r*'s ranging: .31-.62, *see figure 2.5B*). Meanwhile, nonadjacent timepoints did not have significant associations with one another. Interestingly, the strongest correlations were found between T2 and T3 (*r*: 0.62, *see figure 2.5B*).

Discussion:

As infant monkeys mature after birth, their increasing capability to respond adaptively to potential threats is illustrated by the changes in their neuroendocrine and behavioral responses during their exposure to NEC. In this longitudinal study, we observed age-related increases in NEC-related behavioral inhibition across all subjects in our population. This is demonstrated by the significant within-subject increases in freezing duration during 30 minutes NEC from birth to one year, along with significant within-subject decreases in coo-call frequency. Additionally, we also observed increases in monkeys' post-NEC levels of the stress-related hormone cortisol. The ICC performance of cooing, freezing, and cortisol was "good" across all ages, implicating stability of these measures within subjects, even with the dramatic magnitude changes of each measure across development. Our regression analyses assessing the relation

between adjacent ages provides complementary evidence regarding the stability of these measure and their trait-like quality across the developmental time period. Most notably, the Time 1 freezing was significantly predictive of individual differences in freezing at 1 year of age, which suggests that infant expression of threat-related responses may have predictive power beyond this early development period. This finding is especially interesting in the context of recent work in human infants, where reflexive freezing was found to be predictive of psychopathology later in life (Niermann et al., 2019). Given the age-related changes for each component of the composite trait-like score AT, as expected, examination of the age-related change in AT also illustrates a significant increase with development. Our analyses indicate that there is moderate stability of AT across this entire developmental period, which is reflective of its trait-like quality during this early life period of great change.

The age-related findings in this study are generally consistent with the observations made in the 1991 cross-sectional examination of how threat-related responses differ across the first year of life in the monkey (Ned H Kalin et al., 1991). In that study, as in our current data, a decrease in NEC-induced freezing is seen during the first couple weeks of life, which is followed by a subsequent increase in NEC-induced freezing with increasing age. We note that, as in the 1991 cross-section study, because it is difficult to confidently assess freezing behavior shortly after birth, this apparent decrease in freezing around 4-7 weeks should be interpreted with caution. The current data provides a more detailed description of the within subject-changes to threat responses over the first year of life, which have not previously been described with

longitudinal testing. The trajectories of vocalization and freezing appear to mirror one another across this developmental period, and specifically implicates the 12-week age as a significant point of directional shift in the age-related changes. The increase in freezing duration within subject with age, accompanied by the overall decrease in total coo calls expressed within subject with age, illustrates how individuals transition from reacting to the NEC with typical separation-related behaviors in infancy to the more adaptive inhibition of behaviors by one year of age. It is possible that this development is due to the young monkey experiencing increased stress associated with threat, or the monkey's increased capacity to inhibit behaviors, or a combination of both.

The developmental trajectories of age-related changes in post-NEC cortisol are more difficult to interpret, much like other studies examining stress-related cortisol reactivity patterns in early life. We observe a peak in post-NEC cortisol at 12 weeks, after which it seems to undergo a slight decrease and then plateau. Importantly, our within-subject cortisol trajectories demonstrate a period of HPA-axis hypo-responsiveness to threat at the first age of testing, which has been well documented in the literature across primate and rodent species (Levine, 2001; Rosenfeld et al., 1992). This hypo-responsiveness is thought to be partially due to the essential role that major attachment figures play in maintaining baseline cortisol levels, typical diurnal cortisol rhythms, and cortisol reactivity in the presence of everyday stressors (Gunnar et al., 2015; Gunnar & Donzella, 2002; Gunnar & Hostinar, 2015). In human infants, psychological stressors especially (separation or stranger related-stress) seem to have the longest postnatal period where they are unable to stimulate reactivity of the HPA-

axis (Jansen et al., 2010). However, the studies investigating cortisol reactivity to separation or stranger stress have mixed findings across the first couple years of human life. In our data, the within-subject trajectories of post-NEC cortisol appear to plateau between 6 months and 1 year, suggesting a maturation by this point. It is of interest that the ICC(3,k) performance of threat-related cortisol was the highest amongst all other AT components, and also had the highest correlations between different timepoints. This finding suggests that threat-related cortisol is a highly stable measure within individuals over this time period, even with changes between timepoints.

One potential complication in our study examining fear-related responses over time is that each subject is repeatedly exposed to the identical behavioral paradigm with the same intruder. Given that this paradigm relies on the intruder's unfamiliarity to pose a potential threat to the monkey, it is possible that repeated exposures to the stimulus (which aims to maintain a tightly controlled experiment) sacrifices the paradigm's saliency and ability to trigger similar levels of anxiety with additional exposures. However, the observed behavioral changes, especially when considered in conjunction with our observations of increasing levels of post-NEC cortisol across this first 1 year, suggest the saliency of the threat is still present, and that subjects are generally not acclimating to the paradigm. The ability of the monkey to recognize the threat throughout early timepoints is also unclear, and the delay in complex visual processing during this same period (Kiorpes, 2016) may play a role in preventing the presentation of this unfamiliar threat from becoming overly familiar. Most importantly, other studies of repeated, mild, early life stress suggest that it does not necessarily result in more

adaptive responses (e.g. habituation) but instead can result in more extreme or inappropriate threat-related responses (Harlow & Suomi, 1971; Seay et al., 1962). Moreover, studies examining the effects of early life stress and cortisol (Fogelman & Canli, 2018) seem to demonstrate that early life stress does not have long term effects on the reactivity of cortisol to stress. Thus, we believe our data demonstrate that our animals are not habituating to the paradigm, and are experiencing NEC-related stress during the paradigm at 1 year.

Here we have described the within-subject trajectories of threat-related responses across the first year of life. Across the entire study population, we observed a reduction in cooing and in increase in freezing during NEC as monkeys aged from birth to one year. We also observe increases in post-NEC levels of cortisol, suggesting maturation of the HPA-axis and its reactivity to stress during this period. While we did not observe differences between the subjects in the rate of change across development (for cooing, freezing, cortisol, and AT), we did observe differences in magnitude. Given the extended period of postnatal development of many anxiety-related brain regions, an understanding of how regions in the anxiety-related circuit are changing during this period is essential to our ability to understand how they may associate with expression of AT. In the next chapter we turn our focus to the FDG-PET data that was collected in conjunction with the NEC, to explore how threat-related brain function changes during this critical early life development period.

Chapter 3

The Development of Threat-Induced Brain Metabolism during the First Year of

Nonhuman Primate Life

Introduction:

Significance & Rationale

To enhance our understanding of the origins of pathological anxiety, we must turn our attention to its neural substrates. Examination of threat-related brain function is essential for the development of novel biologically-relevant treatments for Anxiety Disorders (AD). Understanding threat-related brain function during the early postnatal developmental period will provide insight into how the organization of anxiety-related neural circuits manifest in expression of anxiety-related behaviors. Given the demonstration of the ongoing development of threat-related behavioral responses during the first year of life (Chapter 2), it follows that underlying brain circuitry contributing to these responses must be changing as well. Whether or not these developmental changes in brain function associate with the changes we observe in Anxious Temperament (AT) is of upmost interest. However, prior to investigating such brain-behavior relationships, we first must characterize how threat-related brain function is changing as a function of age during this dynamic development period. In this chapter, we describe the age-related developmental trajectories of threat-related regional brain metabolism with specific focus on regions with essential roles in anxiety circuitry: dorsal amygdala (dA), bed nucleus of the stria terminalis (BST), posterior orbitofrontal cortex (pOFC), and dorsal lateral prefrontal cortex (dlPFC).

Use of FDG-PET to Assess Regional Brain Metabolism in Primates

Brain imaging is an invaluable approach for non-invasive exploration of the functional correlates of primate behavior. [18]Fluorodeoxyglucose- Positron Emission Tomography imaging ([18]FDG-PET) is of particular relevance because it reflects areas that are metabolically active during specific behavior-related or emotion-related tasks. This technique uses a radioactively labeled analog of glucose ([18]FDG) injected intravenously that gets taken up into, and sequestered by, active neurons. After an injection of [18]FDG, it is taken up over the course of approximately 30 minutes and remains trapped in the cells for an extended amount of time, leaving behind an accumulated signal that can be measured with PET. Thus, [18]FDG-PET allows for the visualization of integrated brain activity that occurred during the 30-minute period following injection. Importantly, in these studies the animal is injected with [18]FDG-PET immediately prior to the start of the 30-minute NEC behavioral testing and is anesthetized immediately following NEC, prior to the PET scan. Therefore, the brain signal is reflective of the prior 30 minutes during which the tracer was taken up by active neurons. The unique advantage of using this technique is that it allows for examination of glucose metabolism that is matched in time to the expression of anxiety-related responses during unrestrained, ethologically-relevant naturalistic behavior. This measure of brain metabolism, which can be specifically associated with a particular experience, lays the way for investigation of how individual differences in brain function may manifest behaviorally during this same experience.

Alterations of Brain Metabolism during Threat Exposure

[18]FDG-PET imaging has been a useful tool for understanding the role of different brain regions in threat- and anxiety-related processing (Baeken et al., 2018; Wang et al., 2017; Yang et al., 2023). It has been especially useful in animal models for visualizing metabolic patterns during conditions stimulating stress(Jahn et al., 2010). While PET imaging at rest does not appear to differentiate between humans with Anxiety Disorders (ADs) and those without (Giordani et al., 1990), it does show powerful potential when used within the context of exposure to threatening contexts. Rodent and NHP studies have demonstrated marked metabolic changes in anxiety-related regions during the experience of threat (Rilling et al., 2004; Sung et al., 2009; Wei et al., 2018). In our lab, we have conducted numerous studies examining rhesus monkeys' NEC-related FDG-PET metabolism in order to probe individual differences in brain metabolism during exposure to potential threat, and how these differences relate to individual differences in Anxious Temperament (AT). In a large cohort of 592 monkeys, NEC-related metabolism of the Ce, BST, and pOFC, among other regions, were shown to be highly predictive of individual differences in AT (Fox, Oler, Shackman, et al., 2015). Importantly, we have also demonstrated heritability in the FDG-PET signal of relevant anxiety-related brain regions, and relative stability of individuals' differences in threat-related brain function for relevant brain regions (Oler et al., 2010). To our knowledge, there have been no studies investigating the changes in threat-related brain metabolism during the early-life period of development of primates, while adaptive threat-related behavioral responses are still emerging.

Changes in ^{18}FDG-PET during Early-life Development (at Rest)

There has been some investigation into how brain metabolism at rest changes over the course of early life development in humans. The ongoing development of the primate brain during infancy and childhood requires a substantial amount of energy. Generally, the changes in uptake of ^{18}FDG-PET at rest during infant development reflect the hierarchical development of the brain during this period. Overall rates of glucose metabolic uptake at birth in humans are about 30% lower than in adults, but dramatically increase until they are 2X higher than adult levels by 3 years, reflecting the increased glucose needs during ongoing postnatal brain development. More specifically, studies have demonstrated the regional metabolic differences across the brain as newborns age from birth, with increased glucose utilization in primary visual, parietal, cingulate, and temporal cortices at 2-3 months, followed by increases in lateral and inferior frontal cortex by 6-8 months, and finally by increased glucose uptake in dorsal and medial frontal regions at 8-12 months (Harry T Chugani, 2018). These dramatic developmental changes at rest highlight the need for more specific investigation of how ^{18}FDG-PET signal is changing during early-life experience of potential threats, as there may be additional developmental differences associated with threat-related metabolic uptake. Chugani's work ((H T Chugani, 1998; H T Chugani et al., 1987; H T Chugani & Phelps, 1986)), and others (Kennedy et al., 1982; Kinnala et al., 1996; London & Howman-Giles, 2015), in particular suggests that the anxiety-relevant regions highlighted from our own ^{18}FDG-PET studies (Ce, BST, pOFC) have

different development rates across this postnatal period. It also suggests that the

dlPFC, whose role in anxiety is implicated by functional connectivity fMRI studies,

utilizes glucose later than these other regions across this developmental period,

implying its role in regulating threat-related responses may be delayed relative to said

regions(Harry T Chugani, 2018; London & Howman-Giles, 2015).

In this chapter, using the developmental cohort and a longitudinal experimental

design of behavioral testing accompanied by [18]FDG-PET, we investigate age-related

changes in glucose uptake within anxiety-relevant regions during 30 minutes of NEC.

More specifically, given the significant role each plays in threat responding, we are

interested in exploring potential differences in the developmental trajectories of threat-

related metabolism in the Ce, BST, pOFC, and dlPFC. Beyond this chapter's initial

characterization of development-related changes in threat-induced brain metabolism,

the current cohort also provides the opportunity to directly correlate individual

differences in regional brain metabolism with AT expression during NEC. Exploration of

the associations between NEC-related AT and FDG-PET signal will be covered in

Chapter 5. Here we start by describing the age-related growth curves of NEC-related

regional brain metabolism over the first year of life in NHPs (rhesus macaques).

Aim of Chapter 3: *Characterize the developmental patterns of regional brain*

metabolism in response to threat exposure across the first year of life. Given the

immaturity of important anxiety-related circuits at birth (especially those involving the

PFC), stress responses may be partially influenced by ongoing postnatal developmental

processes. How brain metabolism during experience of threat changes over the first year of primate life has not been previously described. Here we aim to explore the development of metabolic changes in anxiety-related regions during exposure to NEC across 5 timepoints during the first year of NHP life. We hypothesize that *metabolism in prefrontal brain regions (i.e., dlPFC, pOFC) during NEC will increase across the first year of life, as these regulatory regions mature and infants develop the capacity to more adaptively regulate their emotional responses.* In contrast, we hypothesize that *metabolism in the extended amygdala (i.e., dA, BST) will not increase across development, as these regions are more mature at birth and the influences of developing prefrontal cortical regions may provide a buffer on the threat-related activation of these regions.*

Methods

Review of Timeline & Testing Design

Monkeys were tested 5 times between birth and 1 year (average ages: 11 days, 6 weeks, 12 weeks, 24 weeks, 1 year) with 30 minutes of the No Eye Contact-Condition (NEC) followed by ^{18}FDG-PET imaging (*see figure 3.1*). This approach allows for the simultaneous collection of both the behavioral data and regional brain metabolism in association with NEC, providing the potential to integrate these data for an enhanced understanding of how brain metabolism during threat exposure correlates with threat-related behavioral responses. Details on the behavioral data and NEC testing can be found in Chapter 2; the details of the PET scanning protocol details follow below.

Exploration of the relationships between NEC-related brain metabolism and NEC-related behavior will be covered in Chapter 5.

At each testing age (T1-5), using a tabletop restraint or manual restraint, a catheter was placed, with preference given to the saphenous vein, for intravenous tracer delivery. The [18]FDG was administered (0.5mCi + 1.5mCi/kg), and the animals were immediately transported to a novel testing room and placed in a large mesh testing cage (inner dimensions: 71 cm x 76 cm x 78cm). The familiar experimenter left the room, and approximately one minute later an unfamiliar male intruder entered the testing room and stood still 2.5 meters away from the cage while presenting his profile to the animal and avoiding eye contact for 30 minutes. A heated water pad covered with a towel was placed on the floor of the test cage to maintain body temperature. To ensure that NEC-related brain metabolism was unconfounded by the stress of transfer and blood draw, and to allow for safe transport to the scanner, immediately following testing the animals were anesthetized with ketamine (20 mg/kg) and atropine (0.04 mg/kg) in consultation with veterinary staff. The animals were also administered ketoprofen (5 mg/kg, IM) to reduce inflammation and pain caused by the intubation and placement in ear bars. A rolled-up towel was placed in the transport for comfort, and heated water bags or bottles covered with towels were also placed in the transport to help maintain body temperature.

Prior to PET imaging, atropine sulfate was administered to depress salivary secretion, animals were fitted with an endotracheal tube and placed ventral side-down in a head holder with the head facing down toward the table. Anesthesia was induced

with 5% or less isoflurane, and typically maintained on less than 2% isoflurane. During the scans, heart rate, respiration, and oxygen saturation were monitored continuously throughout the procedure. Body temperature, measured before and after the imaging procedure, was maintained in the scanner with a warm air blanket. Approved isotonic fluids were administered via the indwelling catheter to maintain hydration. Blood glucose was monitored before and after the scanning procedure, and at intervals during the scanning procedure if recommended by veterinary staff. If necessary, supplemental glucose, such as dextrose (alone or mixed with an isotonic fluid) or corn syrup, was given before, during, or after the imaging procedure. Data were collected using a Focus 220 microPET scanner (Siemens Microsystems, Knoxville, TN). The PET scan lasted approximately 90 minutes. A 9-minute transmission scan was initially collected for scatter- and attenuation-correction followed by a 45 emission PET scan, which were reconstructed using standard filtered back projection methods and reflect the integrated brain metabolism that occurred during the 30 minutes of [18]FDG uptake. After the scan, animals were extubated, the catheter was removed, and pressure was placed at the site of injection to prevent leakage. Subjects were monitored continuously until they were able to lift their own head, then they were monitored at least every 15 minutes until sitting up, after which they were monitored every 30 minutes until fully recovered. Once fully recovered, the infants were reunited with their mothers (T1-4) or their cage-mates (T5) in their home cages. One subject's [18]FDG-PET data from Time 1 were lost due to technical difficulties.

Collection and Processing of MRI for Anatomical Reference Template

One week following each 30-minute NEC with [18]FDG-PET, monkeys were scanned while under anesthesia to collect structural and functional brain imaging data for examination of white-matter microstructure, myelination, and functional connectivity (temporal correlations in BOLD signal) across this important developmental period. The analytic processing of the structural- and myelin-related data, along with the investigation of age-related changes in these modalities in this sample, can be reviewed in detail in our recently published studies (Aggarwal et al., 2021; Moody et al., 2022). Our investigation of the developmental trajectories of the resting-state fMRI can be found in Chapter 4.

At each MRI data were collected using a GE Healthcare 3T Discovery MR750 scanner equipped with a custom coil. Monkeys were weighed, initially anesthetized with ketamine (20 mg/kg, IM), and administered atropine sulfate (0.04 mg/kg, IM) and ketoprofen (5 mg/kg). They were then intubated and positioned inside the MRI scanner in the custom 8-channel receive array for NHP imaging with a built-in stereotactic head frame (Clinical MR Solutions). Anesthesia was maintained during scanning with isoflurane (<2% isoflurane/O2) while heart rate and oxygen saturation were monitored. Isotonic fluids were administered, if necessary, to maintain blood glucose levels before, during, or after scanning. Whole brain, 3D T1-weighted images were acquired and reconstructed with 0.625 mm isotropic spatial resolution (Kecskemeti et al., 2016). Details on fMRI scanning parameters and processing can be found in Chapter 4.

The anatomical reference template was created through co-registration of structural MRI scans in ANTS (Avants et al., 2009). Briefly, each subject's structural MRI scans from each timepoint (T = 1-5) were co-registered to create 35 within-subject, across time templates. These 35 individual-subject longitudinal templates were then co-registered together to create an overall population template. The time-averaged population template was then warped into a standard NHP template constructed from 592 animals (Fox, Oler, Shackman, et al., 2015; Shackman et al., 2013). Details on this process can be found in our recently published work ((Aggarwal et al., 2021; Moody et al., 2022). This template was used as the anatomical reference for the rs-fMRI data, as well as for the [18]FDG-PET data (detailed in Chapter 4). The 592 subject template space was also used to delineate population-derived seed masks for functional connectivity analyses.

Scanning Parameters and Imaging Processing

Using the same strategy employed for the longitudinal alignment of the structural MRI data described above, the 5 PET scans from each subject were co-registered to create within-subject, across time [18]FDG-PET templates in ANTs. These 35 individual subject templates were then co-registered together to create an overall longitudinal population [18]FDG-PET template. The time-averaged population template was then co-registered to the MRI template space as used in Chapter 4, to allow for use of ROI masks from the same Calabrese Atlas used for rs-fMRI analyses. The transformations were concatenated and applied to the individual scans in native space so that each

individual scan was in template space. Each individual [18]FDG-PET image was scaled to

its mean signal intensity for each developmental timepoint (intensity normalized so the

mean value for each subject, at each age, was fixed to the same arbitrary value of 5)

followed by application of a 2 mm FWHM smoothing kernel to facilitate across-time and

across-subject analyses and to account for any variability in registration or of underlying

brain anatomy.

Analytical Approach and Statistics

We took a Region of Interest (ROI) based approach for our investigation of the

age-related changes to threat-related brain metabolism. We selected regions that are

important for both the production and the regulation of anxiety-related behavioral and

physiological responses. 3D anatomical masks were created for each ROI from the

Calabrese Monkey Brain Atlas constructed from Paxino's regions (Calabrese et al.,

2015), by co-registering the ROIs into the cohort-population template space and then

performing smoothing and erosion. Atlas-derived ROIs included: bed nucleus of the

stria terminalis (BST), posterior orbital frontal cortex (BA14/ProIso, pOFC), dorsal lateral

prefrontal cortex (dlPFC, BA46 & BA9-46). Instead of using an atlas-defined central

nucleus of the amygdala (Ce) ROI for our examination of threat-related metabolism

changes across development, we chose a hand-drawn dorsal amygdala (dA) seed.

There have been few studies exploring the subdivisions of the amygdala in early infancy

(Medina et al., 2023), with little evidence of the presence of a true Ce region in early

infancy (Chareyron et al., 2012). Moreover, the MRI resolution in our population does

not allow us to validate the presence of the Ce ourselves. We chose to use a dorsal amygdala (dA) ROI instead, which mostly contains the Ce, but is hand-drawn on our NHP population template to incorporate a larger area of coverage. This more grossly defined dA seed may help account for major structural differences across these early ages. We also use this hand-drawn mask as the seed for our functional connectivity analyses (to be discussed in Chapter 4).

To examine how differences in regional metabolism changed over the developmental period, we also computed a difference score (Δ) with our frontal and dA ROIs: a dlPFC-dA FDG-PET Δ, and a pOFC-dA FDG-PET Δ. These values represent the difference in metabolism of these regions during the 30 minutes of NEC. Our interest in these measures stems from the hypothesis that they may represent relative metabolism of regions during experience of NEC, and could reveal associations with developmental changes in AT, as well as relations with underlying functional connectivity between these regions at rest.

The shapes of the developmental growth curves were determined using within-subject linear mixed effects modelling in R (Bates et al., 2015). The within-subject changes with age were assessed for each ROI, while controlling for any effects of gestation length and sex. Models included a random effect for intercept; inclusion of a random slope effect for age did not improve the performance or fit of any models. We determined the best growth shape across this first-year developmental period by estimating models with Maximum Likelihood and using Bayesian Information Criterion (BIC) to compare models considering linear, logarithmic, quadratic, cubic, and *a priori*

age-related growth shapes in threat-related metabolism. These methods are similar to the approach used in Chapter 2. In cases when comparison between models yielded similar BIC values (<2 units difference between BIC), visual inspection of individual growth curves was used to evaluate the best fit for the data. To correct for multiple comparisons, we used the Bonferroni method. With four regions of interest, & three delta values, our threshold for significance of within-subject age-related trajectories is adjusted to $p=0.007$. All reported developmental trajectory findings below pass this corrected threshold, and can be interpreted as highly significant. With 10 between-timepoint pairwise comparisons, our adjusted threshold for significance is $p<0.005$. We still report correlations with a $p<0.05$ as trending, but these should be considered exploratory and interpreted with caution.

Results:
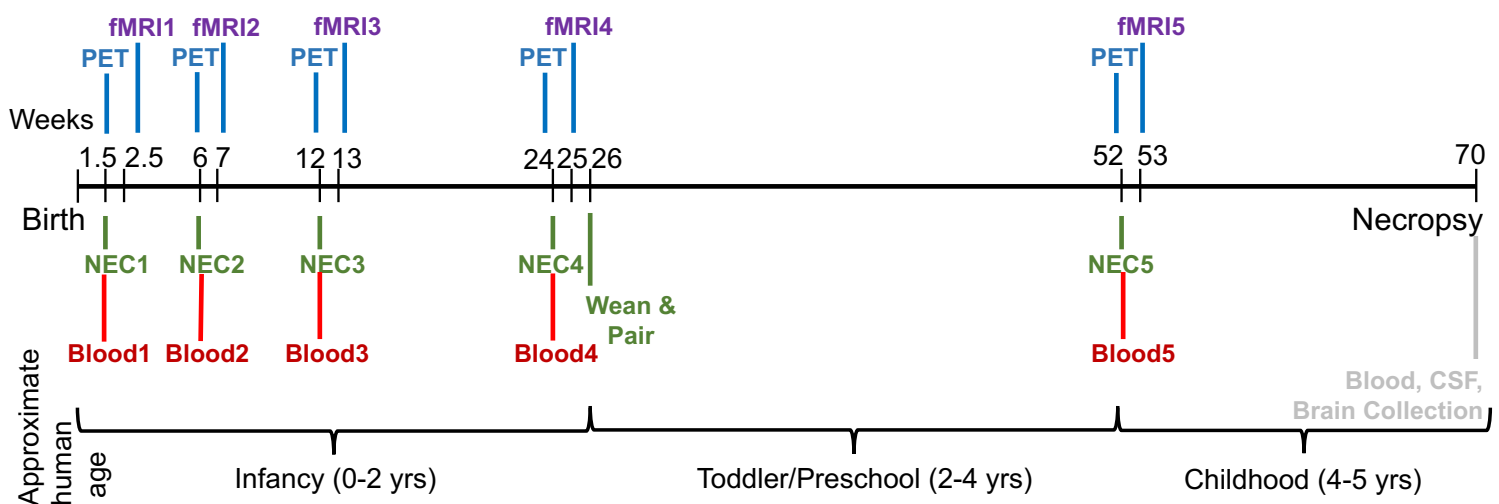
Figure 3.1 – full timeline of study, with testing points of NEC with ^{18}FDG-PET indicated by bold blue "PET"

		Linear	Logarithmic	Quadratic	Cubic	*A priori*
dA	AIC	-87.96551	-155.584	-158.7038	-163.1265	-162.2103
	BIC	-68.97679	-136.5953	-136.5503	-137.808	-133.7272
pOFC (BA14, ProIso)	AIC	-126.8454	-156.708	-178.3036	-177.3154	-178.816
	BIC	-107.8566	-137.7193	-156.1501	-151.9972	-150.3329
dlPFC (BA46, 9-46)	AIC	12.09377	-69.45688	-45.77749	-93.02355	95.16162
	BIC	31.08248	-50.4618	-23.62399	-67.70526	-66.67855
BST	AIC	-26.22689	-113.2959	-109.4392	-129.3149	-127.4297
	BIC	-7.238173	-94.3072	-87.28569	-103.9966	-98.94662
pOFC-dA	AIC	-216.6845	-218.3196	-228.0478	-230.8574	-229.5453
	BIC	-197.6958	-199.3309	-205.8943	-205.5391	-201.0622
dlPFC-dA	AIC	159.0835	41.18577	69.67346	31.30644	37.40747
	BIC	178.0722	60.17448	91.82696	56.62473	65.89054
BST-dA	AIC	-209.7411	-206.117	-215.291	-223.2293	-224.5547
	BIC	-190.7524	-187.1283	-193.1375	-197.9111	-196.0717

Table 3A – AIC and BIC values for each age-related growth curve, best growth shape highlighted

	dlPFC	pOFC	BST	dAmy
ICC(3,k)	0.00000017	.77	.621	.36
p value	0.48	0.00000000025	0.000041	0.038

Table 3B – ICC, and associated p-values for each region of interest, assessing stability of individual subjects across all ages

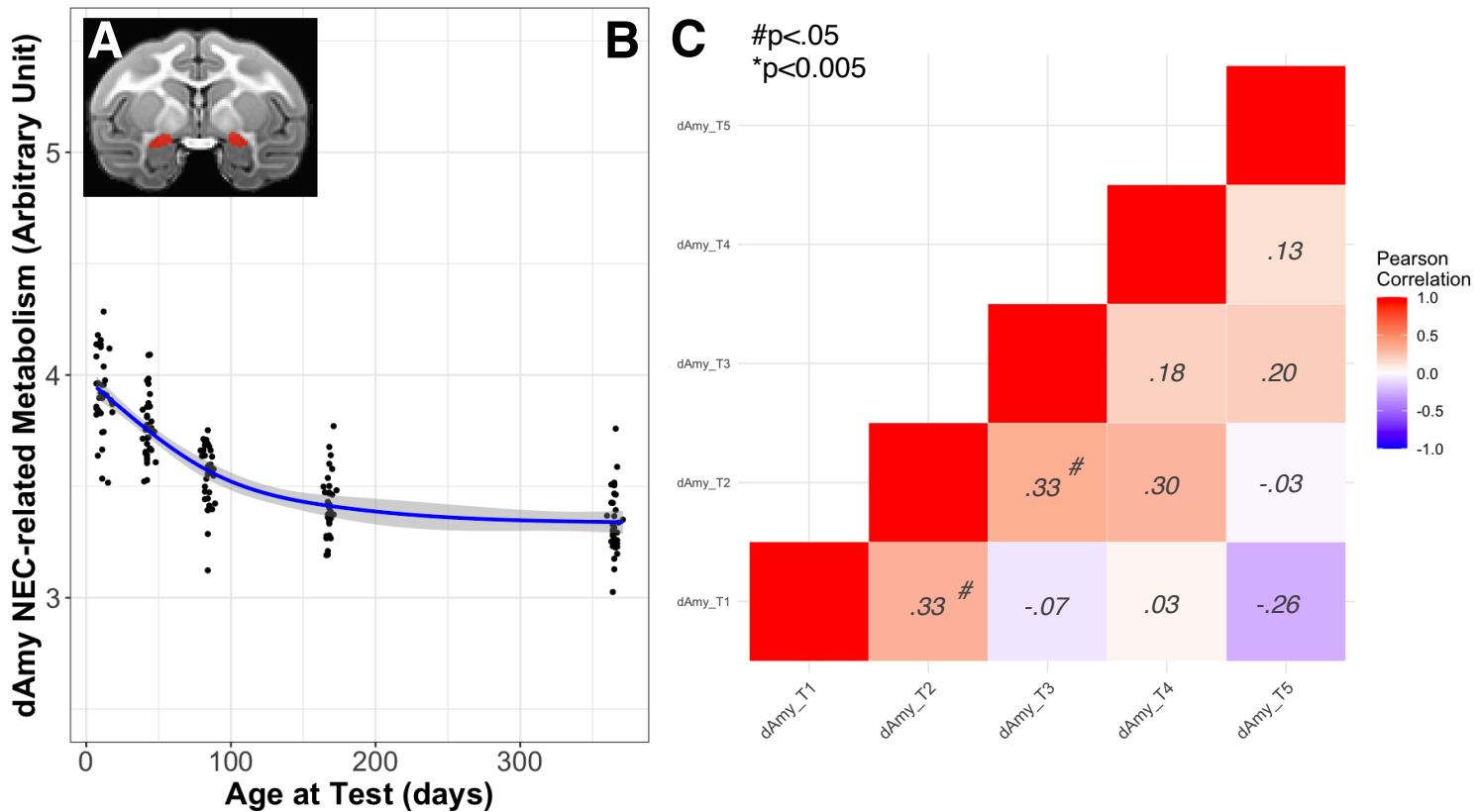Decrease in NEC-related dorsal amygdala metabolism with increasing age

Figure 3.2 – A) coronal view of dA mask, B) cubic age-related within-subject changes in dA NEC-related metabolism, p<2x10^{-16}, C) pairwise correlations testing associations across different timepoints, significance threshold adjusted for multiple comparisons

Over the first year of life, infant monkeys show a marked decrease in dA (*see figure 3.2A)* metabolism during 30 minutes of NEC. The best growth shape for the change was determined to be cubic (p<2x10^{-16}, *see figure 3.2B*), with the most rapid changes happening between 1.5-12 weeks, a less rapid decrease between 12-24 weeks, and an apparent plateau from 24 weeks to 1 year. Considering stability within subjects, ICC(3,k) performance was poor (.36, p<0.038, *see table 3B*). We used pairwise regression analyses to examine stability of individual differences across timepoints (*see figure 3.2C)*, and only found positive correlations between adjacent early timepoints (T1vT2: *r* =.33; T2vT3: *r* =.33). Interestingly, there was a modest

negative correlation between NEC-related dA metabolism at 1.5 weeks and 1 year ($r = -0.26$).

Decrease in NEC-related BST metabolism with increasing age
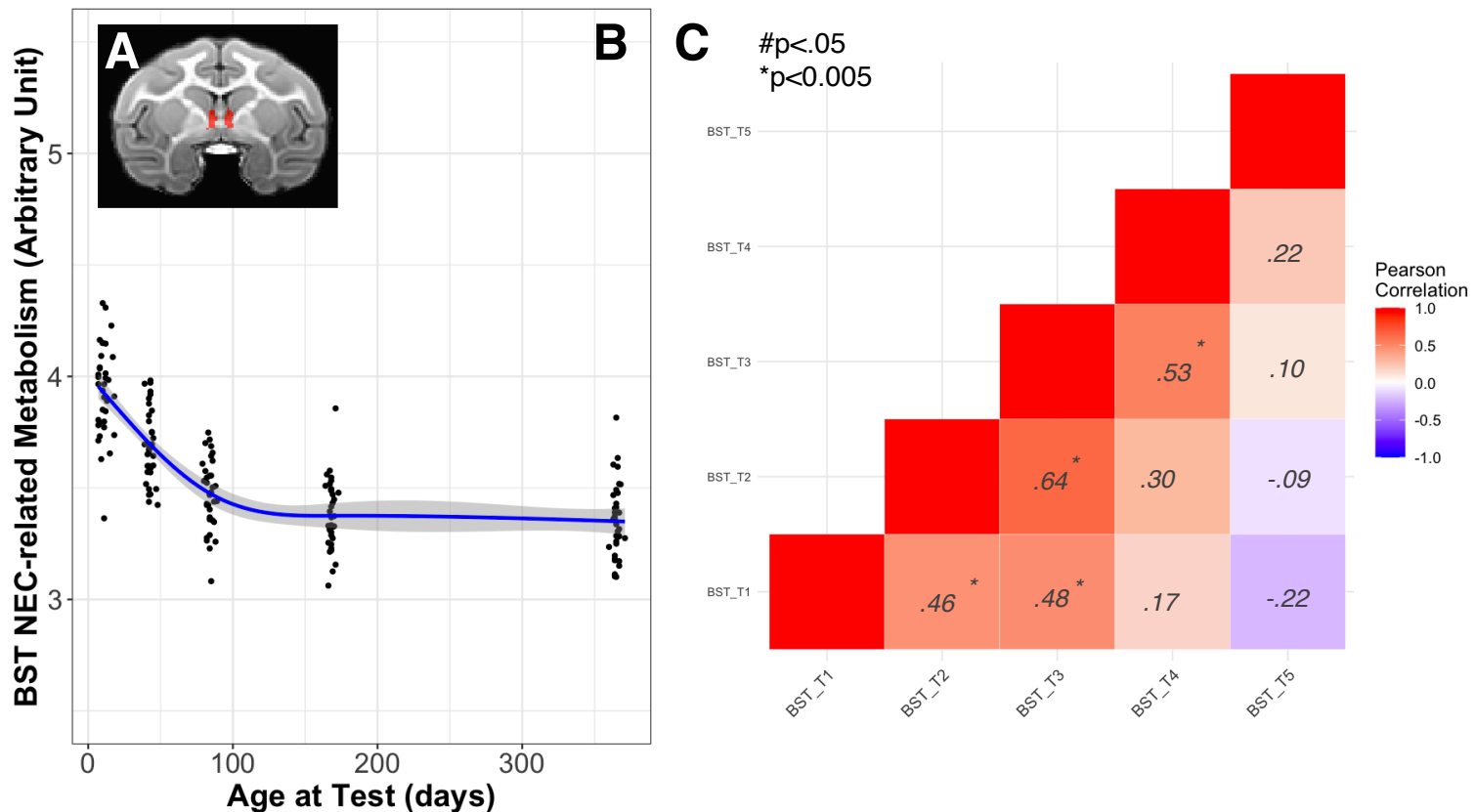
Figure 3.3 – A) coronal view of BST mask, B) cubic age-related within-subject developmental trajectory for NEC-related BST metabolism, p<2x10⁻¹⁶, C) pairwise correlations between individual differences across different timepoints, significance threshold adjusted for multiple comparisons

Monkeys showed a significant decrease in NEC-related BST metabolism while aging from birth to 1 year, with the best fit for the age-related changes determined as cubic (*see Table 3A*), with a steep decrease from 1.5-12 weeks, a less steep decrease from 12 weeks to 24 weeks, and a plateau between 24 weeks and 1 year ($p<2x10^{-16}$, *see figure 3.3B*). Regarding stability of individual differences within subjects, ICC(3,k) performance was good (.621, p<0.000041, *See Table 3B*). Regression analyses

assessing stability of individual differences across timepoints (*see figure 3.3C)* revealed

some strong correlations amongst early timepoints (*r*'s ranging .46-.64) with other

associations ranging from weak to good (-.09-.53)

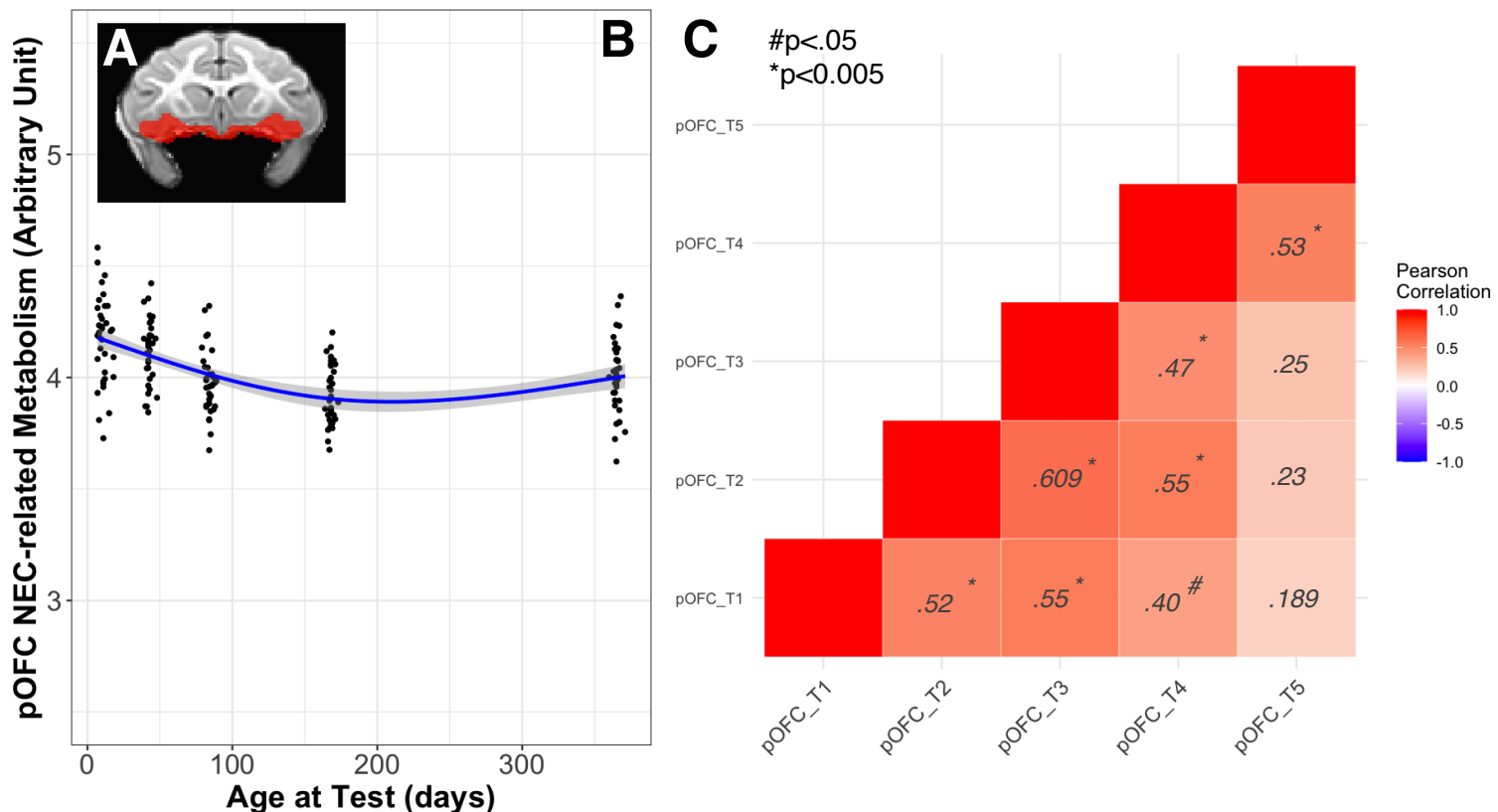Changes in pOFC metabolism during 30 minutes NEC over the first year of life

Figure 3.4 – A) coronal view of pOFC mask B) quadratic age-related within-subject developmental trajectory for NEC-related pOFC metabolism, p<2x10^{-16}, C) pairwise correlations between individual differences across timepoints, significance threshold adjusted for multiple comparisons

We found the best fit for the age-related within-subjects changes across the first

year of life to be quadratic (*see Table 3A),* such that monkeys show a continuous

decrease of NEC-related FDG metabolism from 1.5-24 weeks, followed by a slight

increase from 24 weeks to 1 year (p<2x10^{-16}, *see figure 3.4B*). Regarding stability of

individual differences in NEC-related pOFC metabolism, ICC(3,k) performance was

excellent (.77, p<2.5e-10, *see Table 3B*), and regression analyses across timepoints

found positive correlations (*r*'s ranging .18-.61), with especially strong correlations

between adjacent timepoints of NEC-testing (*r*'s ranging .47-.61).

Increases in NEC-related dlPFC metabolism during first year of life

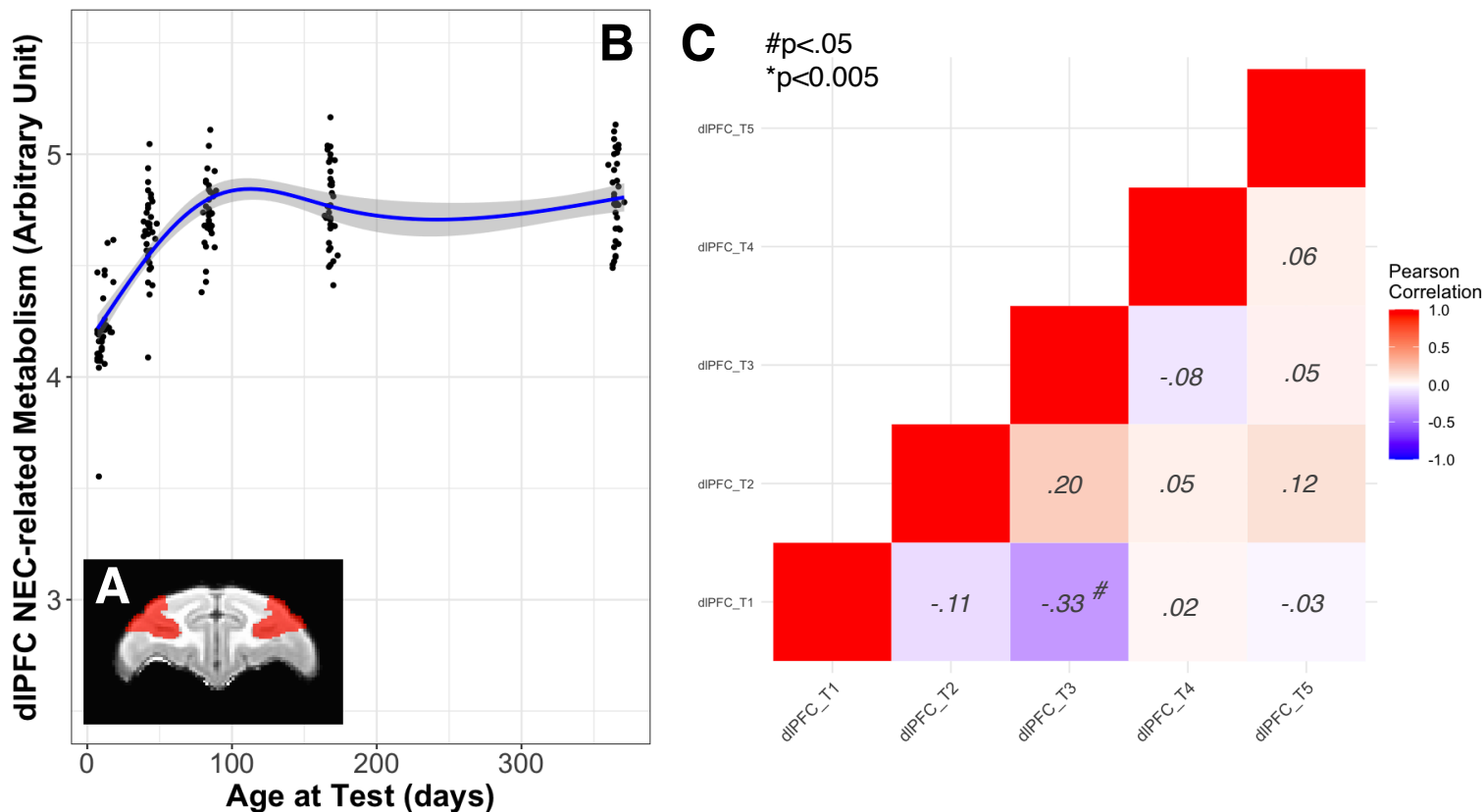*Figure 3.5 – A) coronal view of dlPFC mask B) within-subject age-relate developmental trajectory for NEC-related dlPFC metabolism, p<2x10^{-16}, C) pairwise correlations between individual differences across timepoints, significance threshold adjusted for multiple comparisons*

Over the first year of life, within individuals, dlPFC metabolism during 30 minutes

of NEC showed a dramatic increase, with the best age-related growth shape fit

determined as cubic (*See Table 3A*, $p<2x10^{-16}$). Individuals showed an increase

between 1.5-12 weeks, a slight decrease between 12-24 weeks, and finally a slight

increase from 24 weeks to 1 year (*see figure 3.5B*). ICC(3,k) performance was poor

(0.00000017, p=0.48, *see Table 3B*), and regression analyses between timepoints

revealed no significant correlations across timepoints (r's ranging -.33 - .2, *see figure*

3.5C).

Changes to differences between BST-, pOFC-, dlPFC- and dA NEC-related metabolism
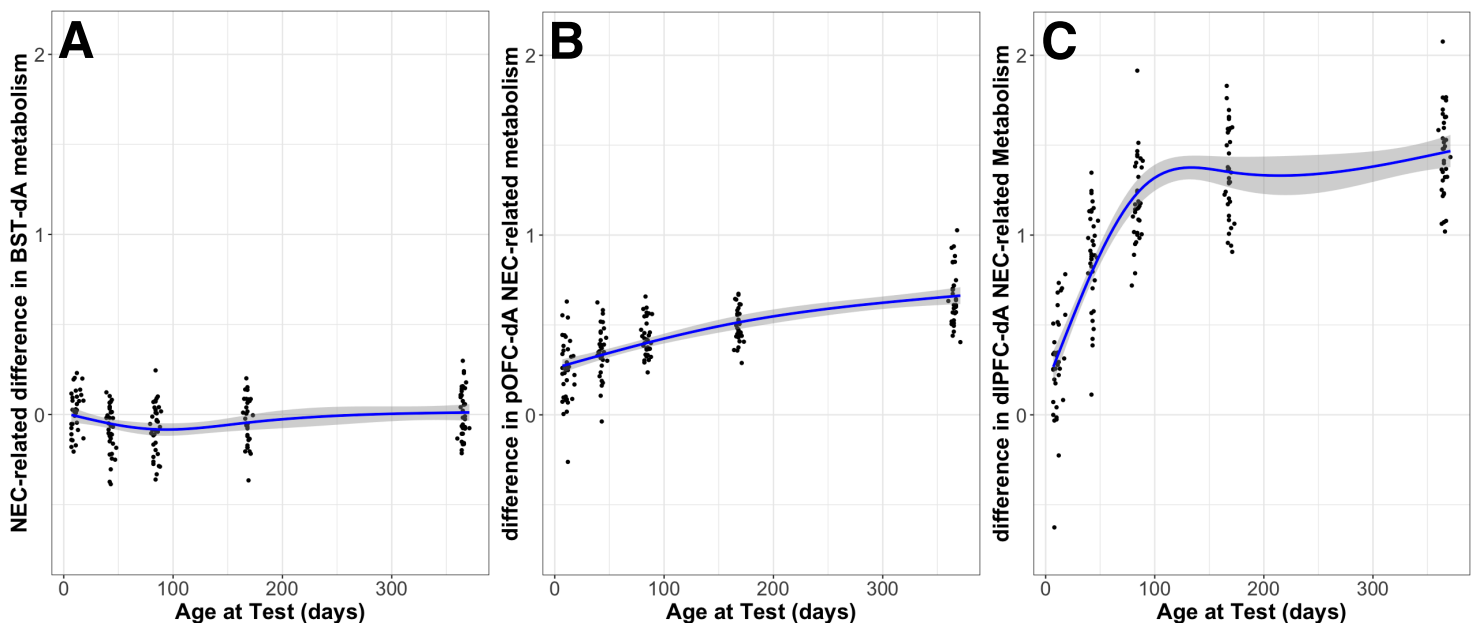
over the first year of life

Figure 3.6 - A) cubic age-related within-subject trajectory for differences between BST-dA NEC-related metabolism, p<0.00004364, B) quadratic age-related within-subject developmental trajectory for differences between pOFC-dA NEC-related metabolism, p<2.2x10^{-16}, C) cubic age-related within-subject developmental trajectory between dlPFC-dA NEC-related metabolism, p<2x10^{-16}

To enhance our understanding in the differences between dA metabolism and

our other ROIs during 30 minutes of NEC, we computed "delta" (Δ) values for the

difference between 1) BST & dA, 2) pOFC & dA, and 3) dlPFC & dA, (ROI – dA)

metabolism during 30 minutes of NEC. We found different shapes for the age-related

trajectories of each delta, with the best fit for each being as follows: 1) BST-dA Δ is

cubic, 2) pOFC-dA Δ is quadratic, 3) dlPFC-dA Δ is cubic (see *Table 3A).* More

specifically, the differences in BST and dA metabolism showed a slight decrease from 1.5-12 weeks, a slight increase from 12-24 weeks, followed by a plateau between 24 weeks- 1 year (p<0.00004364, *see figure 3.6A*). The difference between pOFC and dA metabolism during NEC increases quadratically with age, with a more rapid increase from 1.5-24 weeks and a less dramatic increase from 24 weeks- 1 year (p<2.2×10^{-16}, see *Figure 3.6B).* The difference between dlPFC and dA metabolism during NEC increases in a cubic manner, with a sharp increase from 1.5 weeks to 12 weeks, followed by a minor decrease to 24 weeks, and then finishing with a slight increase to 1 year (p<2×10^{-16}, *see figure 3.6C).*

Discussion

In the first year of NHP life, the metabolic uptake of anxiety-related brain regions during exposure to NEC show distinct age-related changes. Overall, these data suggest dA, BST, and pOFC regions become less metabolically active during the experience of NEC as monkeys age from 1.5 weeks to 1 year, while dlPFC becomes more active during this period. Components of the extended amygdala, including the dA and BST, show similar developmental trajectories between 1.5 weeks and 1 year. These regions demonstrate a pattern of steep decrease in their NEC-related metabolism, with an apparent plateau as they approach 1 year. In contrast, the pOFC shows only a modest decrease during this period, and the dlPFC shows a dramatic *increase* in its metabolism during NEC. It is particularly interesting that these regions also display different levels of stability within individuals. While individual differences in threat-related metabolism of

the pOFC and BST show "excellent" and "good" stability, respectively, threat-related

metabolism of the dA and dlPFC do not seem to be particularly stable. It is notable that

these differences in stability do not seem to simply relate to magnitude changes across

development, as the dA and BST have similar trajectories but differ in their stability. The

regional differences in stability suggest the involvement of dA and dlPFC in the

processing of threat-related stress is changing over time, while the BST and pOFC

maintain a similar threat-related response within individuals across time. Taken

together, these findings suggest dynamic changes/patterns in distinct regions

associated with stress responses. Our data illustrate a shift from relatively equal

involvement of these subcortical and cortical regions in threat-related responses to

greater cortical than subcortical involvement by 1 year old.

As previewed in the introduction, [18]FDG uptake in the brain while at rest

undergoes significant change across this period due to the ongoing developmental

events occurring throughout the brain. As the brain continues to undergo rapid volume

and surface area expansion during postnatal development (Kim et al., 2020; Kovacs-

Balint et al., 2021; Malkova et al., 2006), regional brain metabolism follows a similar

pattern of increases across the cortex, with subcortical regions increasing first, followed

by increases in higher-order cortical regions (Harry T Chugani, 2018). In the present

study, we must consider that any observed differences in threat-related metabolism

during this early-life period may be partially influenced by the underlying developmental

changes in regional metabolism across the brain overall. We did not obtain baseline

[18]FDG-PET in this study, so we are unable to directly address how these underlying

changes in [18]FDG-PET metabolism may be influencing our threat-related findings. However, there are a couple of observations that increase confidence that we have captured individual differences in true threat-related metabolism during this period. First, the dramatic regional differences in glucose uptake at rest (H T Chugani & Phelps, 1986; Harry T Chugani, 2018) are observed mostly during the first year of human life, which roughly translates to the first 12 weeks of NHP life. This implies that the developmental baseline complications to our dataset would primarily be in the first 3 timepoints. Importantly, primary cortices have a notable increase by 2-3 months in humans, which corresponds to our first timepoint (~ 1-2 weeks in NHPs), and our testing expands beyond the period of significant baseline [18]FDG-PET development implicated by the literature. Finally, the distinct directions and growth shapes of the above described age-related trajectories suggest that regions are not universally increasing metabolism based simply on needs for ongoing developmental processes.

To further illustrate the differences between regional glucose uptake during NEC across development, we examined the age-related changes in the computed "deltas" between our regions of interest. As we are specifically interested in considering how increased functionality of the prefrontal cortices may contribute to the emergence of threat-related responses, and the engagement of the dA during these responses, we focused on deltas between the BST-, pOFC-, dlPFC- and dA metabolism. We found pOFC, dlPFC, and BST displayed greater NEC-related metabolism than the dA at 1 year compared to 1.5 weeks, while the shape of each delta's age-related trajectory was unique. The dlPFC-dA delta showed the greatest increase with age, while the BST-dA

delta showed the least. These delta measures reflect the relative engagement of these regions during stress exposure. As monkeys age, prefrontal and other frontal regions have increasing involvement during the experience of stress. Meanwhile, the components of the extended amygdala show smaller differences in total change across this period. Put another way, the subcortical components show similar relative threat-related metabolism across development, while cortical components are becoming more differentiated by 1 year. Together these delta data, along with the individual trajectories, demonstrate a shift from more equal limbic/prefrontal engagement at birth towards greater prefrontal metabolism during experience of threat at 1 year. To our knowledge, there have not been other studies characterizing the differences in subcortical and cortical threat-related [18]FDG-PET metabolism across early life development in this manner. The examination of these deltas may provide a unique approach for examination of how threat-related brain function is associated with threat-related responses within individuals.

As with the behavioral data, there may be concern that repeated exposure to this paradigm results in its loss of saliency and/or habituation of monkeys' responses. While the age-related decrease of dA and BST metabolism during this first year of life could be interpreted as supporting a habituation of brain responses to this paradigm, the dramatic increase in the dlPFC metabolism seems to directly refute that possibility. Certainly, if brain responses are habituating with the paradigm, it is not occurring across all of our regions of interest. Here our data have demonstrated dramatic changes to the metabolism in important anxiety-related regions across the first year of NHP life.

Importantly, regions differ from each other both in terms of their age-related changes and their stability within subjects across this period. To our knowledge, there are no other studies examining the early life changes in brain metabolism during stress exposure longitudinally in NHPs. Our findings present novel within-subject developmental trajectories of the changes in these responses over the first year of life. Of particular interest will be whether individual differences in these regions associate with individual differences in the expression of the trait-like measure Anxious Temperament (AT). These research questions will be explored in Chapter 5, and in the next chapter we will expand our understanding of the neural circuitry underlying threat-processing through the examination of fMRI connectivity at rest. While examination of the "deltas" above provides some insight into how differences between regional metabolism occur over this period, perhaps a better approach to investigating relationships between regions is through functional connectivity analyses with fMRI. We will explore the changes in temporal correlativity between the dA and the pOFC, dlPFC, and BST, to complement the findings using ^{18}FDG-PET imaging described above and to better understand how resting state brain dynamics develop during the first year of NHP life.

Chapter 4

The Development of Resting-State Dorsal Amygdala Functional Connectivity during the

First year of Nonhuman Primate Life

Introduction:

Significance and Rationale

Functional Magnetic Resonance Imaging (fMRI) is a useful methodological approach for exploring the underlying neural circuitry of threat-related responses and trait anxiety. Specifically, resting state (rs)- fMRI is a useful tool in both nonhuman primates (NHPs) and humans to examine how the dynamics of the brain while at rest associate with the expression of pathological anxiety. Neural circuit dynamics revealed by fMRI studies implicate potential targets both for the investigation of causal links between brain regions and expression of anxiety (i.e. use of DREADDs) and eventually for use in therapeutics such as TMS, or TiBS, which seek to alter brain functionality using a region-specific approach to ameliorate extreme pathological anxiety. Regarding interpretability, rs-fMRI is thought to be representative of stable set points in brain function that may reflect trait characteristics of circuitry (van den Heuvel & Hulshoff Pol, 2010). These trait circuitry characteristics may further associate with threat-related brain function or trait characteristics of threat-related responses. In this chapter, we describe the changes in resting-state signatures of anxiety-related brain regions during the first year of nonhuman primate (NHP) life.

The Utility of Functional Connectivity in Anxiety Disorders (ADs) Research

In the previous chapter, we describe distinct developmental trajectories for the NEC-related brain metabolism of subcortical (dorsal amygdala, dA; bed nucleus of the

stria terminalis, BST) and cortical regions (posterior orbitofrontal cortex, pOFC; dorsal lateral prefrontal cortex, dlPFC) involved in threat-related responses. To enhance our understanding of the changes to threat-related brain function postnatally, we are interested in describing the intrinsic functional connectivity between different anxiety-related brain regions at rest. While [18]FDG-PET measures a cumulative signal of regional brain metabolism over a ~30-minute period, fMRI measures relative Blood Oxygenation Level Dependent (BOLD) signal across regions over time. An elevated BOLD signal is reflective of a higher ratio of oxygenated to deoxygenated blood, which is interpreted as demonstrating greater activation. The collection of data with this time-series approach allows temporal correlation analyses to examine the "functional connectivity" between regions of interest (ROIs). Seed-based functional connectivity is one approach that examines the time course of BOLD signal pattern changes across the brain by computing, on a voxel-wise level, the correlation between each voxel's time course and the time course of the chosen seed (ROI). In these analyses, we produce 3-dimensional images of the brain, where each voxel represents its temporal correlation with the predefined seed. Strong functional connectivity between regions is thought to reflect greater coordination of function, whereas weak or low levels of connectivity are thought to implicate less functional coordination between these regions.

Given its significance in mediating threat-related responses, we have adopted an amygdala-focused approach to investigate the temporal correlations and resting functional dynamics with other brain regions. In our work, as well as in other studies (L J Gabard-Durnam et al., 2018; Laurel J Gabard-Durnam et al., 2014; Hamm et al., 2014;

Toazza et al., 2016), investigation of how individual differences in functional connectivity

between anxiety-related brain regions associate with individual differences in anxiety

responses have used whole amygdala or dorsal amygdala (dA) seeds. For example, rs-

fMRI analyses using a functionally-derived central nucleus of the amygdala (Ce) seed

found that humans and NHPs with higher levels of anxiety showed decreased functional

connectivity between the Ce and dlPFC (Birn et al., 2014a). Another study of NHPs

illustrated increased Ce-BST functional connectivity in association with increased AT

(Fox et al., 2018; Oler et al., 2012). Together these findings generally suggest that

pathological anxiety is associated with increased functional connectivity within the

extended amygdala, but decreased functional connectivity between the amygdala and

important regulatory regions such as the dlPFC. While this relationship has been

demonstrated in preadolescent monkeys (Birn et al., 2014b, 2014a), how these

relationships manifest in infant development is less clear. Many of the brain regions that

have significant functional connectivity with the amygdala at rest in mature individuals

are undergoing significant changes structurally (Teffer & Semendeferi, 2012) and

functionally (see data in prior chapter) during early infancy, and we are particularly

interested in how dA connectivity with different anxiety-related regions changes across

development.

Implications of Functional Connectivity in the Early-life Developmental Period

Until recently, the characteristics of the resting-state functional dynamics in

threat-related neural circuitry, and brain circuitry overall, during infancy have not been

well characterized. Over the past decade, the use of fMRI functional connectivity analyses in human and NHP infants has made great strides in enhancing our understanding of infant brain development. Studies of resting-state fMRI in human infants highlight that neonates show evidence of the anterior-posterior components of the Default Mode Network (DMN, considered the predominant network in the brain at rest), a strengthening of its components' connectivity across the first year of human life, and an achievement of adult-like topology by 1 year (Wen et al., 2019; H. Zhang et al., 2019). Also, in early infancy, there is evidence of basic functional connectivity patterns for the primary neural circuitry underlying the most basic of brain functions (Fransson et al., 2007; Wen et al., 2019). There has been less work specifically examining anxiety-related circuitry in this early life period (Gee, Gabard-Durnam, et al., 2013), though the strengthening of amygdala-frontal cortex functional connectivity (thought to be important in the regulation of adaptive anxiety expression) seems to continue from childhood through adolescence and adulthood, suggesting a particularly extended development of this network throughout life (L J Gabard-Durnam et al., 2018; Laurel J Gabard-Durnam et al., 2014).

NHPs are a useful model for longitudinal examination of anxiety-related circuitry across the lifespan. Initial studies of functional connectivity in monkeys demonstrate the measurability of functional networks throughout life under anesthesia and also, most importantly, demonstrate the presence of definable networks early in life (Rao et al., 2021). The data from these young monkeys under anesthesia further suggest that the developmental patterns of functional connectivity across development in NHPs are

similar to those seen in human infants. Specific exploration of the functional connectivity between anxiety-related brain regions during infant development remains relatively understudied. In this chapter, we examine within-subject longitudinal changes of resting-state fMRI across 5 timepoints by exploring the developmental trajectories of dorsal amygdala (dA) functional connectivity with posterior orbitofrontal cortex (pOFC), bed nucleus of the stria terminalis (BST), and the dorsolateral prefrontal cortex (dlPFC).

Aim of Chapter 4: *Describe the developmental trajectories of anxiety-related regions with fMRI-based connectivity measures at rest.* The early-life developmental characteristics of the primate anxiety circuit remain relatively unexplored; and because of the known role of the Ce in AT, the purpose of this aim is to characterize the development of dorsal amygdala functional connectivity with other components of anxiety-related network over the first year of life**.** We hypothesize that *the connectivity between the dorsal amygdala and prefrontal regions, such as the dlPFC and pOFC, will strengthen across the first 3 months of life, a time at which young monkeys have the capacity to adaptively regulate their threat-related responses.* Meanwhile, we predict that *the connectivity within the extended amygdala (i.e., between dorsal Amygdala and BST), will be present throughout early life and will not demonstrate age-related changes across development.*

Methods:

Study Timeline & Testing Design

Monkeys were followed longitudinally and periodically assessed for behavioral

and physiological characteristics of trait anxiety as detailed in Chapter 2 (*see figure 2.1).*

Echo planer Magnetic Resonance Imaging (MRI) was performed on all 35 subjects in

parallel with the five behavioral testing timepoints, providing functional brain data from

similar ages to investigate the developmental trajectories of resting brain connectivity in

anxiety-related neural circuitry. The average ages at MRI scans were: 19, 50, 92, 175,

and 374 days. In one subject, the functional MRI scan from the fourth timepoint was lost

due to technical difficulties during the scanning protocol. This subject was not included

in age-related longitudinal voxel-wise analyses (remaining n = 34). For ROI-based

analyses, this subject's missing time 4 measurement was replaced with an average

value for the ROI, computed from the other 34 subjects' time 4 measurements. No other

timepoints, or timepoints in any other subject, were dropped from the analyses.

Scanning Parameters and Image Processing

One week following each 30-minute NEC with ^{18}FDG-PET, monkeys were

scanned while under anesthesia to collect structural and functional brain imaging data

for examination of white-matter microstructure, myelination, and functional connectivity

(temporal correlations in BOLD signal) across this important developmental period. The

analytic processing of the structural- and myelin-related data, along with the

investigation of age-related changes in these modalities in this sample, can be reviewed

in detail in our recently published studies (Aggarwal et al., 2021; Moody et al., 2022). Here, we focus on the examination of individual differences in functional connectivity between important regions of the anxiety-related network using resting-state fMRI (rs-fMRI) scans. All ROI images are overlaid on a 592 subject population template (Fox, Oler, Shackman, et al., 2015) for anatomical reference.

At each MRI data were collected using a GE Healthcare 3T Discovery MR750 scanner equipped with a custom coil. Monkeys were weighed, initially anesthetized with ketamine (15 mg/kg, IM), and administered atropine sulfate (0.04 mg/kg, IM) and ketoprofen (5 mg/kg). They were then intubated and positioned inside the MRI scanner in the custom 8-channel receive array for NHP imaging with a built-in stereotactic head frame (Clinical MR Solutions). Anesthesia was maintained during scanning with isoflurane (<2% isoflurane/O2) while heart rate and oxygen saturation were monitored. Isotonic fluids were administered, if necessary, to maintain blood glucose levels before, during, or after scanning. Whole brain, 3D T1-weighted images were acquired and reconstructed with 0.625 mm isotropic spatial resolution (MPnRAGE, Kecskemeti et al., 2016). Functional MRI was obtained using 2D T2*weighted echo-planar image (EPI) prescription with the following parameters: TR/TE = 2100/25 ms, Flip angle = 70 degrees, FOV = 100x100x100 mm, Matrix = 64x64x38 voxels, voxel size = 2.2 X 2 X 2.2 mm. Volumes were acquired every 2.1 seconds, with a total of 38 individual slices of 2.2 mm thickness for 450 timepoints.

The anatomical reference template was created through co-registration of structural MRI scans in ANTs (Avants et al., 2009). Briefly, each subject's structural MRI

scans from each timepoint (T = 1-5) were co-registered to create 35 within-subject, across time templates. These 35 individual-subject longitudinal templates were then co-registered together to create an overall population template. The time-averaged population template was then warped into a standard NHP template constructed from 592 animals (Fox, Oler, Shackman, et al., 2015). Details on this process can be found in our recently published work (Aggarwal et al., 2021; Moody et al., 2022). This template was used as the anatomical reference for the rs-fMRI data, as well as for the [18]FDG-PET data (detailed in Chapter 3). The 592 subject template space was also used to delineate population-derived seed masks for functional connectivity analyses.

The 4D time-series volumes from each subject were reconstructed into single files with 450 time-linked volumes and fit to a field map. Following reconstruction, the EPI data were processed in AFNI (Cox, 1996) using a standard pipeline (Birn et al., 2014b). Data were corrected for B0-field distortions, orientation, motion artifacts, physiological noise, and slice-timing differences. Each subject's image for each timepoint was then warped to their transformed subject template using warps derived from the creation of the population template (see above), followed by segmentation to produce cerebrospinal fluid (CSF), white matter (WM), and grey matter (GM) masks. Finally, scaled maps were subjected to a nuisance regression to address any remaining artifacts, spatially smoothed (4mm FWHM Gaussian), and bandpass filtered (0.01-0.1 Hz). Each subject's data at each timepoint was visually inspected to ensure the quality of processing steps and the quality of the final images to be used for subsequent functional connectivity analyses.

Selection and use of Seeds for Functional Connectivity Analyses

We used a seed-based approach for our resting-state functional connectivity analyses, focusing on neural circuitry relevant to the production, regulation, and expression of anxiety. Given the rapid ongoing structural changes in the cortex during the immediate postnatal period of infant development, it is important to consider the potentially dramatic differences in the underlying brain structure between timepoints. To account for these differences in the voxel-wise computation of 3D functional connectivity maps, inverse warps were developed from the co-registration process of the population template construction. These subject- and timepoint-unique warps were then applied to each seed during the computation process for each subject, at each age. ROIs were inspected in native space to ensure proper translation. This gives us confidence that the subsequent seed-based functional connectivity maps account for individual differences in underlying anatomy.

Given the dramatic differences in both brain size and discreteness of brain regions across this developmental sample, we chose to use a hand-drawn dorsal amygdala seed instead of an atlas-defined "Central Nucleus" seed. There is limited study on the structure and/or presence of subnuclei in the amygdala during early infant development (Chareyron et al., 2012; Medina et al., 2023; Scott et al., 2016). The findings bring into question the validity of using a "Central Nucleus" seed during earliest developmental timepoints. Therefore, we chose to use a structurally defined dorsal amygdala seed, originally hand-drawn on the 592-population template (Fox, Oler, Shackman, et al., 2015). This dorsal Amygdala (dA) region is comprised mostly of Ce,

but was subsequently adjusted by hand to incorporate a larger area of coverage (*see*

figure 4.2), which may help account for major structural differences across these early

ages. A posterior cingulate cortex seed, derived from a rhesus monkey brain atlas

(Calabrese et al., 2015) was used for examination of the default mode network.

Description of Functional Connectivity Analyses

Functional connectivity analyses were performed by extracting the time series for

our seeds (dA, and posterior cingulate), and running whole-brain temporal correlations.

Subsequent connectivity values were Fischer-z transformed. To visualize the

components of the Default Mode Network (DMN), we conducted voxel-wise functional

connectivity analyses using an anatomically defined posterior cingulate seed (*see*

Appendix A.2). We computed group-averaged posterior cingulate connectivity maps

within each timepoint to visualize and inspect the DMN components at each age. We

further tested for any developmental effects within the DMN with voxel-wise analyses

testing the effects of postnatal age, while controlling for gestation length and sex, on the

functional connectivity of the posterior cingulate. Visualization of the DMN at each age,

along with age-related changes can be found in the Appendix A.2. Most importantly, the

temporal and anterior poles of the DMN were present at every age, suggesting the

capability of our measure to detect meaningful relationships regarding basic circuitry.

We explored anxiety-related networks by conducting functional connectivity

analyses with a dA seed. Individual subject connectivity maps in each timepoint were

visually inspected (at significance threshold p<0.005) for error or outliers. After some

minor corrections, no subjects or timepoints needed to be excluded from subsequent analyses. Any variable with repeated measurements was mean centered within-subject, while gestation length and sex were mean centered across the entire population. Variables with a single measurement were mean centered across the entire group.

We took an ROI-based approach to explore age-related changes in amygdala functional connectivity, focusing on regions previously implicated as important for anxiety regulation neural circuitry. Using 3D masks defined by and derived from the Paxino's rhesus monkey brain atlas (Calabrese et al., 2015) co-registered to the NHP population template, we extracted average functional connectivity in the following regions for the dorsal amygdala seed: BST, pOFC (BA14,ProIso), and dlPFC (BA46 and BA9-46). All visualizations of seeds, masks, and voxelwise results are overlaid on the study cohort -592 structural population template.

Statistical Analyses for Evaluation of Age-Related Developmental Trajectories

All statistical analyses were conducted in R. We used within-subject linear mixed effects models (Bates et al., 2015) to investigate age-related changes to amygdala functional connectivity in our ROIs, while controlling for gestation length, sex, and including a random intercept. The same approach for testing and determining best developmental growth shape was used as described in Chapter 2 for behavioral data. We tested linear, logarithmic, quadratic, cubic, and *a priori* (details in Chapter2) models for describing within-subject changes with increasing age. Akaike and Bayesian Information Criteria were used to determine which growth shape best fit the data.

Similar to what we observed in prior chapters, we did not find that inclusion of a random slope improved the fit or performance of our models for any region of interest. We used the Bonferroni method to correct for multiple comparisons. With three regions of interest, our threshold for significance of within-subject age-related trajectories is adjusted to p=0.02. All reported developmental trajectory findings below pass this corrected threshold, and can be interpreted as highly significant. With 10 between-timepoint pairwise comparisons, our adjusted threshold for significance is p<0.005. We still report correlations with a p<0.05 as trending, but these should be considered exploratory and interpreted with caution.

To explore whether individual differences in the functional connectivity between dA and the BST, pOFC, dlPFC predicted individual differences in NEC-related FDG-PET metabolism of these regions, we computed timepoint centered values of each variable of interest. By adjusting values to be centered within each age of testing, we account for magnitude differences across different ages. This allows for testing of main-effect associations between functional connectivity and FDG-PET measures, as well as for interactions of these relationships with age. With 6 comparisons in these analyses our adjusted threshold for significance is p=0.0083. We report findings less than p=0.05 as trending associations.

Results:
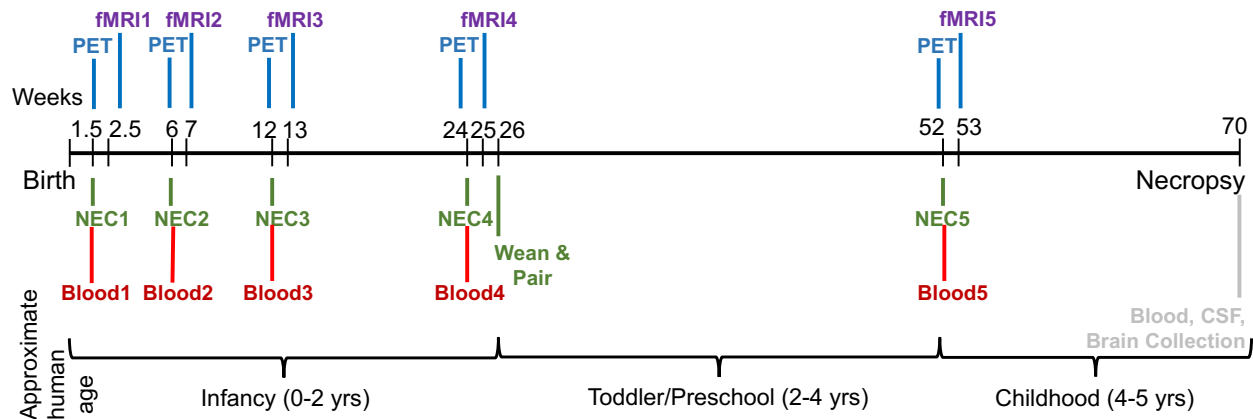
Figure 4.1 – full study timeline, fMRI testing timepoints are bolded with purple text
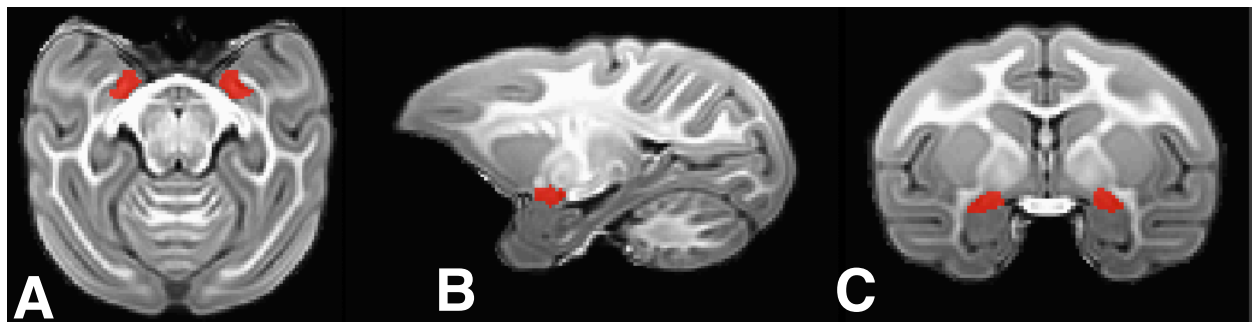
Figure 4.2 – horizontal (A), sagittal (B), and (C) coronal views of the dorsal amygdala seed used for functional connectivity analyses

		Linear	Logarithmic	Quadratic	Cubic	*a priori*
dA-dlPFC	AIC	-771.8899	-776.2787	-784.7248	-791.4897	-789.3364
	BIC	-752.9012	-757.29	-762.5713	-766.1714	-760.8534
dA-pOFC	AIC	-617.846	-615.7985	-616.0772	-614.1043	-613.1435
	BIC	-598.8573	-596.8098	-593.9237	-588.786	-584.6604
dA-BST	AIC	-335.2116	-338.2331	-336.1618	-334.5468	-333.5504
	BIC	-316.2229	-319.2444	-314.0083	-309.2285	-305.0674

Table 4A – AIC/BIC values for different age-related growth curves. Best fit AIC/BIC values are highlighted

	dlPFC-dA connectivity	pOFC-dA connectivity	BST-dA connectivity
ICC (3,k)	.388	.373	0.113
p-value	0.026	0.032	.31

Table 4B – ICC performance and corresponding p-value for two-way mixed effects intraclass correlation analyses for consistency

Dorsal amygdala-BST resting state functional connectivity increases with aging
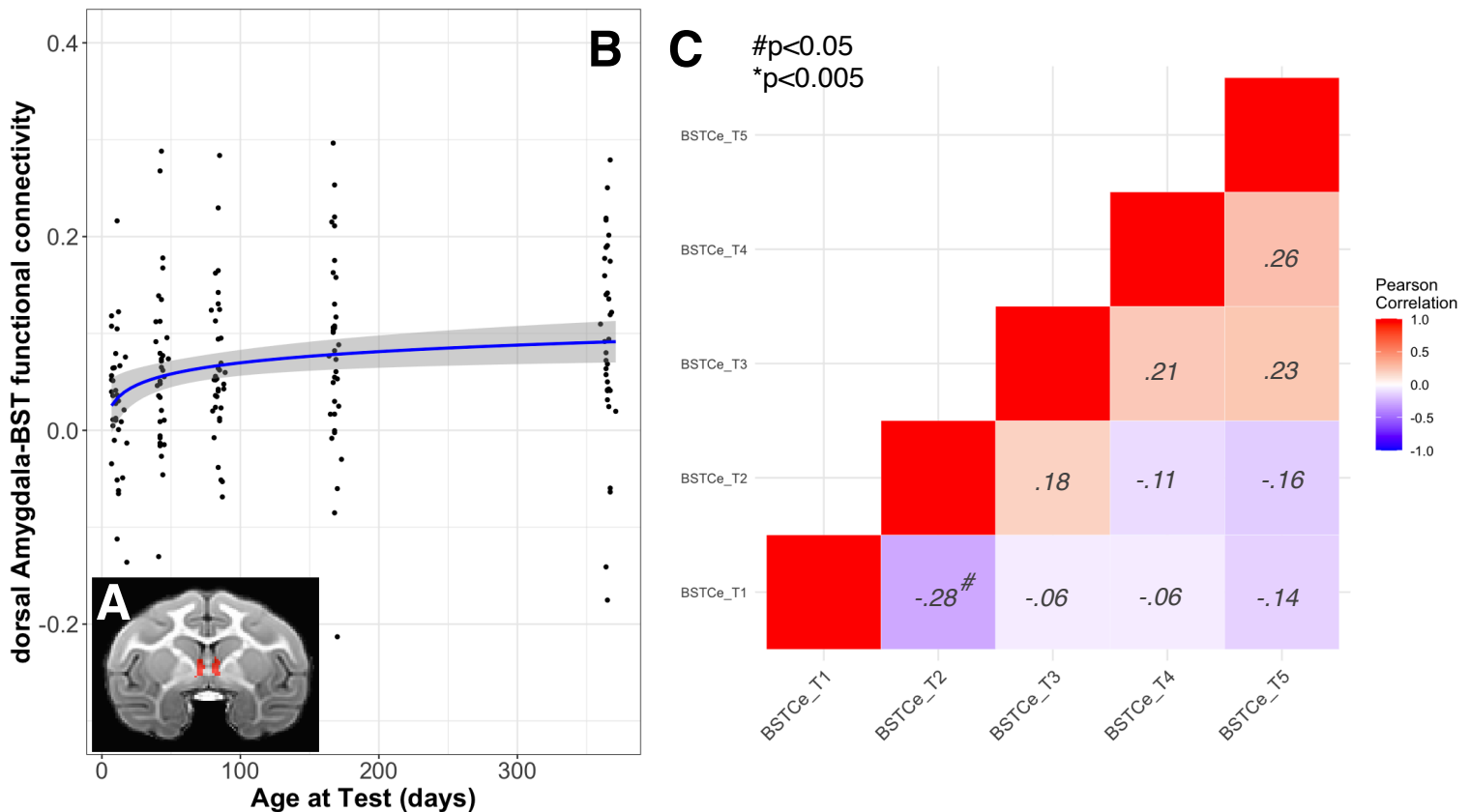
Figure 4.3 – A) coronal view of BST mask, B) within-subject developmental trajectory depicting best fit logarithmic age-related changes, p<0.0009472, C) pairwise correlations exploring between timepoint relationships

Across the first year of life, we observed a significant, though modest, logarithmic increase within-subjects in the functional connectivity between the dorsal amygdala and the BST (p<0.0009472, *See figure 4.3, see Table 4A),* with the most rapid change occurring from 2.5-7 weeks, followed by a plateau to 1 year of age. Regression analyses examining stability of individual differences across timepoints did not identify significant correlations between any timepoints (*r*'s ranging from -0.28 to 0.26). ICC(3,k) performance on BST-dorsal amygdala connectivity was poor (.113, p = .31) indicating low stability of individual differences in BST-connectivity within subject.

Dorsal Amygdala- pOFC resting state functional connectivity increases with aging
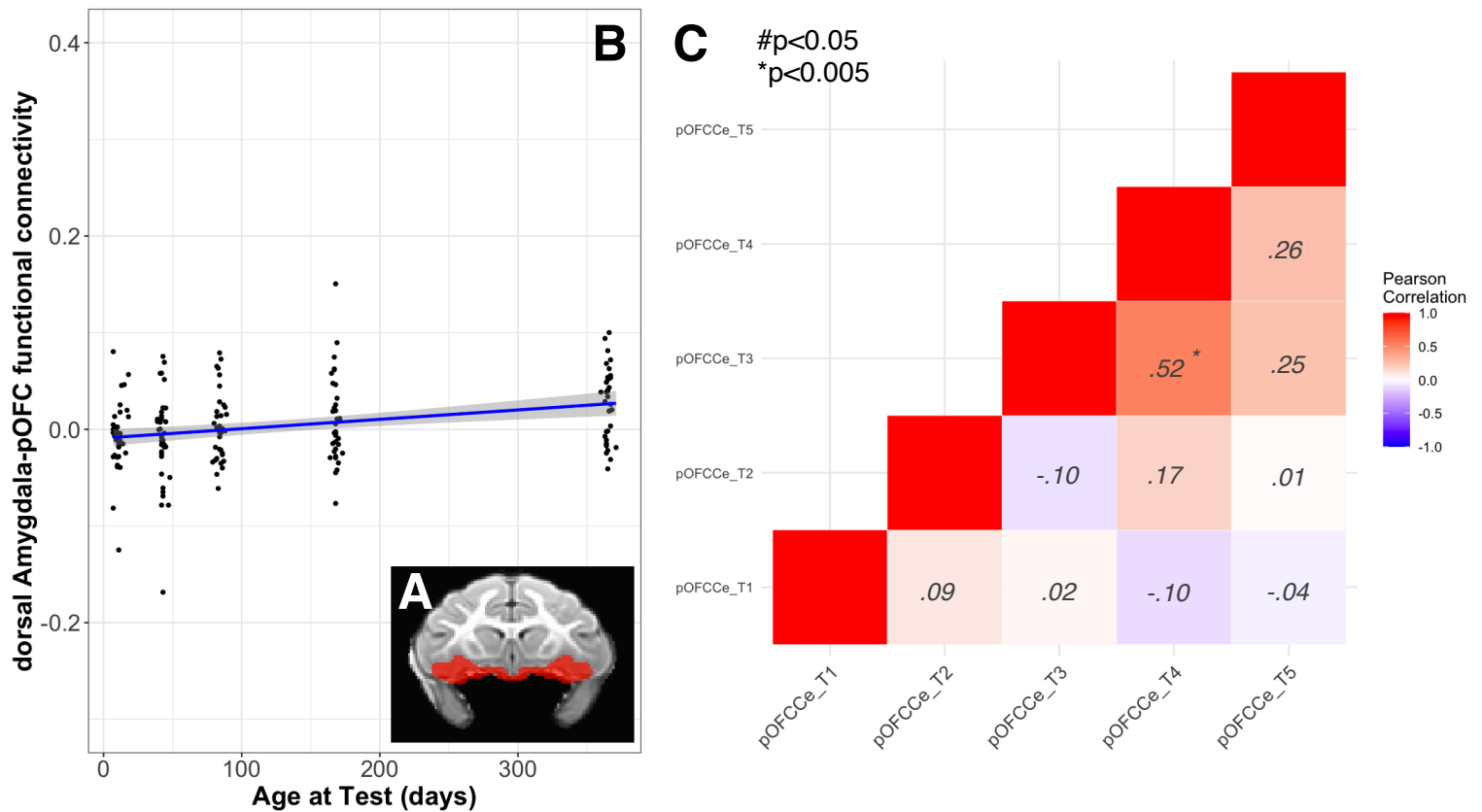
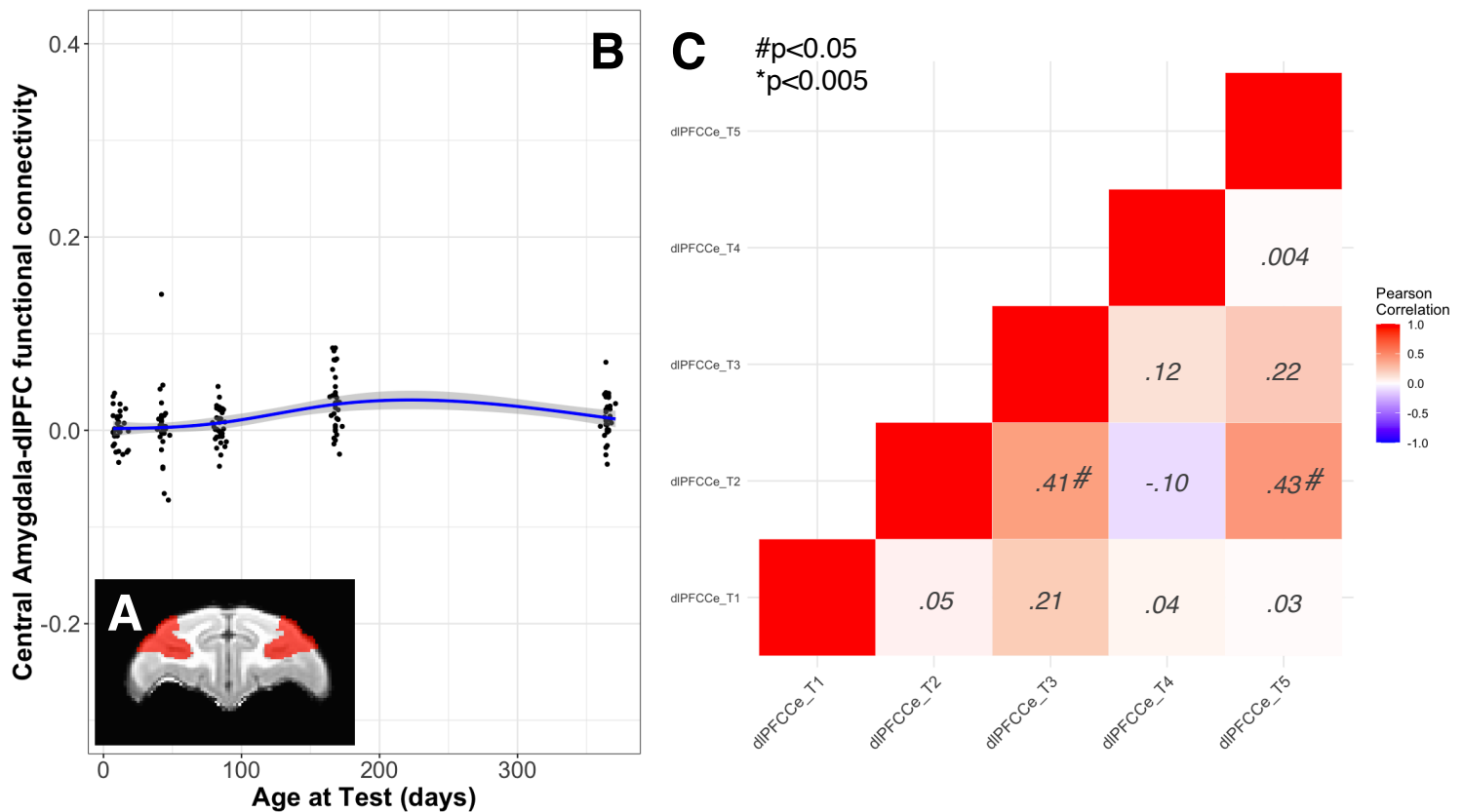*Figure 4.4 – A) coronal view of pOFC mask, B) within-subject developmental trajectory of dA-pOFC functional connectivity, depicted with linear best fit, p<0.0000233, C) pairwise correlations examining relationships between expression levels across timepoints*

Within subjects, while aging from 2.5 weeks to 1 year, we observed a significant, slight, linear increase in the functional connectivity between dorsal amygdala and the pOFC (p<0.0000233, *See figure 4.4, See Table 4A*). Regarding stability of individual differences, ICC(3,k) performance was poor (.373, p=0.032, *Table 4B*). Regression analyses across timepoints found mostly weak correlations (*r*'s ranging -.10-.26), with the exception of a positive correlation between T3 and T4 (r = .52).

Dorsal amygdala – dlPFC resting state functional connectivity changes with aging

Figure 4.5 – A) coronal section depicting dlPFC mask, B) within-subject developmental trajectory of dA-dlPFC functional connectivity, depicted with best fit cubic age-related changes, p<0.000000404, C) pairwise correlations of relationships between timepoints

Within subjects over the first year of life, we observed a slight increase in the functional connectivity between the dorsal amygdala and the dlPFC. The best growth shape for age-related changes was determined to be cubic (*See table 4A),* with a slight increase from 2.5-13 weeks, a more rapid increase from 13-25 weeks, followed by a slight decrease from 25 weeks to 1 year (p<0.000000404, *See figure 4.5).* For our assessment of stability in individual differences, ICC(3,k) performance was poor (0.388,p = 0.026, *see Table 4B*) and regression analyses across timepoints revealed weak to moderate correlations (*r*'s range: .004 - .43,).

The relations of NEC-related metabolism and dA functional connectivity across subjects
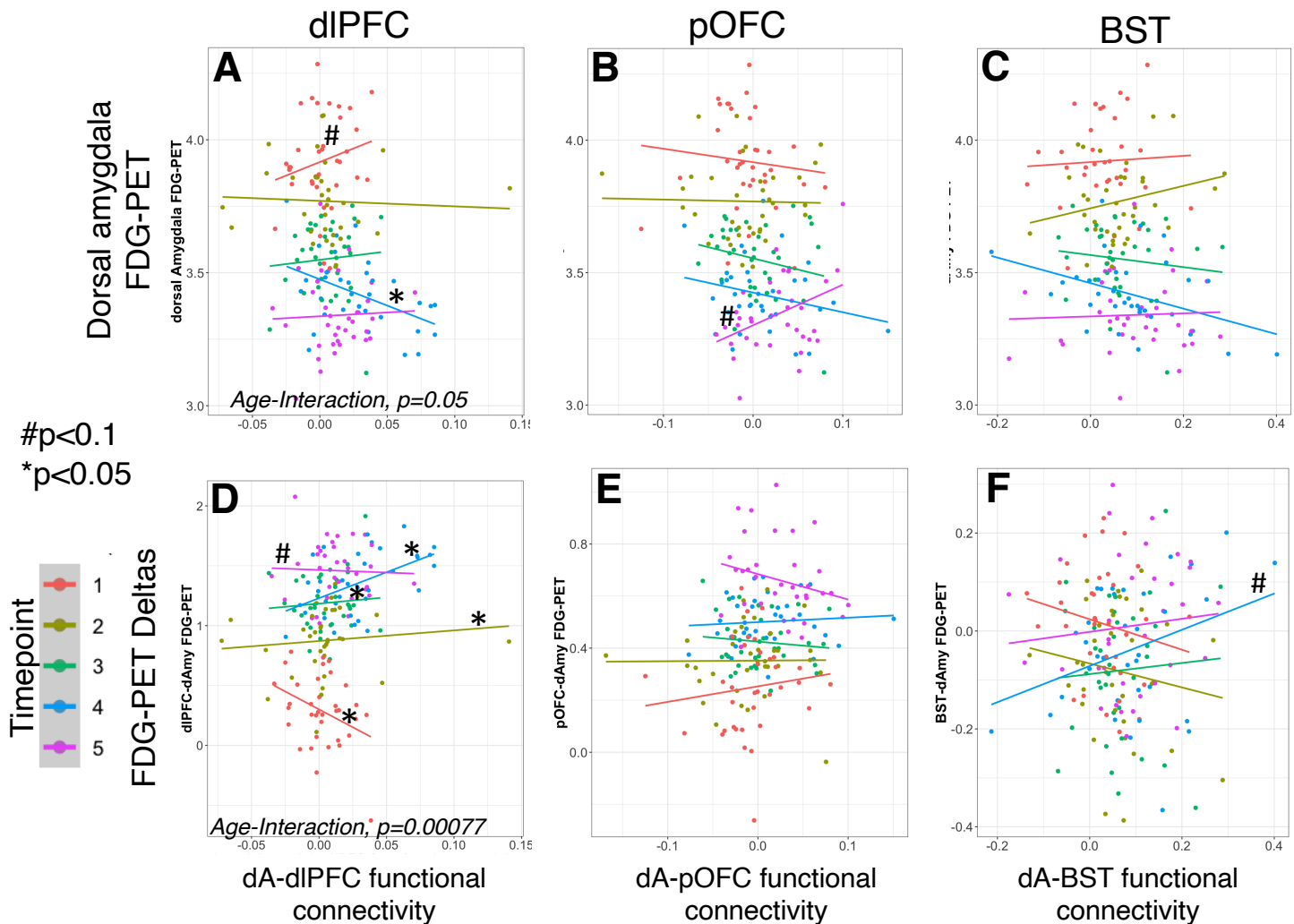
Figure 4.6 – depictions of the associations between functional connectivity of A) dA-dlPFC and dA NEC-related metabolism, of B) dA-pOFC and dA NEC-related metabolism, of C) dA-BST and dA NEC-related metabolism, of D) dA-dlPFC and the difference in dlPFC & dA NEC-related metabolism; of E) dA-pOFC and the difference in pOFC & dA NEC-related metabolism, and of F) dA-BST and the difference between BST & dA NEC-related metabolism

When looking for associations between the dA metabolism and functional

connectivity between the dA and the previously selected regions, BST, pOFC, dlPFC,

we used a statistical model that incorporates age as interactive term. While we did not

find any significant main effects, we did find a significant interaction between dA- dlPFC

functional connectivity and age as predictive of NEC-related dA metabolism (*see figure*

4.6A, p=0.05). At the youngest ages (red), greater functional connectivity between dA and dlPFC was significantly associated with greater dA threat-related metabolism (p=0.07). With increasing age, this relationship switched direction, with greater dlPFC-dA functional connectivity predicting less dA threat-related metabolism (Within T4 associations, p=0.02). We found no main effects or age-interaction for relationships between dA-pOFC (main-effect, p=0.55; age-interaction, p=0.11) and dA-BST (main-effect, p=0.98; age-interaction, p=0.16) and dA metabolism (*see figure 4.6B and 4.6C).*

　　We next explored the difference in metabolism between the dA and these regions as a measure that might be more relevant to individual differences in resting state functional connectivity between dA and these regions. No significant main effects were observed. However, we found a significant interaction between dA-dlPFC functional connectivity and age, such that we found dA-dlPFC functional connectivity to changes its relationships with the difference between dA and dlPFC metabolism with increased age (p=0.000774, *see figure 4.6B*). At youngest ages, greater functional connectivity between dlPFC-dA was associated with less of a difference between dlPFC and dA metabolism (within T1 association, p=0.022). As monkeys age, this relationship switches direction, such that greater functional connectivity between the dlPFC and dA is associated with a greater difference between the metabolism of these regions (within T2 association, p=0.02; within T3 association, p=0.03; within T4 association, p=0.007, within T5 association, p=0.06). We did not find any main effect or age-interaction associations between dA-pOFC and dA-BST functional connectivity and the differences

in dA and pOFC (main-effect, p=0.39; age-interaction, p=0.53) and dA and BST NEC-related metabolism (main-effect, p=0.41; age-interaction, p=0.21).

Discussion:

As monkeys age from 2.5 weeks to 1 year, the functional connectivity of the dorsal amygdala (dA) with the BST, pOFC, and dlPFC generally shows an increase with age. However, the shape of the age-related changes for each region's connectivity with the dA were different. The BST shows its most rapid change earliest in development, the pOFC displays a consistent and gradual change, while the dlPFC shows a later and directional shift in its trajectory. These data suggest an overall age-related strengthening in the connectivity within the extended amygdala, and also between the dA and important prefrontal components, likely supporting the regulation of the amygdala and/or the expression of anxiety. While these overall increases in functional connectivity occur, there is little stability within individuals across this developmental period. This may be due to the inherent increased variability of fMRI functional connectivity data and/or noise in the resting-state fMRI measure. The overall increases in functional connectivity are bolstered by the findings of global increases to structural connectivity in this same cohort (Aggarwal et al., 2021). It is important to note that the existence of structural connections between two regions does not necessarily directly translate to functional connectivity between them. However, the significant changes that have been observed in these same animals in relation to white matter integrity across the brain during development likely facilitates more effective communication between

distal regions, resulting in stronger functional connections between them. In particular, the increase in myelination observed in the uncinate fasciculus (white matter tract connecting pOFC & amygdala) could be contributing towards the improved functional connectivity observed between the dA and pOFC with development. Future work can test this relationship to more specifically explore the associations between functional and structural connectivity in this development cohort.

Studies in human and NHP infants demonstrate that during development of neural circuitry, local connections within neural circuits strengthen first, after which connections are established with more distant regions. Studies examining functional connectivity across the brain show that in early life, functional connectivity increases amongst local, or between proximal, regions first, followed by increases in functional connectivity between more distal regions (Rao et al., 2021; Wen et al., 2019; H. Zhang et al., 2019). Some functional connectivity between distant regions of the brain is already present at birth (De Asis-Cruz et al., 2015), though evidence shows distant connections undergo significant strengthening with continued development (Fransson et al., 2007; Wen et al., 2019). Here, using a seed-based approach, our data follows this same pattern. In relation to the dA, we observed the most rapid increase from 2.5-7 weeks in the dA-BST functional connectivity. Meanwhile, connectivity between the dA and dlPFC, the dlPFC being the most distal region, undergoes the greatest changes in its dA connectivity towards the end of the first year. In contrast, the pOFC-dA connectivity shows a gradual increase across the first year. These findings align with the literature describing changes in functional connectivity in early life; there are general

increases in the functional coordination between core components of networks, although different components may have different phases of development. The connectivity between the dA-BST, the extended amygdala, matures earlier, followed by a later maturation of the functional connectivity between the dA with frontal regions, a process that likely extends beyond our period of study.

A unique feature of this study cohort is the longitudinal, parallel collection of two different types of functional brain imaging (FDG-PET during threat exposure, rs-fMRI) across a period with dramatic brain development. This provides a unique opportunity to test the cross-modality associations between these two different methods, one using fMRI to assess measures of functional connectivity, and another using FDG-PET to assess threat-related metabolic activity. We thought it was particularly interesting to examine the difference in metabolism between two regions as a potential correlate of resting-state functional connectivity. To our knowledge, the relation between these two parameters of brain activity has not been systematically examined. We found no relationships between individual differences in threat-related metabolism of the dA, or in the difference between dA and BST or dA and pOFC metabolism, in association with the functional connectivity between these regions. We did, however, find significant interactions between dlPFC-dA functional connectivity and age as it predicts dA metabolism, and the difference between dlPFC and dA metabolism. This demonstrates that as monkeys age, the relationship between functional connectivity of the dlPFC-dA and the metabolism of these regions/delta changes its direction. It is curious that we find associations between our functional imaging approaches for some regions and not

others, but this is still somewhat consistent with prior work from our lab. We have previously shown, in older animals, dlPFC-Ce functional connectivity to be predictive of Ce metabolism (Birn et al., 2014b, 2014a), which is generally consistent with the age-related interaction we observe here. Additionally, in another study of primates, we did not find a significant relation between BST-Ce connectivity and BST metabolism (Fox et al., 2018; Oler et al., 2012), which is also consistent with our current findings. In fact, for Ce-BST connectivity and BST metabolism, while both were predictive of AT in a large sample of monkeys (n = 378), each imaging modality accounted for different variance in AT (Fox et al., 2018).

Here our data illustrates the general increases in functional connectivity both within the extended amygdala and with its more distal regulatory components (pOFC, dlPFC), while also demonstrating unique developmental age-related trajectories for each regions' connectivity with the dA. The stability of these measures is somewhat poor. These data, in conjunction with the NEC-related FDG-PET data, demonstrate the developmental trajectories of both threat-related and resting-state brain function during the first year of life in rhesus monkeys. Alongside these alterations, we have also described the dramatic age-related changes in the threat-related responses in these same individuals. These changes in brain function may be associated with the changes observed in trait characteristics of anxiety during this same period. With an understanding of how anxiety-relevant brain regions change during early life, we can begin the exploration of how individual differences in brain function associate with individual differences in AT across this period of significant development.

Chapter 5

Exploring Relationships between the Individual Differences of Trait Anxiety and of

Threat-Related or Resting-State Brain Function

Introduction:

Thus far, we have described the developmental trajectories of threat-related responses, threat-associated brain metabolism, and resting-state functional connectivity between threat-related regions. Our age-related findings for each of these distinct measures provide novel insights into how threat responses and brain function in threat-related regions are changing within individuals across the crucial postnatal period of development. As monkeys age from birth to one year, they show increasing levels of adaptive threat-related behaviors during exposure to No Eye Contact (NEC), a shift towards greater prefrontal metabolism during experience of threat, along with general increases in the prefrontal functional connectivity of the dorsal amygdala. With this longitudinal cohort of monkeys, our findings illustrate that the behavioral development of adaptive threat responses occurs in parallel with the ongoing development of neural circuitry. Our age-related trajectories suggest a developmental shift, such that by 1 year of age monkeys exhibit mature anxiety-related responses with concomitant developmental changes in the neural circuitry that underlies these responses. With the detailed characterization in this cohort, we have established an excellent framework for the examination of adaptive and maladaptive threat responses over the course of early development. In high AT preadolescent monkeys, and children with ADs, there are alterations in both the functional and structural components of the neural circuitry involving prefrontal regulation of subcortical structures such as components of the extended amygdala (Birn et al., 2014b; Tromp, Williams, et al., 2019). Given our data demonstrating developmental changes in both adaptive threat-related responses and

limbic-prefrontal neural circuitry during early life, we focus on an understanding of how individual differences in brain function relate to individual differences in AT across this critical period. In this chapter, we explore how threat-related metabolism in anxiety-related brain regions, as well as dorsal amygdala functional connectivity with prefrontal regions, associate with individual differences in AT in NHPs across the first year of life.

Aim of Chapter 5: *Characterize how individual differences in extended amygdala and prefrontal brain function relate to individual differences in trait anxiety across the early life developmental period.* We hypothesize that *the threat-related metabolism in the extended amygdala (BST, Ce) across the first year of life will be associated with AT, however, metabolism in prefrontal cortical regulatory regions (dlPFC, pOFC) will only predict individual differences in AT towards the end of the first year.* We also predict that *at younger ages fMRI-based functional connectivity between dA and BST will be significantly correlated with the expression of AT, whereas it will not be until near the end of the first year of development when significant relations between dA-dlPFC and dA-pOFC connectivity and AT emerge.*

<u>Methods:</u>

All data for the following analyses were prepared and manipulated as described in Chapter 2 (Trait-like anxiety responses), Chapter 3 (^{18}Flurodeoxyglucose – Positron Emission Tomography), and Chapter 4 (resting-state functional Magnetic Resonance Imaging). As age-related developmental trajectories for our variables of interest have

been previously described, the statistical analyses in this chapter are focused on exploring main-effect and age-interaction relationships between functional brain imaging measures and anxiety-related responses. Given the absence of within-subject slope differences across the population for both behavioral and brain imaging variables of interest, we chose to examine associations and interactions of these variables while considering only magnitude differences between timepoints within subjects. To adjust for these age-related magnitude differences across all variables, we adjusted our longitudinal variables by centering them around the mean within each timepoint/at each age of testing. To correct for multiple comparisons, we used the Bonferroni method to adjust our p-value threshold. With four ROIs (dorsal amygdala (dA), bed nucleus of the stria terminalis (BST), posterior orbitofrontal cortex (pOFC), dorsal lateral prefrontal cortex (dlPFC), our adjusted p-value threshold for 4 comparisons is p = 0.0125. While several findings reviewed below would not pass multiple comparison correction, we still discuss them in any case as we are working within a small population, and the effect sizes of the findings we are trying to replicate are relatively small. Given the potentially small changes in our small study cohort, we don't want to miss relationships that we may not be fully powered to find in this small population. We use a threshold of p<0.01 for significant findings and a threshold of p<0.1 for reporting trends.

Results:
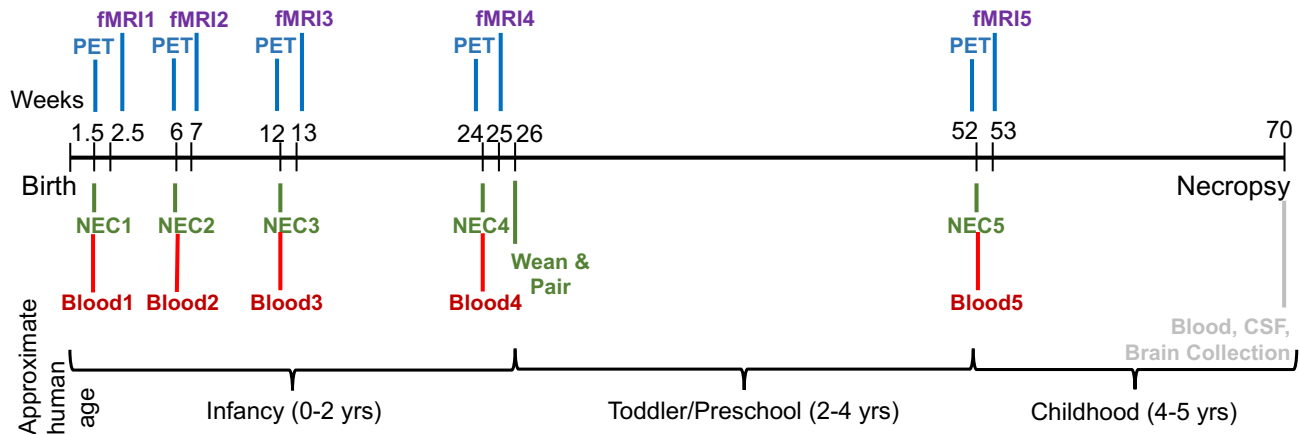
Figure 5.1 – Full project timeline, depicting parallel fMRI and NEC with FDG-PET

Threat-related metabolism in the extended amygdala in association with AT

When examining the relation between dA NEC-related metabolism and AT, there was no main effect of dA metabolism (p=0.8) and no interaction with age (p=0.95). For BST, we observed a trend for a main effect (p=0.061) such that increased NEC-related metabolism was associated with increased AT (*see figure 5.2A*), and no interaction with age (p = 0.43). Taken together these findings provide some support for the involvement of the extended amygdala in AT over the first year of life as the relation between BST metabolism with AT trends in a positive direction.

Threat-related metabolism in the prefrontal cortex in association with AT

We observed no main effect between pOFC metabolism and AT (p= 0.74). We did find a trend for age-related interaction with AT. With maturation, at the one-year assessment, we found that less pOFC metabolism predicted higher AT (p<0.08). When examining the relation between NEC-related metabolism in the dlPFC and AT, we
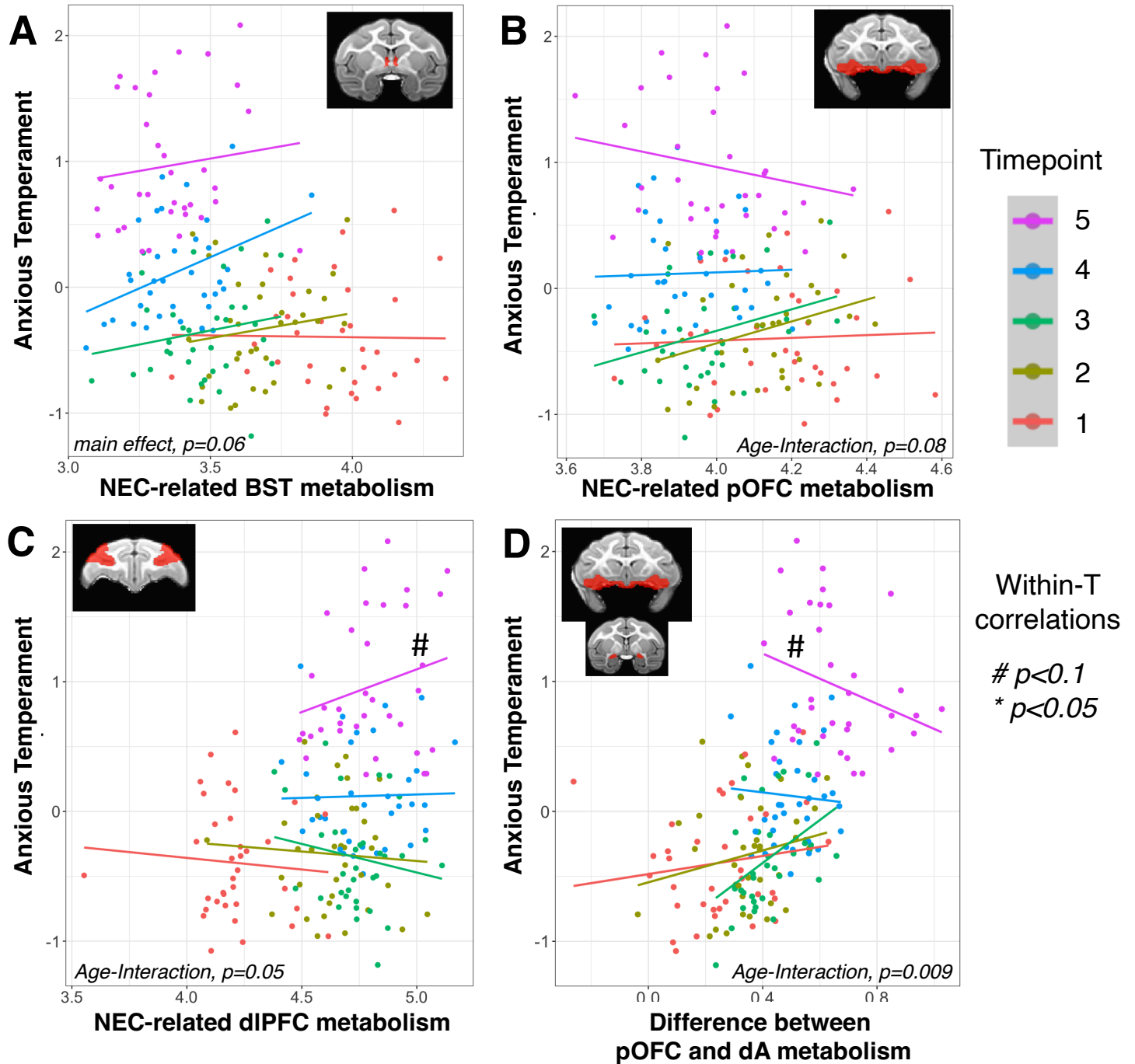
Figure 5.2 – associations between NEC-related brain metabolism and AT; A) NEC-related BST metabolism shows trend for prediction of AT across ages (main effect, p=0.06); B) pOFC metabolism shows trend for age-interaction in prediction of AT (interaction, p=0.08); C) dlPFC metabolism shows trend for age-interaction (p=0.05), trend for within T5 association (p = 0.07); D) difference between pOFC and dA metabolism show significant age interaction (p<0.009), trend for within T5 association (p=0.06)

observed no main effect. However, we did observe an age-related interaction (p=0.05, *see figure 5.2B),* such that dlPFC metabolism did not predict AT across the first 4 assessments up to 6 months of age, but at 1 year of age greater dlPFC metabolism was moderately associated with higher AT (within-T5 association, p = 0.07). Together, these findings suggest that the associations between pOFC and dlPFC with AT are occurring during the later maturation phases and can be detected at 1 year of life. It is noteworthy that the associations with AT are in opposite directions, such that at 1 year of age, pOFC metabolism is negatively correlated with AT, whereas dlPFC metabolism is positively correlated with AT.

The differences between PFC and dA threat-related metabolism in association with AT

We did not find a main effect of the difference between pOFC and dA metabolism in the prediction of AT. However, we found a significant interaction with age as it predicts AT (p<0.009, *see figure 5.2C*), with the difference between the pOFC and dA having no predictive relationship with AT at the younger ages (1.5 weeks – 6 months), eventually shifting, such that at 1-year smaller differences between pOFC and dA metabolism predicted higher AT (within T5 association, p = 0.06, *figure 5.2C*). There was no main effect when examining the difference in dlPFC and dA metabolism in relation with AT (p=0.3), or age-interaction. The finding at 1 year of age, where less of a difference between pOFC and dA metabolism is associated with higher AT, and a greater difference is associated with lower AT, suggests the possibility that this

difference measure reflects the regulatory capacity of the pOFC in relation to dA

metabolism.

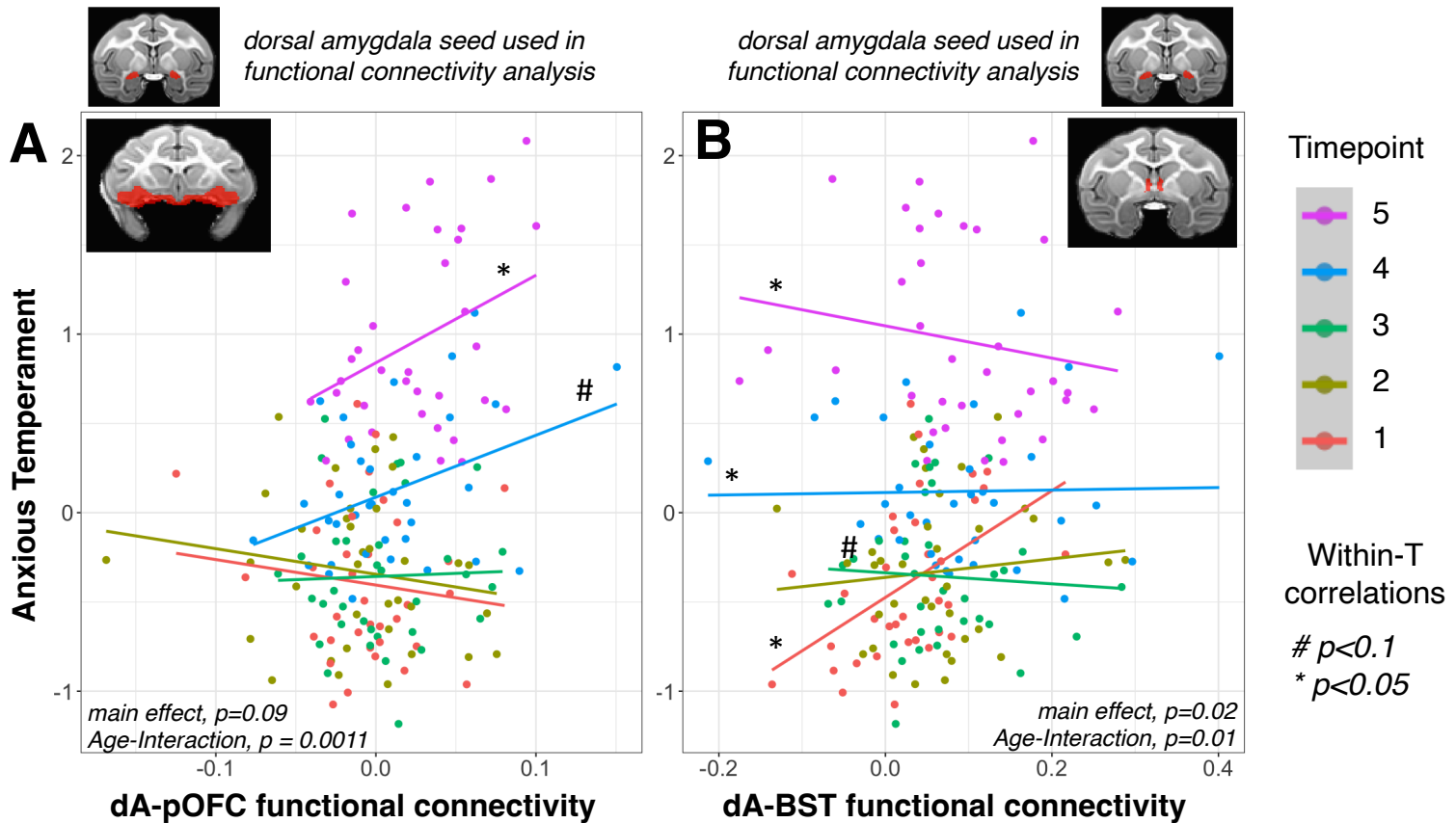Dorsal amygdala functional connectivity in association with AT

Figure 5.2 – Associations between dA- functional connectivity and AT, A) dA-pOFC functional connectivity shows significant age-interaction in prediction of AT (p=0.0011), trend for within T4 (p=0.07) and within T5 (p = 0.03); B) dA-BST functional connectivity shows significant age-interaction in predict of AT (p = 0.01), trend for within T1 (p=0.03), within T4(p=0.049), and within T5 (p=0.02) associations.

When examining the relationship between dA-BST functional connectivity and

AT, we found a trend for a main effect such that overall lower dA-BST functional

connectivity was associated with higher AT (p=0.02, uncorrected). We also found a

significant age-related interaction (p=0.01, corrected), with increased dA-BST functional

connectivity at 2 weeks (within-T1 association, p = 0.03) being associated with higher

AT, while at 24 weeks (within-T4 association, p=0.049) and 1 year (within-T5

association, p= 0.02), increased dA-BST functional connectivity was associated with

lower AT. This finding is intriguing, as the direction of the relation at 1 year of age is not

consistent with our prior data in older animals (average was 1.8 years, (Fox et al.,

2018)).

When examining the relationship between dA-pOFC functional connectivity and

AT, our model suggests a trend for a main effect such that greater dA-pOFC functional

connectivity is predictive of higher AT (p=0.09). We found a significant age-interaction

(p=0.0011, *see figure 5.2A*), suggesting no significant relationship between dA-pOFC

functional connectivity and AT between 1.5 weeks and 24 weeks, but a transition to

greater dA-pOFC functional connectivity predicting higher AT at 6 months and 1 year

(within T4 association: p = 0.07; within-T5 association: p=0.03). There were no main

effect or age-interaction associations between dA-dlPFC functional connectivity and AT.

Conclusion:

Across early development in this sample, we find interesting associations

between threat-related brain metabolism and AT, and also between resting-state

functional connectivity and AT. The findings also reveal a number of interesting age-

related interactions. We note that while many of these results do not pass multiple

correction threshold, we still consider them of value in this unique and relatively small

sample.

Associations between NEC-related Metabolism and AT

We found a trend for higher BST metabolism predicting higher AT, across all ages. We also found trends for age-related interactions between dlPFC metabolism and AT and between pOFC metabolism and AT. In both cases, the strongest relationships were observed at 1 year of age, where increased dlPFC metabolism was associated with higher AT, and increased pOFC metabolism was associated with lower AT. There was a trend for an interaction with pOFC-dA delta and age such that a smaller difference between pOFC and dA metabolism predicted higher AT at 1 year of age.

The BST metabolism finding is consistent with results from our study of NEC-related metabolism and AT in a sample of 592 animals (mean age= 1.8 years), whereas the lack of a dA metabolism relation with AT is not consistent (Fox, Oler, Shackman, et al., 2015; Shackman et al., 2013). The lack of significant relations between dA metabolism and AT could be due to the relatively small sample of (n = 35) infant monkeys used in this study, as the prior study with the large sample (n = 592) was sufficiently powered to detect small effects. The pOFC metabolism findings, suggesting a decrease in pOFC metabolism at 1 year to be associated with higher AT, are also not consistent with the data from the large sample, where we observed increased pOFC metabolism in association with high levels of AT (Fox, Oler, Shackman, et al., 2015). The current data is also inconsistent with a recent study in rhesus monkeys (Kenwood et al., 2023), which demonstrated that lesioning of white matter tracts passing through the pOFC results in decreased freezing behavior during NEC. However, our findings do support a more traditional understanding of a top-down regulatory role of the prefrontal

cortex. Our findings, in conjunction with the mixed evidence in the literature (Stawicka et al., 2022; Zikopoulos et al., 2017), provide support for a bi-directional role of the pOFC in the regulation of anxiety.

We note that the median age of the animals in the large sample study was 1.8, with only 2.5% of animals at 1 year of age or younger, and none below 9 months of age. Together our findings suggest that BST metabolism during NEC shows a consistent relationship with the expression of AT throughout development, while dlPFC and pOFC metabolism, along with the difference between pOFC and dA metabolism, appear not to relate to AT until later in development. This may reflect an emergence of the regulatory role of the prefrontal cortices in threat-related brain function at 1 year of life. Taken together these findings may point to time-related differences in the associations between limbic regions and prefrontal regions with expression of AT in monkeys. As noted above, positive correlations between BST metabolism in AT are present early in life and continue throughout the first year, whereas significant relations between AT and pOFC metabolism (and AT and dlPFC metabolism), only appear at 6 months – 1 year of age.

Associations with Resting-state Dorsal Amygdala fMRI Connectivity and AT

When assessing the resting-state data we found interactions that pass multiple comparison corrections. Specifically, significant age-related interactions were observed with the dA-BST functional connectivity and dA-pOFC functional connectivity as they predict AT. At 1 year, increased dA-pOFC functional connectivity was associated with

higher AT, while increased dA-BST functional connectivity was associated with lower AT. It is unclear why the dA-BST functional connectivity finding here is not in the direction that would be predicted from our prior findings acquired in somewhat older animals (average age; 1.84 years), and may suggest a different relationship between dA-BST functional connectivity and AT during early-life development. The significant association between dA-pOFC functional connectivity with AT at 1 year of age has not previously been described. It is notable that we do not find a relationship between dA-dlPFC and AT, as we had hypothesized based on results from previous studies (Birn et al., 2014b, 2014a). Again, the ages of the monkeys from this study were much older than in the current study (median age = 2.69); therefore, these discrepant findings may be due to the extended postnatal maturation of the dlPFC (Kolk & Rakic, 2022; Petrides et al., 2012; Teffer & Semendeferi, 2012; Tsujimoto, 2008).

In summary, some of the findings from this young cohort are consistent with findings from previous studies in older animals, and others are not. It is important to emphasize that the findings from this current study reflect maturational processes occurring up to 1 year of age, which may be quite different from animals in the 1.5-2 year range. In the final chapter, we will synthesize these findings with those from the prior four chapters and present our interpretation of this work.

Chapter 6

Discussion & Implications

Summary of Study & Findings across Development

In the preceding chapters I have explored the development of threat-related behavior, threat-related brain metabolism, and resting-state amygdala functional connectivity to understand the earliest developmental features of Anxious Temperament (AT). AT a composite score that combines expression of freezing, cooing, and blood cortisol. Understanding the antecedents of AT and the emergence of its underlying neural substrates is of particular importance as high levels of AT during childhood increase the likelihood of later development of anxiety-related disorders and other stress-related psychopathology(Kagan & Snidman, 1999; Kodal et al., 2018; Walter et al., 2020).

Generally, during the first year of nonhuman primate (NHP) life, we provide evidence for the emergence of threat-related behavioral inhibition, accompanied by a shift from relatively similar limbic/prefrontal engagement to greater prefrontal engagement during threat, and increases in intrinsic functional connectivity of the amygdala. We chose to focus on anxiety-related components of the extended amygdala, the dorsal amygdala (dA) and bed nucleus of stria terminalis (BST), along with frontal cortical regions that play key roles in the regulation of threat-related responses, the posterior orbital frontal cortex (pOFC) and the dorsal lateral prefrontal cortex (dlPFC). While these regions show distinct shapes in their growth trajectories across development, there are some similarities in the pattern of their age-related changes, especially when considered in the context of behavioral response trajectories. In particular, the behavioral data suggested a directional shift in trajectories at 12

weeks. In the FDG-PET data, we similarly see a critical shift in trajectories around 12-week of age in some regions. This is the point at which NEC-related dA and BST metabolism begin to plateau, and the NEC-related dlPFC metabolism shows a directional shift, prior to plateauing. The exception to this is NEC-related pOFC metabolism, which changes direction somewhat later (at 24 weeks). This indicates that at 12-weeks of age, there is a critical shift in the behavioral and brain responses to threat. Regarding behavior, this transitional point may reflect a switch from the dominance of one set of behavioral responses- maternal separation related responses aimed at reducing threat by maternal retrieval- to another -behavioral inhibition that serves to protect the maturing infant in its mothers' absence. The age-related changes in dA functional connectivity with the BST, pOFC, and dlPFC are modest, and are characterized by gradual maturation-related increases in connectivity. Taken together with the FDG-PET data, these findings suggest dynamic functional changes involving components of anxiety-related circuitry.

Understanding the extent to which anxiety-related behavioral and functional imaging measures are stable early in life is important, as it provides insight into the earliest ages at which individual differences in the development of AT can be predictive of later pathological anxiety. Regarding stability, behavioral and cortisol responses to NEC show the highest levels of consistency within subjects across time as measured with Intraclass Correlation Analyses (ICC(3,k)). Interestingly, in some regions NEC-related metabolism also show high levels of stability (BST, pOFC). The ICC(3,k) stability of functional connectivity data did not perform as well, which is perhaps indicative of the

relative noise in this measure. Alternatively, it is possible that there is less actual stability in the functional connectivity over the first year of life in primates. However, it appears that NEC-related responses (behavioral, physiological, along with select brain regions' metabolism) do show trait-like characteristics across this period of great change.

Interpretation of Regional NEC-related Metabolism Associations with AT

Given our interest in exploring threat-related brain function in relation to AT, and our demonstration that specific brain regions in older animals predict individual differences in AT, we are especially interested in exploring these relationships during this critical development period. We find that threat-related metabolism of BST is predictive of AT throughout this developmental period. Meanwhile, it is not until later in this developmental period that we find NEC-related pOFC and dlPFC metabolism to be predictive of AT. This supports the idea that expression of AT at 1 year is associated with engagement of pOFC or dlPFC as a regulatory component of the anxiety-circuit. Notably, we observed that decreased pOFC metabolism predicted increased AT at 1 year of age, which, on the one hand is in the opposite direction to the association found in our larger cohort of study (Fox, Oler, Shackman, et al., 2015), or suggested by the pOFC lesion study (Kenwood et al., 2023). Our data also demonstrated that the difference between pOFC and dA NEC-related metabolism is predictive of AT, where a greater difference in metabolism was associated with lower AT. While not consistent with prior findings, these results fit well with the traditional explanation for top-down

regulation of emotion involving orbitofrontal cortical regions (Dixon et al., 2017; Jones & Graff-Radford, 2021), which would suggest that greater pOFC engagement results in lower AT.

Interpretation of Dorsal Amygdala Functional Connectivity Associations with AT

In this longitudinal developmental study of dA functional connectivity we observed the interactive effects of age when assessing the relationships between dA-BST connectivity and AT as well as between dA-pOFC connectivity and AT. dA-BST functional connectivity changes from a positive relationship with AT at 1.5 weeks to a negative relationship by 1 year. The directionality change in the relationship between dA-BST functional connectivity and AT with is of particular interest, and is not consistent with our prior findings in older animals. As noted in Chapter 5, the mean age of the group with the prior finding of increased dA-BST functional connectivity in association with higher AT (1.8 years,(Fox et al., 2018)) is greater than the most mature age in our cohort.

The dA-pOFC functional connectivity shows no associations with AT at 1.5 weeks, and an emergence of an association between dA-pOFC functional connectivity and AT at 1 year, such that greater dA-pOFC functional connectivity was predictive of higher AT. These functional connectivity findings are somewhat similar to the timing of the changes seen in the relations between NEC-related metabolism and AT. In both modalities, we demonstrated the involvement of extended amygdala in the expression of AT throughout development, a finding that supports and adds to the large body of

evidence implicating the extended amygdala in threat-responding (Jacqueline A Clauss et al., 2019; Feola et al., 2021; Fox et al., 2018; Fox, Oler, Tromp, et al., 2015; Oler et al., 2012). The PET data highlights involvement of the BST, while the fMRI data suggests a role for intrinsic connectivity between dA and BST in the expression and developmental dynamics of AT. Within prefrontal regions, the PET data suggests associations between dA-pOFC functional connectivity and AT at 1 year, which is a similar time course to the dynamics of pOFC metabolism as it relates to AT.

The lack of associations between dA-dlPFC connectivity and AT is also inconsistent with earlier data and could be due to the fact that dlPFC continues to develop far beyond the termination point in this study (Teffer & Semendeferi, 2012). The role played by dlPFC in regulating the anxiety circuit in young adult animals may rely on further development of additional regions not tested here (such Area 32 and Area 25 carrying polysynaptic connections through the anterior cingulate cortex from the dlPFC to the BLA (Kenwood et al., 2022; Zikopoulos et al., 2017)), prior to its engagement during threat-processing or in the expression of AT. Importantly, the prior finding of dA-dlPFC connectivity relating to AT was found in an older cohort of primates (mean age = 2.69,(Birn et al., 2014b)), which supports the possibility that continued maturation of the dlPFC is necessary to observe its relation with AT. In fact, studies exploring the functional connectivity of the amygdala in humans from 3 months-5 years old were unable to identify significant associations between the amygdala and prefrontal cortices (typically found later in adolescence, (Laurel J Gabard-Durnam et al., 2014; Gee, Gabard-Durnam, et al., 2013) during this period (L J Gabard-Durnam et al., 2018).

Implications of these Findings in the Context of Development

Here, in the first longitudinal study of concomitant rhesus brain and anxiety-related behavioral development, we demonstrate changes to anxiety-related metabolism and resting-state brain function in association with anxiety-related responses within-subjects. Our findings depict a framework for understanding the developmental trajectory of the brain circuitry underlying expression of adaptive and maladaptive anxiety during infancy and childhood. Below we describe a circuitry model, incorporating the extended amygdala and prefrontal regulatory regions, to illustrate how each region's role in AT changes from ages 1.5 weeks to 1 year. The data suggests that just after birth, monkeys with higher AT have increases in NEC-related BST metabolism, along with greater intrinsic extended amygdala (dA and BST) functional connectivity. At 1- year, higher AT continues to be associated with increased BST metabolism, along with an emergence of associations with greater dlPFC threat-related metabolism and a smaller difference between pOFC and dA metabolism. Higher AT at 1 year is also associated with increased dA-pOFC functional connectivity and decreased dA-BST functional connectivity. Overall, these finding support our initial hypotheses regarding the associations between brain function and AT during this period: associations between the extended amygdala and AT are apparent throughout the first year, while those between the frontal cortex and AT are only apparent closer to 1 year. The age-interactions between prefrontal (pOFC, dlPFC) NEC-related metabolism and dA-pOFC functional connectivity with AT support a delayed engagement of these

regions in threat-related behavior. We note that these findings are associational and cannot assess causality.

Within the context of overall brain development, our findings largely support a hierarchical model of development. Functionality of the core extended amygdala components of anxiety-related circuitry are relevant to the expression of AT throughout early-life development, while the functionality of prefrontal regulatory regions is only apparent after undergoing additional postnatal development, when the expression of anxiety begins to resemble the adaptive responses typical of preadolescent monkeys.

Unanswered Questions and Future Directions

Unanswered questions remain that are worthy of continued exploration with further research. Repeated testing is a necessary aspect of longitudinal studies. However, as noted in prior Chapters repeated testing has the potential to influence both the anxiety responses of our subjects (Hinde & Spencer-Booth, 1971), as well as neural circuit organization occurring over the period of study(Gee, Gabard-Durnam, et al., 2013; Herzberg & Gunnar, 2020). There was no obvious evidence of habituation to the NEC in our subjects, as evident by the elevated cortisol and inhibited responses with increasing age. Moreover, the highest levels of AT were at 1 year of age. It is also possible that the repeated testing could enhance anxiety related- behaviors. Regarding our examination of brain function, we chose to focus specifically on the extended amygdala and prefrontal regions that have previously been implicated as components of anxiety-related neural circuitry. Further work could expand our investigation beyond

these regions, taking a more brain-wide or network-based approach to examine the associations between anxiety-behavior and brain function. Additionally, more detailed examination of pOFC sub regions may further elaborate the associations of pOFC regulation with anxiety responses.

The Significance of this Work for Understanding the Pathophysiology of Anxiety Disorders

The work presented in this dissertation uses a classic NHP model of the risk to develop pathological anxiety to characterize the within-subject development of adaptive threat responses in association with developing prefrontal-limbic neural circuitry. Importantly, threat-related behavioral, hormonal, and several neural measures show good stability within individuals, suggesting they present trait-like features that are identifiable during the earliest stages of postnatal development. Because AT in children and preadolescent monkeys is a risk factor for the development of pathological anxiety, these findings characterized during the first year of life hold the potential for identifying at risk individuals very early in life. The brain metabolism data demonstrates a shift from similar levels of threat-related metabolism occurring across limbic and prefrontal regions limbic during the first months of life to a relative increase in prefrontal metabolism by 1 year of age, which is comparable to ~3-4 years old in human children. In parallel, with fMRI, we observed general increases in prefrontal-amygdala frunctional connectivity with maturation from infancy to 1 year of life, suggesting a developmental increase in the synchronization of the function of these regions. Interestingly, examination of the

associations between individual differences in AT with brain function implicate the BST and pOFC as being particularly important in the development of threat-related responding. These relationships between anxiety-related neural circuitry and AT differ somewhat from that observed in older preadolescent monkeys, suggesting that continuing developmental processes influence the neural circuitry underlying the expression of adaptive and pathological anxiety.

Our NHP data shows that the trait-like aspects of anxious temperament, which have been demonstrated later in childhood, begin to emerge at birth. This suggests the possibility of identifying children at risk to develop anxiety disorders during their first few years of life. This work also points to the BST and pOFC as being related to the expression of trait-like anxiety during the first year of life in rhesus monkeys and suggests further developmental studies of these regions will help to better understand the risk to develop anxiety disorders at a neural level. These findings also suggest that modifying the developmental trajectories of these regions may be strategies that will result in increasing resilience and decreasing risk. Overall, the new data established by the studies presented in this thesis provide a developmental framework for understanding the risk to develop stress-related psychopathology at behavioral and neural levels at the earliest stages of life. These data, along with other work, provide the neuroscientific basis for conceptualizing early-life interventions in at-risk children with the hope of reducing the lifelong suffering that many of these children face.

References

Aggarwal, N., Moody, J. F., Dean, D. C., Tromp, D. P. M., Kecskemeti, S. R., Oler, J. A., Alexander, A. L., & Kalin, N. H. (2021). Spatiotemporal dynamics of nonhuman primate white matter development during the first year of life. *NeuroImage*, *231*, 117825. https://doi.org/10.1016/j.neuroimage.2021.117825

Alheid, G. F., & Heimer, L. (1988). New perspectives in basal forebrain organization of special relevance for neuropsychiatric disorders: the striatopallidal, amygdaloid, and corticopetal components of substantia innominata. *Neuroscience*, *27*(1), 1–39. https://doi.org/10.1016/0306-4522(88)90217-5

Avants, B., Tustison, N. J., & Song, G. (2009). Advanced Normalization Tools: V1.0. *The Insight Journal*. https://doi.org/10.54294/uvnhin

Baeken, C., Wu, G.-R., & De Raedt, R. (2018). Dorsomedial frontal cortical metabolic differences of comorbid generalized anxiety disorder in refractory major depression: A [(18)F] FDG PET brain imaging study. *Journal of Affective Disorders*, *227*, 550–553. https://doi.org/10.1016/j.jad.2017.11.066

Barrett, H. C. (2012). A hierarchical model of the evolution of human brain specializations. *Proceedings of the National Academy of Sciences of the United States of America*, *109 Suppl*(Suppl 1), 10733–10740. https://doi.org/10.1073/pnas.1201898109

Bates, D., Mächler, M., Bolker, B., & Walker, S. (2015). Fitting Linear Mixed-Effects Models Using lme4. *Journal of Statistical Software*, *67*(1), 1–48.

https://doi.org/10.18637/jss.v067.i01

Battaglia, M. (2015). Separation anxiety: at the neurobiological crossroads of adaptation and illness. *Dialogues in Clinical Neuroscience, 17*(3), 277–285. https://pubmed.ncbi.nlm.nih.gov/26487808

Biederman, J., Rosenbaum, J. F., Bolduc-Murphy, E. A., Faraone, S. V, Chaloff, J., Hirshfeld, D. R., & Kagan, J. (1993). A 3-year follow-up of children with and without behavioral inhibition. *Journal of the American Academy of Child and Adolescent Psychiatry, 32*(4), 814–821. https://doi.org/10.1097/00004583-199307000-00016

Birn, R. M., Shackman, A. J., Oler, J. A., Williams, L. E., McFarlin, D. R., Rogers, G. M., Shelton, S. E., Alexander, A. L., Pine, D. S., Slattery, M. J., Davidson, R. J., Fox, A. S., & Kalin, N. H. (2014a). Evolutionarily conserved prefrontal-amygdalar dysfunction in early-life anxiety. *Molecular Psychiatry, 19*(8), 915–922. https://doi.org/10.1038/mp.2014.46

Birn, R. M., Shackman, A. J., Oler, J. A., Williams, L. E., McFarlin, D. R., Rogers, G. M., Shelton, S. E., Alexander, A. L., Pine, D. S., Slattery, M. J., Davidson, R. J., Fox, A. S., & Kalin, N. H. (2014b). Extreme early-life anxiety is associated with an evolutionarily conserved reduction in the strength of intrinsic functional connectivity between the dorsolateral prefrontal cortex and the central nucleus of the amygdala. *Molecular Psychiatry, 19*(8), 853. https://doi.org/10.1038/mp.2014.85

Bowlby, J. (2008). *Attachment.* Basic books.

Britton, J. C., Lissek, S., Grillon, C., Norcross, M. A., & Pine, D. S. (2011). Development of anxiety: the role of threat appraisal and fear learning. *Depression and Anxiety,*

28(1), 5–17. https://doi.org/10.1002/da.20733

Brooker, R. J., Buss, K. A., Lemery-Chalfant, K., Aksan, N., Davidson, R. J., & Goldsmith, H. H. (2013). The development of stranger fear in infancy and toddlerhood: normative development, individual differences, antecedents, and outcomes. *Developmental Science, 16*(6), 864–878. https://doi.org/10.1111/desc.12058

Calabrese, E., Badea, A., Coe, C. L., Lubach, G. R., Shi, Y., Styner, M. A., & Johnson, G. A. (2015). A diffusion tensor MRI atlas of the postmortem rhesus macaque brain. *NeuroImage, 117*, 408–416. https://doi.org/10.1016/j.neuroimage.2015.05.072

Cassell, M. D., Freedman, L. J., & Shi, C. (1999). The intrinsic organization of the central extended amygdala. *Annals of the New York Academy of Sciences, 877*, 217–241. https://doi.org/10.1111/j.1749-6632.1999.tb09270.x

Chareyron, L. J., Lavenex, P. B., Amaral, D. G., & Lavenex, P. (2012). Postnatal development of the amygdala: A stereological study in macaque monkeys. *The Journal of Comparative Neurology, 520*(9), 1965–1984. https://doi.org/10.1002/cne.23023

Chavira, D. A., Stein, M. B., & Malcarne, V. L. (2002). Scrutinizing the relationship between shyness and social phobia. *Journal of Anxiety Disorders, 16*(6), 585–598. https://doi.org/10.1016/s0887-6185(02)00124-x

Chugani, H T. (1998). A critical period of brain development: studies of cerebral glucose utilization with PET. *Preventive Medicine, 27*(2), 184–188.

https://doi.org/10.1006/pmed.1998.0274

Chugani, H T, & Phelps, M. E. (1986). Maturational changes in cerebral function in infants determined by 18FDG positron emission tomography. *Science (New York, N.Y.)*, *231*(4740), 840–843. https://doi.org/10.1126/science.3945811

Chugani, H T, Phelps, M. E., & Mazziotta, J. C. (1987). Positron emission tomography study of human brain functional development. *Annals of Neurology*, *22*(4), 487–497. https://doi.org/10.1002/ana.410220408

Chugani, Harry T. (2018). Imaging Brain Metabolism in the Newborn. *Journal of Child Neurology*, *33*(13), 851–860. https://doi.org/10.1177/0883073818792308

Clauss, J A, Avery, S. N., & Blackford, J. U. (2015). The nature of individual differences in inhibited temperament and risk for psychiatric disease: A review and meta-analysis. *Progress in Neurobiology*, *127–128*, 23–45. https://doi.org/10.1016/j.pneurobio.2015.03.001

Clauss, Jacqueline A, Avery, S. N., Benningfield, M. M., & Blackford, J. U. (2019). Social anxiety is associated with BNST response to unpredictability. *Depression and Anxiety*, *36*(8), 666–675. https://doi.org/10.1002/da.22891

Clauss, Jacqueline A, & Blackford, J. U. (2012). Behavioral inhibition and risk for developing social anxiety disorder: a meta-analytic study. *Journal of the American Academy of Child and Adolescent Psychiatry*, *51*(10), 1066-1075.e1. https://doi.org/10.1016/j.jaac.2012.08.002

Cox, R. W. (1996). AFNI: software for analysis and visualization of functional magnetic resonance neuroimages. *Computers and Biomedical Research, an International*

Journal, *29*(3), 162–173. https://doi.org/10.1006/cbmr.1996.0014

De Asis-Cruz, J., Bouyssi-Kobar, M., Evangelou, I., Vezina, G., & Limperopoulos, C. (2015). Functional properties of resting state networks in healthy full-term newborns. *Scientific Reports*, *5*, 17755. https://doi.org/10.1038/srep17755

Dixon, M. L., Thiruchselvam, R., Todd, R., & Christoff, K. (2017). Emotion and the prefrontal cortex: An integrative review. *Psychological Bulletin*, *143*(10), 1033–1081. https://doi.org/10.1037/bul0000096

Donahue, C. J., Glasser, M. F., Preuss, T. M., Rilling, J. K., & Van Essen, D. C. (2018). Quantitative assessment of prefrontal cortex in humans relative to nonhuman primates. *Proceedings of the National Academy of Sciences of the United States of America*, *115*(22), E5183–E5192. https://doi.org/10.1073/pnas.1721653115

Feola, B., Melancon, S. N. T., Clauss, J. A., Noall, M. P., Mgboh, A., Flook, E. A., Benningfield, M. M., & Blackford, J. U. (2021). Bed nucleus of the stria terminalis and amygdala responses to unpredictable threat in children. *Developmental Psychobiology*, *63*(8), e22206. https://doi.org/10.1002/dev.22206

Fogelman, N., & Canli, T. (2018). Early life stress and cortisol: A meta-analysis. *Hormones and Behavior*, *98*, 63–76. https://doi.org/10.1016/j.yhbeh.2017.12.014

Fox, A. S., & Kalin, N. H. (2014). A translational neuroscience approach to understanding the development of social anxiety disorder and its pathophysiology. *The American Journal of Psychiatry*, *171*(11), 1162–1173. https://doi.org/10.1176/appi.ajp.2014.14040449

Fox, A. S., Oler, J. A., Birn, R. M., Shackman, A. J., Alexander, A. L., & Kalin, N. H.

(2018). Functional Connectivity within the Primate Extended Amygdala Is Heritable and Associated with Early-Life Anxious Temperament. *The Journal of Neuroscience : The Official Journal of the Society for Neuroscience*, *38*(35), 7611–7621. https://doi.org/10.1523/JNEUROSCI.0102-18.2018

Fox, A. S., Oler, J. A., Shackman, A. J., Shelton, S. E., Raveendran, M., McKay, D. R., Converse, A. K., Alexander, A., Davidson, R. J., Blangero, J., Rogers, J., & Kalin, N. H. (2015). Intergenerational neural mediators of early-life anxious temperament. *Proceedings of the National Academy of Sciences of the United States of America*, *112*(29), 9118–9122. https://doi.org/10.1073/pnas.1508593112

Fox, A. S., Oler, J. A., Tromp, D. P. M., Fudge, J. L., & Kalin, N. H. (2015). Extending the amygdala in theories of threat processing. *Trends in Neurosciences*, *38*(5), 319–329. https://doi.org/10.1016/j.tins.2015.03.002

Fox, A. S., Shelton, S. E., Oakes, T. R., Converse, A. K., Davidson, R. J., & Kalin, N. H. (2010). Orbitofrontal cortex lesions alter anxiety-related activity in the primate bed nucleus of stria terminalis. *The Journal of Neuroscience : The Official Journal of the Society for Neuroscience*, *30*(20), 7023–7027. https://doi.org/10.1523/JNEUROSCI.5952-09.2010

Fox, A. S., Shelton, S. E., Oakes, T. R., Davidson, R. J., & Kalin, N. H. (2008). Trait-like brain activity during adolescence predicts anxious temperament in primates. *PloS One*, *3*(7), e2570–e2570. https://doi.org/10.1371/journal.pone.0002570

Fransson, P., Skiöld, B., Horsch, S., Nordell, A., Blennow, M., Lagercrantz, H., & Aden, U. (2007). Resting-state networks in the infant brain. *Proceedings of the National*

Academy of Sciences of the United States of America, *104*(39), 15531–15536. https://doi.org/10.1073/pnas.0704380104

Gabard-Durnam, L J, O'Muircheartaigh, J., Dirks, H., Dean, D. C. 3rd, Tottenham, N., & Deoni, S. (2018). Human amygdala functional network development: A cross-sectional study from 3 months to 5 years of age. *Developmental Cognitive Neuroscience*, *34*, 63–74. https://doi.org/10.1016/j.dcn.2018.06.004

Gabard-Durnam, Laurel J, Flannery, J., Goff, B., Gee, D. G., Humphreys, K. L., Telzer, E., Hare, T., & Tottenham, N. (2014). The development of human amygdala functional connectivity at rest from 4 to 23 years: a cross-sectional study. *NeuroImage*, *95*, 193–207. https://doi.org/10.1016/j.neuroimage.2014.03.038

Gee, D. G., Gabard-Durnam, L. J., Flannery, J., Goff, B., Humphreys, K. L., Telzer, E. H., Hare, T. A., Bookheimer, S. Y., & Tottenham, N. (2013). Early developmental emergence of human amygdala-prefrontal connectivity after maternal deprivation. *Proceedings of the National Academy of Sciences of the United States of America*, *110*(39), 15638–15643. https://doi.org/10.1073/pnas.1307893110

Gee, D. G., Humphreys, K. L., Flannery, J., Goff, B., Telzer, E. H., Shapiro, M., Hare, T. A., Bookheimer, S. Y., & Tottenham, N. (2013). A developmental shift from positive to negative connectivity in human amygdala-prefrontal circuitry. *The Journal of Neuroscience : The Official Journal of the Society for Neuroscience*, *33*(10), 4584–4593. https://doi.org/10.1523/JNEUROSCI.3446-12.2013

Giordani, B., Boivin, M. J., Berent, S., Betley, A. T., Koeppe, R. A., Rothley, J. M., Modell, J. G., Hichwa, R. D., & Kuhl, D. E. (1990). Anxiety and cerebral cortical

metabolism in normal persons. *Psychiatry Research*, *35*(1), 49–60.

https://doi.org/10.1016/0925-4927(90)90008-t

Global Burden of Disease Collaborative Network. (2019). *Global Burden of Disease Study 2019 (GBD 2019)*.

Gunnar, M. R., & Donzella, B. (2002). Social regulation of the cortisol levels in early human development. *Psychoneuroendocrinology*, *27*(1–2), 199–220.

https://doi.org/10.1016/s0306-4530(01)00045-2

Gunnar, M. R., & Hostinar, C. E. (2015). The social buffering of the hypothalamic-pituitary-adrenocortical axis in humans: Developmental and experiential determinants. *Social Neuroscience*, *10*(5), 479–488.

https://doi.org/10.1080/17470919.2015.1070747

Gunnar, M. R., Hostinar, C. E., Sanchez, M. M., Tottenham, N., & Sullivan, R. M. (2015). Parental buffering of fear and stress neurobiology: Reviewing parallels across rodent, monkey, and human models. *Social Neuroscience*, *10*(5), 474–478.

https://doi.org/10.1080/17470919.2015.1070198

Hamm, L. L., Jacobs, R. H., Johnson, M. W., Fitzgerald, D. A., Fitzgerald, K. D., Langenecker, S. A., Monk, C. S., & Phan, K. L. (2014). Aberrant amygdala functional connectivity at rest in pediatric anxiety disorders. *Biology of Mood & Anxiety Disorders*, *4*(1), 15. https://doi.org/10.1186/s13587-014-0015-4

Hansen, E. W. (1966). The Development of Maternal and Infant Behavior in the Rhesus Monkey. *Behaviour*, *27*(1–2), 107–148.

https://doi.org/https://doi.org/10.1163/156853966X00128

Harlow, H. F., & Suomi, S. J. (1971). Social recovery by isolation-reared monkeys. *Proceedings of the National Academy of Sciences of the United States of America*, *68*(7), 1534–1538. https://doi.org/10.1073/pnas.68.7.1534

HARLOW, H. F., & ZIMMERMANN, R. R. (1959). Affectional responses in the infant monkey; orphaned baby monkeys develop a strong and persistent attachment to inanimate surrogate mothers. *Science (New York, N.Y.)*, *130*(3373), 421–432. https://doi.org/10.1126/science.130.3373.421

Henderson, H. A., Pine, D. S., & Fox, N. A. (2015). Behavioral inhibition and developmental risk: a dual-processing perspective. *Neuropsychopharmacology : Official Publication of the American College of Neuropsychopharmacology*, *40*(1), 207–224. https://doi.org/10.1038/npp.2014.189

Herzberg, M. P., & Gunnar, M. R. (2020). Early life stress and brain function: Activity and connectivity associated with processing emotion and reward. *NeuroImage*, *209*, 116493. https://doi.org/10.1016/j.neuroimage.2019.116493

Hinde, R. A., & Spencer-Booth, Y. (1967). The behaviour of socially living rhesus monkeys in their first two and a half years. *Animal Behaviour*, *15*(1), 169–196. https://doi.org/https://doi.org/10.1016/S0003-3472(67)80029-0

Hinde, R. A., & Spencer-Booth, Y. (1971). Effects of Brief Separation from Mother on Rhesus Monkeys. *Science*, *173*(3992), 111 LP – 118. https://doi.org/10.1126/science.173.3992.111

Jahn, A. L., Fox, A. S., Abercrombie, H. C., Shelton, S. E., Oakes, T. R., Davidson, R. J., & Kalin, N. H. (2010). Subgenual prefrontal cortex activity predicts individual

differences in hypothalamic-pituitary-adrenal activity across different contexts. *Biological Psychiatry*, *67*(2), 175–181. https://doi.org/10.1016/j.biopsych.2009.07.039

Janak, P. H., & Tye, K. M. (2015). From circuits to behaviour in the amygdala. *Nature*, *517*(7534), 284–292. https://doi.org/10.1038/nature14188

Jansen, J., Beijers, R., Riksen-Walraven, M., & de Weerth, C. (2010). Cortisol reactivity in young infants. *Psychoneuroendocrinology*, *35*(3), 329–338. https://doi.org/10.1016/j.psyneuen.2009.07.008

Jiang, X., & Nardelli, J. (2016). Cellular and molecular introduction to brain development. *Neurobiology of Disease*, *92*(Pt A), 3–17. https://doi.org/10.1016/j.nbd.2015.07.007

Jones, D. T., & Graff-Radford, J. (2021). Executive Dysfunction and the Prefrontal Cortex. *Continuum (Minneapolis, Minn.)*, *27*(6), 1586–1601. https://doi.org/10.1212/CON.0000000000001009

Kagan, J., Reznick, J. S., & Gibbons, J. (1989). Inhibited and uninhibited types of children. *Child Development*, *60*(4), 838–845.

Kagan, J., Reznick, J. S., & Snidman, N. (1987). The physiology and psychology of behavioral inhibition in children. *Child Development*, *58*(6), 1459–1473.

Kagan, J., & Snidman, N. (1999). Early childhood predictors of adult anxiety disorders. *Biological Psychiatry*, *46*(11), 1536–1541. https://doi.org/10.1016/s0006-3223(99)00137-7

Kalin, N H. (1993). The neurobiology of fear. *Scientific American*, *268*(5), 94–101.

https://doi.org/10.1038/scientificamerican0593-94

Kalin, N H, & Shelton, S. E. (1989). Defensive behaviors in infant rhesus monkeys: environmental cues and neurochemical regulation. *Science*, *243*(4899), 1718 LP – 1721. https://doi.org/10.1126/science.2564702

Kalin, N H, Shelton, S. E., Davidson, R. J., & Kelley, A. E. (2001). The primate amygdala mediates acute fear but not the behavioral and physiological components of anxious temperament. *The Journal of Neuroscience : The Official Journal of the Society for Neuroscience*, *21*(6), 2067–2074. https://doi.org/10.1523/JNEUROSCI.21-06-02067.2001

Kalin, Ned H, Shelton, S. E., & Davidson, R. J. (2004). The Role of the Central Nucleus of the Amygdala in Mediating Fear and Anxiety in the Primate. *The Journal of Neuroscience*, *24*(24), 5506 LP – 5515. https://doi.org/10.1523/JNEUROSCI.0292-04.2004

Kalin, Ned H, Shelton, S. E., & Davidson, R. J. (2007). Role of the primate orbitofrontal cortex in mediating anxious temperament. *Biological Psychiatry*, *62*(10), 1134–1139. https://doi.org/10.1016/j.biopsych.2007.04.004

Kalin, Ned H, Shelton, S. E., & Takahashi, L. K. (1991). Defensive Behaviors in Infant Rhesus Monkeys: Ontogeny and Context-dependent Selective Expression. *Child Development*, *62*(5), 1175–1183. https://doi.org/10.1111/j.1467-8624.1991.tb01598.x

Kecskemeti, S., Samsonov, A., Hurley, S. A., Dean, D. C., Field, A., & Alexander, A. L. (2016). MPnRAGE: A technique to simultaneously acquire hundreds of differently

contrasted MPRAGE images with applications to quantitative T1 mapping. *Magnetic Resonance in Medicine*, *75*(3), 1040–1053. https://doi.org/10.1002/mrm.25674

Keller, A. S., Sydnor, V. J., Pines, A., Fair, D. A., Bassett, D. S., & Satterthwaite, T. D. (2023). Hierarchical functional system development supports executive function. *Trends in Cognitive Sciences*, *27*(2), 160–174. https://doi.org/10.1016/j.tics.2022.11.005

Kennedy, C., Sakurada, O., Shinohara, M., & Miyaoka, M. (1982). Local cerebral glucose utilization in the newborn macaque monkey. *Annals of Neurology*, *12*(4), 333–340. https://doi.org/10.1002/ana.410120404

Kenwood, M. M., Kalin, N. H., & Barbas, H. (2022). The prefrontal cortex, pathological anxiety, and anxiety disorders. *Neuropsychopharmacology : Official Publication of the American College of Neuropsychopharmacology*, *47*(1), 260–275. https://doi.org/10.1038/s41386-021-01109-z

Kenwood, M. M., Oler, J. A., Tromp, D. P. M., Fox, A. S., Riedel, M. K., Roseboom, P. H., Brunner, K. G., Aggarwal, N., Murray, E. A., & Kalin, N. H. (2023). Prefrontal influences on the function of the neural circuitry underlying anxious temperament in primates. *Oxford Open Neuroscience*, *2*. https://doi.org/10.1093/oons/kvac016

Kessler, R. C., Berglund, P., Demler, O., Jin, R., Merikangas, K. R., & Walters, E. E. (2005). Lifetime Prevalence and Age-of-Onset Distributions of DSM-IV Disorders in the National Comorbidity Survey Replication. *Archives of General Psychiatry*, *62*(6), 593–602. https://doi.org/10.1001/archpsyc.62.6.593

Kim, J., Jung, Y., Barcus, R., Bachevalier, J. H., Sanchez, M. M., Nader, M. A., & Whitlow, C. T. (2020). Rhesus Macaque Brain Developmental Trajectory: A Longitudinal Analysis Using Tensor-Based Structural Morphometry and Diffusion Tensor Imaging. *Cerebral Cortex (New York, N.Y. : 1991)*, *30*(8), 4325–4335. https://doi.org/10.1093/cercor/bhaa015

Kinnala, A., Suhonen-Polvi, H., Aärimaa, T., Kero, P., Korvenranta, H., Ruotsalainen, U., Bergman, J., Haaparanta, M., Solin, O., Nuutila, P., & Wegelius, U. (1996). Cerebral metabolic rate for glucose during the first six months of life: an FDG positron emission tomography study. *Archives of Disease in Childhood. Fetal and Neonatal Edition*, *74*(3), F153-7. https://doi.org/10.1136/fn.74.3.f153

Kiorpes, L. (2016). The Puzzle of Visual Development: Behavior and Neural Limits. *The Journal of Neuroscience : The Official Journal of the Society for Neuroscience*, *36*(45), 11384–11393. https://doi.org/10.1523/JNEUROSCI.2937-16.2016

Kodal, A., Fjermestad, K., Bjelland, I., Gjestad, R., Öst, L.-G., Bjaastad, J. F., Haugland, B. S. M., Havik, O. E., Heiervang, E., & Wergeland, G. J. (2018). Long-term effectiveness of cognitive behavioral therapy for youth with anxiety disorders. *Journal of Anxiety Disorders*, *53*, 58–67. https://doi.org/https://doi.org/10.1016/j.janxdis.2017.11.003

Kolk, S. M., & Rakic, P. (2022). Development of prefrontal cortex. *Neuropsychopharmacology : Official Publication of the American College of Neuropsychopharmacology*, *47*(1), 41–57. https://doi.org/10.1038/s41386-021-01137-9

Kovacs-Balint, Z. A., Payne, C., Steele, J., Li, L., Styner, M., Bachevalier, J., &

    Sanchez, M. M. (2021). Structural development of cortical lobes during the first 6

    months of life in infant macaques. *Developmental Cognitive Neuroscience*, *48*,

    100906. https://doi.org/10.1016/j.dcn.2020.100906

Kovner, R., Souaiaia, T., Fox, A. S., French, D. A., Goss, C. E., Roseboom, P. H., Oler,

    J. A., Riedel, M. K., Fekete, E. M., Fudge, J. L., Knowles, J. A., & Kalin, N. H.

    (2019). Transcriptional Profiling of Primate Central Nucleus of the Amygdala

    Neurons to Understand the Molecular Underpinnings of Early Life Anxious

    Temperament. *BioRxiv*, 808279. https://doi.org/10.1101/808279

Levine, S. (2001). Primary social relationships influence the development of the

    hypothalamic--pituitary--adrenal axis in the rat. *Physiology & Behavior*, *73*(3), 255–

    260. https://doi.org/10.1016/s0031-9384(01)00496-6

Lewis, J. G., & Elder, P. A. (1985). An enzyme-linked immunosorbent assay (ELISA) for

    plasma cortisol. *Journal of Steroid Biochemistry*, *22*(5), 673–676.

    https://doi.org/10.1016/0022-4731(85)90222-5

London, K., & Howman-Giles, R. (2015). Voxel-based analysis of normal cerebral

    [18F]FDG uptake during childhood using statistical parametric mapping.

    NeuroImage, *106*, 264–271. https://doi.org/10.1016/j.neuroimage.2014.11.047

Luis-Joaquin, G.-L., Lourdes, E.-F., & José A, M.-M. (2020). Behavioral Inhibition in

    Childhood as A Risk Factor for Development of Social Anxiety Disorder: A

    Longitudinal Study. *International Journal of Environmental Research and Public*

    Health, *17*(11). https://doi.org/10.3390/ijerph17113941

Makropoulos, A., Aljabar, P., Wright, R., Hüning, B., Merchant, N., Arichi, T., Tusor, N.,

Hajnal, J. V, Edwards, A. D., Counsell, S. J., & Rueckert, D. (2016). Regional

growth and atlasing of the developing human brain. *NeuroImage*, *125*, 456–478.

https://doi.org/10.1016/j.neuroimage.2015.10.047

Malik, F., & Marwaha, R. (2023). *Developmental Stages of Social Emotional*

Development in Children.

Malkova, L., Heuer, E., & Saunders, R. C. (2006). Longitudinal magnetic resonance

imaging study of rhesus monkey brain development. *The European Journal of*

Neuroscience, *24*(11), 3204–3212. https://doi.org/10.1111/j.1460-

9568.2006.05175.x

Medina, L., Abellán, A., Morales, L., Pross, A., Metwalli, A. H., González-Alonso, A.,

Freixes, J., & Desfilis, E. (2023). Evolution and Development of Amygdala

Subdivisions: Pallial, Subpallial, and Beyond. *Brain, Behavior and Evolution*, *98*(1),

1–21. https://doi.org/10.1159/000527512

Mental Health and Substance Use, W. H. (2022). *Mental Health and COVID-19: Early*

Evidence of the pandemic's impact. WHO/2019-

nCoV/Sci_Brief/Mental_health/2022.1

Moody, J. F., Aggarwal, N., Dean, D. C. 3rd, Tromp, D. P. M., Kecskemeti, S. R., Oler,

J. A., Kalin, N. H., & Alexander, A. L. (2022). Longitudinal assessment of early-life

white matter development with quantitative relaxometry in nonhuman primates.

NeuroImage, *251*, 118989. https://doi.org/10.1016/j.neuroimage.2022.118989

Mueller, S. A. L., Oler, J. A., Roseboom, P. H., Aggarwal, N., Kenwood, M. M., Riedel,

M. K., Elam, V. R., Olsen, M. E., DiFilippo, A. H., Christian, B. T., Hu, X., Galvan, A., Boehm, M. A., Michaelides, M., & Kalin, N. H. (2023). DREADD-mediated amygdala activation is sufficient to induce anxiety-like responses in young nonhuman primates. In *bioRxiv : the preprint server for biology*. https://doi.org/10.1101/2023.06.06.543911

Niermann, H. C. M., Tyborowska, A., Cillessen, A. H. N., van Donkelaar, M. M., Lammertink, F., Gunnar, M. R., Franke, B., Figner, B., & Roelofs, K. (2019). The relation between infant freezing and the development of internalizing symptoms in adolescence: A prospective longitudinal study. *Developmental Science*, *22*(3), e12763. https://doi.org/10.1111/desc.12763

Oler, J. A., Birn, R. M., Patriat, R., Fox, A. S., Shelton, S. E., Burghy, C. A., Stodola, D. E., Essex, M. J., Davidson, R. J., & Kalin, N. H. (2012). Evidence for coordinated functional activity within the extended amygdala of non-human and human primates. *NeuroImage*, *61*(4), 1059–1066. https://doi.org/10.1016/j.neuroimage.2012.03.045

Oler, J. A., Fox, A. S., Shelton, S. E., Rogers, J., Dyer, T. D., Davidson, R. J., Shelledy, W., Oakes, T. R., Blangero, J., & Kalin, N. H. (2010). Amygdalar and hippocampal substrates of anxious temperament differ in their heritability. *Nature*, *466*(7308), 864–868. https://doi.org/10.1038/nature09282

Petrides, M., Tomaiuolo, F., Yeterian, E. H., & Pandya, D. N. (2012). The prefrontal cortex: Comparative architectonic organization in the human and the macaque monkey brains. *Cortex*, *48*(1), 46–57.

https://doi.org/https://doi.org/10.1016/j.cortex.2011.07.002

Rao, B., Xu, D., Zhao, C., Wang, S., Li, X., Sun, W., Gang, Y., Fang, J., & Xu, H. (2021). Development of functional connectivity within and among the resting-state networks in anesthetized rhesus monkeys. *NeuroImage, 242*, 118473. https://doi.org/10.1016/j.neuroimage.2021.118473

Rapee, R. M., Creswell, C., Kendall, P. C., Pine, D. S., & Waters, A. M. (2023). Anxiety disorders in children and adolescents: A summary and overview of the literature. *Behaviour Research and Therapy, 168*, 104376. https://doi.org/10.1016/j.brat.2023.104376

Rheingold, H. L., & Eckerman, C. O. (1973). Fear of the stranger: a critical examination. *Advances in Child Development and Behavior, 8*, 185–222. https://doi.org/10.1016/s0065-2407(08)60496-6

Rilling, J. K., Winslow, J. T., & Kilts, C. D. (2004). The neural correlates of mate competition in dominant male rhesus macaques. *Biological Psychiatry, 56*(5), 364–375. https://doi.org/10.1016/j.biopsych.2004.06.027

Roozendaal, B., McEwen, B. S., & Chattarji, S. (2009). Stress, memory and the amygdala. *Nature Reviews. Neuroscience, 10*(6), 423–433. https://doi.org/10.1038/nrn2651

Roseboom, P. H., Mueller, S. A. L., Oler, J. A., Fox, A. S., Riedel, M. K., Elam, V. R., Olsen, M. E., Gomez, J. L., Boehm, M. A., DiFilippo, A. H., Christian, B. T., Michaelides, M., & Kalin, N. H. (2021). Evidence in primates supporting the use of chemogenetics for the treatment of human refractory neuropsychiatric disorders.

Molecular Therapy : The Journal of the American Society of Gene Therapy, *29*(12), 3484–3497. https://doi.org/10.1016/j.ymthe.2021.04.021

Rosenfeld, P., Suchecki, D., & Levine, S. (1992). Multifactorial regulation of the hypothalamic-pituitary-adrenal axis during development. *Neuroscience and Biobehavioral Reviews*, *16*(4), 553–568. https://doi.org/10.1016/s0149-7634(05)80196-4

SAH, P., FABER, E. S. L., LOPEZ DE ARMENTIA, M., & POWER, J. (2003). The Amygdaloid Complex: Anatomy and Physiology. *Physiological Reviews*, *83*(3), 803–834. https://doi.org/10.1152/physrev.00002.2003

Santiago, A., Aoki, C., & Sullivan, R. M. (2017). From attachment to independence: Stress hormone control of ecologically relevant emergence of infants' responses to threat. *Current Opinion in Behavioral Sciences*, *14*, 78–85. https://doi.org/10.1016/j.cobeha.2016.12.010

Scott, J. A., Grayson, D., Fletcher, E., Lee, A., Bauman, M. D., Schumann, C. M., Buonocore, M. H., & Amaral, D. G. (2016). Longitudinal analysis of the developing rhesus monkey brain using magnetic resonance imaging: birth to adulthood. *Brain Structure & Function*, *221*(5), 2847–2871. https://doi.org/10.1007/s00429-015-1076-x

Seay, B., Hansen, E., & Harlow, H. F. (1962). MOTHER-INFANT SEPARATION IN MONKEYS*. *Journal of Child Psychology and Psychiatry*, *3*(3-4), 123–132. https://doi.org/10.1111/j.1469-7610.1962.tb02047.x

Shackman, A. J., Fox, A. S., Oler, J. A., Shelton, S. E., Davidson, R. J., & Kalin, N. H.

(2013). Neural mechanisms underlying heterogeneity in the presentation of anxious temperament. *Proceedings of the National Academy of Sciences of the United States of America*, *110*(15), 6145–6150. https://doi.org/10.1073/pnas.1214364110

Stawicka, Z. M., Massoudi, R., Oikonomidis, L., McIver, L., Mulvihill, K., Quah, S. K. L., Cockcroft, G. J., Clarke, H. F., Horst, N. K., Wood, C. M., & Roberts, A. C. (2022). Differential Effects of the Inactivation of Anterior and Posterior Orbitofrontal Cortex on Affective Responses to Proximal and Distal Threat, and Reward Anticipation in the Common Marmoset. *Cerebral Cortex (New York, N.Y. : 1991)*, *32*(7), 1319–1336. https://doi.org/10.1093/cercor/bhab240

Sung, K.-K., Jang, D.-P., Lee, S., Kim, M., Lee, S.-Y., Kim, Y.-B., Park, C.-W., & Cho, Z.-H. (2009). Neural responses in rat brain during acute immobilization stress: a [F-18]FDG micro PET imaging study. *NeuroImage*, *44*(3), 1074–1080. https://doi.org/10.1016/j.neuroimage.2008.09.032

Swartz, J. R., Phan, K. L., Angstadt, M., Fitzgerald, K. D., & Monk, C. S. (2014). Dynamic changes in amygdala activation and functional connectivity in children and adolescents with anxiety disorders. *Development and Psychopathology*, *26*(4 Pt 2), 1305–1319. https://doi.org/10.1017/S0954579414001047

Teffer, K., & Semendeferi, K. (2012). Human prefrontal cortex: evolution, development, and pathology. *Progress in Brain Research*, *195*, 191–218. https://doi.org/10.1016/B978-0-444-53860-4.00009-X

Toazza, R., Franco, A. R., Buchweitz, A., Molle, R. D., Rodrigues, D. M., Reis, R. S., Mucellini, A. B., Esper, N. B., Aguzzoli, C., Silveira, P. P., Salum, G. A., & Manfro,

G. G. (2016). Amygdala-based intrinsic functional connectivity and anxiety

disorders in adolescents and young adults. *Psychiatry Research. Neuroimaging*,

257, 11–16. https://doi.org/10.1016/j.pscychresns.2016.09.010

Tovote, P., Fadok, J. P., & Lüthi, A. (2015). Neuronal circuits for fear and anxiety.

Nature Reviews Neuroscience, *16*(6), 317–331. https://doi.org/10.1038/nrn3945

Tromp, D. P. M., Fox, A. S., Oler, J. A., Alexander, A. L., & Kalin, N. H. (2019). The

Relationship Between the Uncinate Fasciculus and Anxious Temperament Is

Evolutionarily Conserved and Sexually Dimorphic. *Biological Psychiatry*, *86*(12),

890–898. https://doi.org/https://doi.org/10.1016/j.biopsych.2019.07.022

Tromp, D. P. M., Williams, L. E., Fox, A. S., Oler, J. A., Roseboom, P. H., Rogers, G.

M., Benson, B. E., Alexander, A. L., Pine, D. S., & Kalin, N. H. (2019). Altered

Uncinate Fasciculus Microstructure in Childhood Anxiety Disorders in Boys But Not

Girls. *The American Journal of Psychiatry*, *176*(3), 208–216.

https://doi.org/10.1176/appi.ajp.2018.18040425

Tsujimoto, S. (2008). The prefrontal cortex: functional neural development during early

childhood. *The Neuroscientist : A Review Journal Bringing Neurobiology, Neurology

and Psychiatry*, *14*(4), 345–358. https://doi.org/10.1177/1073858408316002

van den Heuvel, M. P., & Hulshoff Pol, H. E. (2010). Exploring the brain network: a

review on resting-state fMRI functional connectivity. *European

Neuropsychopharmacology : The Journal of the European College of

Neuropsychopharmacology*, *20*(8), 519–534.

https://doi.org/10.1016/j.euroneuro.2010.03.008

van der Horst, F. C. P., Leroy, H. A., & van der Veer, R. (2008). "When strangers meet":
John Bowlby and Harry Harlow on attachment behavior. *Integrative Psychological & Behavioral Science*, *42*(4), 370–388. https://doi.org/10.1007/s12124-008-9079-2

Walter, H. J., Bukstein, O. G., Abright, A. R., Keable, H., Ramtekkar, U., Ripperger-Suhler, J., & Rockhill, C. (2020). Clinical Practice Guideline for the Assessment and Treatment of Children and Adolescents With Anxiety Disorders. In *Journal of the American Academy of Child and Adolescent Psychiatry* (Vol. 59, Issue 10, pp. 1107–1124). https://doi.org/10.1016/j.jaac.2020.05.005

Wang, X., Zhang, J., Yuan, Y., Li, T., Zhang, L., Ding, J., Jiang, S., Li, J., Zhu, L., & Zhang, K. (2017). Cerebral metabolic change in Parkinson's disease patients with anxiety: A FDG-PET study. *Neuroscience Letters*, *653*, 202–207. https://doi.org/10.1016/j.neulet.2017.05.062

Wehry, A. M., Beesdo-Baum, K., Hennelly, M. M., Connolly, S. D., & Strawn, J. R. (2015). Assessment and treatment of anxiety disorders in children and adolescents. *Current Psychiatry Reports*, *17*(7), 52. https://doi.org/10.1007/s11920-015-0591-z

Wei, K., Bao, W., Zhao, Z., Zhou, W., Liu, J., Wei, Y., Li, M., Wu, X., Liu, B., Du, Y., Gong, W., & Dong, J. (2018). Changes of the brain activities after chronic restraint stress in rats: A study based on (18)F-FDG PET. *Neuroscience Letters*, *665*, 104–109. https://doi.org/10.1016/j.neulet.2017.11.047

Wen, X., Zhang, H., Li, G., Liu, M., Yin, W., Lin, W., Zhang, J., & Shen, D. (2019). First-year development of modules and hubs in infant brain functional networks. *NeuroImage*, *185*, 222–235. https://doi.org/10.1016/j.neuroimage.2018.10.019

Yang, X., Yang, G., Wang, R., Wang, Y., Zhang, S., Wang, J., Yu, C., & Ren, Z. (2023). Brain glucose metabolism on [18F]-FDG PET/CT: a dynamic biomarker predicting depression and anxiety in cancer patients. *Frontiers in Oncology*, *13*, 1098943. https://doi.org/10.3389/fonc.2023.1098943

Zhang, B., Suarez-Jimenez, B., Hathaway, A., Waters, C., Vaughan, K., Noble, P. L., Fox, N. A., Suomi, S. J., Pine, D. S., & Nelson, E. E. (2012). Developmental changes of rhesus monkeys in response to separation from the mother. *Developmental Psychobiology*, *54*(8), 798–807. https://doi.org/10.1002/dev.21000

Zhang, H., Shen, D., & Lin, W. (2019). Resting-state functional MRI studies on infant brains: A decade of gap-filling efforts. *NeuroImage*, *185*, 664–684. https://doi.org/10.1016/j.neuroimage.2018.07.004

Zikopoulos, B., Höistad, M., John, Y., & Barbas, H. (2017). Posterior Orbitofrontal and Anterior Cingulate Pathways to the Amygdala Target Inhibitory and Excitatory Systems with Opposite Functions. *The Journal of Neuroscience : The Official Journal of the Society for Neuroscience*, *37*(20), 5051–5064. https://doi.org/10.1523/JNEUROSCI.3940-16.2017

Zimmerman, P. H., Bolhuis, J. E., Willemsen, A., Meyer, E. S., & Noldus, L. P. J. J. (2009). The Observer XT: a tool for the integration and synchronization of multimodal signals. *Behavior Research Methods*, *41*(3), 731–735. https://doi.org/10.3758/BRM.41.3.731

Acknowledgements

Putting together a dissertation is humbling experience. There are many people without whom this dissertation could never have been possible, I will do my best to acknowledge them all here. I start by highlighting professional acknowledgements.

First, I must acknowledge my PhD mentor, Dr. Ned Kalin. I feel grateful and honored that you trusted me to take the helm of such an amazing research project, and that you pushed me to explore ideas and approaches I never considered. Working with you has been educating, engaging, inspiring, and will forever set the standard for my expectations from primary investigators. I have such great respect for the way you lead your lab, and the way you push us all to be better researchers, scientists, and people. Thank you for creating a research environment and workplace that I am excited and proud to be a part of everyday.

Thank you to my committee, Drs. Rasmus Birn, Ryan Herringa, Chiara Cirelli, and Anita Bhattacharyya, who have been encouraging and enthusiastic members of my team. It has been a pleasure getting to know you all during my graduate education, and I am grateful to have had the advisement of such talented and influential scientists on my PhD project.

There are number of people who specifically contributed to this NHP anxiety development study, and without whom I could never have done such an ambitious PhD project. I want to first acknowledge Jonathan Oler, who has been a part of this project, and my mentorship, since the beginning and has been a tremendous help especially during my writing process. Lisa Williams and Patrick Roseboom have been supportive

helping me understanding fMRI processing and analyses. I could not have become a neuroimager without his mentorship and support.

Dr. Amy Cochran was an essential advisor for my statistical analyses, especially in the approach of determining best fit for developmental growth curves and exploring developmental interactions. I am grateful for her expertise.

There many other Kalin lab members and collaborators who have been essential colleagues and mentors in my development as a scientist including: Dr. Do Tromp, Dr. Sascha Mueller, Dr. Margaux Kenwood, Dr. Rothem Kovner, Dr. Drew Fox, Dr. Melissa Brotman, Dr. Josh Cruz, Ashton Barber, Courtney Olson, Dr. Dan McFarlin, Gina Bednarek, and Dee French. You all make the Kalin lab a wonderful place to work.

My research career began with some mentors and coworkers that inspired my choice to pursue a PhD – Dr. Etienne Sibille, Dr. Marianne Seney, Beverly French, Dr. Georgia Vasilakis, and Micah Shelton – Thank you for helping me realize my dream and for setting me up for success.

Thank you to the A-team of the Neuroscience Training Program office, Angela Norris, Ana Garic, and the NTP director Dr. Ari Rosenberg. I love this program, and am so grateful for all the opportunities I had here. Thank you for putting so much of yourself into this program, and for welcoming and respecting me as be a part of the team.

Special acknowledgement to the NTP community- my fellow grad students have been great inspirations in my work and in my life. Your support, passion, and love carried me through the hard times.

Now for the personal acknowledgements-

I must start by acknowledging my family, whom I am incredibly lucky to call my best friends. I want to thank my parents, Jim Puralewski and Ruth Ann Francis, for all the choices and sacrifices they made in their lives, in order to provide me with the opportunities that brought me here. I owe everything to them, and am forever grateful for the life they have given me, and the tools they taught me to leave each place better than I found it.

A super special acknowledgement to my sister, Hannah Puralewski, my best friend and the other half of my soul. You have taken care of me through the hardest parts of this journey, and hyped me up when I needed it most. Thank you for inspiring me throughout life, and reminding me always that science is for the betterment of the community. With a community focused approach in research, we can change the world.

To my brothers, Joseph and Jacob Puralewski, thank you for protecting and pushing me always, and being my unwavering supporters and cheerleaders. I am so appreciative of your pride in my work, even if you struggle to understand exactly what I'm doing. I couldn't have asked for better older brothers.

Thank you to my partner in life, Dr. Akshay Kohli, for inspiring me to be a better scientist and better person. One of the best things I got from moving here and joining the NTP was you. Your unconditional love and support are something I didn't know I deserved prior to meeting you. I love you and our dreams together; I can't wait for us to make them come true.

Appendix

A.1 – detailed description of behavioral scores

Human Intruder Paradigm (HIP) Behaviors and Vocalizations
updated 3/15/22 MKR & CB

Movement "State" Behaviors:

FA **Falling Down:** Loss of grip, balance, or collapse of one or more arms or legs causing the subject to plunge, drop, tumble or slip. *(frequency; except in the Developmental study where it's a duration)*
 Falling Down (infants only): Any loss of postural stability that results in at least a 90 degree drop in the torso and head. Duration of fall ends when stability of posture is regained either by infant righting itself or by infant gripping the cage enough to regain control of supporting its torso and head. *(duration)*

FF **Freezing:** A period of at least 3 seconds characterized by no vocalizations and no movement other than isolated movements of the head, or slight body movements used to maintain posture. May be scored with self-directed behaviors. (*duration*)

HU **Huddle:** Self enclosed, fetal like position with the head at or lower than the shoulders. (*duration*)

HV **Hypervigilance:** A state of at least 3 seconds of inhibited movement that includes a single body part moving in isolation, or any two or more body parts moving together in synchrony. May be scored with self-directed behaviors. Sometimes coded as SS using Noldus. (*duration*)

IN **Dump:** Previously known as "inactive". Scored when subject is <u>not</u> doing another movement behavior (FA/FF/HU/HV/LO/LOST/LY/RE/US). "Dump" does <u>not</u> mean inactivity. Subject may be doing other action behaviors (EH/EN/LS/PE/SD/TG) and/or vocalizing (BA/GI/SH/VO/VV). *(duration)*

LO **Locomotion:** Ambulation of one or more full steps at any speed. Includes such behaviors as dropping from ceiling to floor or swinging cage shake. May be scored with other action behaviors. (*duration*)

LOST **Stereo Locomotion:** Any repetitive, patterned, and rhythmic movement, singly or in combination. The first occurrence during a test session is scored after three cycles. Thereafter, it is scored whenever it occurs unless a new pattern is developed. May be scored with other action behaviors. (*duration*)

LY   **Lying Down:** Animal is lying down ventrally, dorsally, or on its side. May be scored with other action behaviors. (*duration*)

OM   **Other Movement (infants only):** Movement that does not result in full ambulation of locomotion. Any flailing, reaching, standing, or posture stabilizing that involves movement of at least two independent body parts (arm/torso, arm/arm, leg/arm, leg/torso, etc.). This is considered immature locomotion. *(duration)*

RE   **Resting:** Animal is inactive with eyes closed and in the opinion of the tester is sleeping. (*duration*)

US   **Unsteady:** Any wobbly or wavering movement of the head and/or body. May be scored with other action behaviors. (*duration*)

Action Behaviors:

EH   **Experimenter Hostility:** Any hostile behavior directed at or stimulated by the presence of the intruder (e.g., head bobbing, ear flapping, cage shaking, open mouth threat, etc.). May be scored with any behavior except freezing (FF), hypervigilance (HV), huddle (HU), or resting (RE). Cannot be scored during the Alone condition. *(duration)*

EN   **Environment Explore:** Any manual or oral exploration of manipulation of the physical surroundings such as cage, pan, droppings, hair, urine, or chow. Includes non-locomotive cage shaking. *(duration)*

LS   **Lip Smack:** Repeatedly pressing the lips together and pulling them apart quickly. May be scored with any behavior except freezing (FF), hypervigilance (HV), huddle (HU), or resting (RE). *(duration)*

SD   **Self-Directed:** Any self-directed behaviors which includes SM (self-mouth), SG (self-groom), SC (self-clasp), SF (self-sex), and SA (self-aggression). *(duration)*

TG   **Teeth Grinding:** Any visual and/or audible gnashing of the teeth. May be scored with any behavior except freezing (FF), hypervigilance (HV), huddle (HU), or resting (RE). *(duration)*

Vocalizations:

BA   **Bark:** Vocalization made by forcing air through vocal chords from the abdomen producing a short, rasping low frequency sound. *(frequency)*

GI **Girn:** A soft intermittent complex nasal warbling sound. It is a quiet sound of variable duration of approximately 500 msec and a peak frequency of about 800 Hz. *(frequency)*

SH **Shriek:** Harsh shrill sound made by pulling back the lips. This vocalization is high pitched with little change in frequency. *(frequency)*
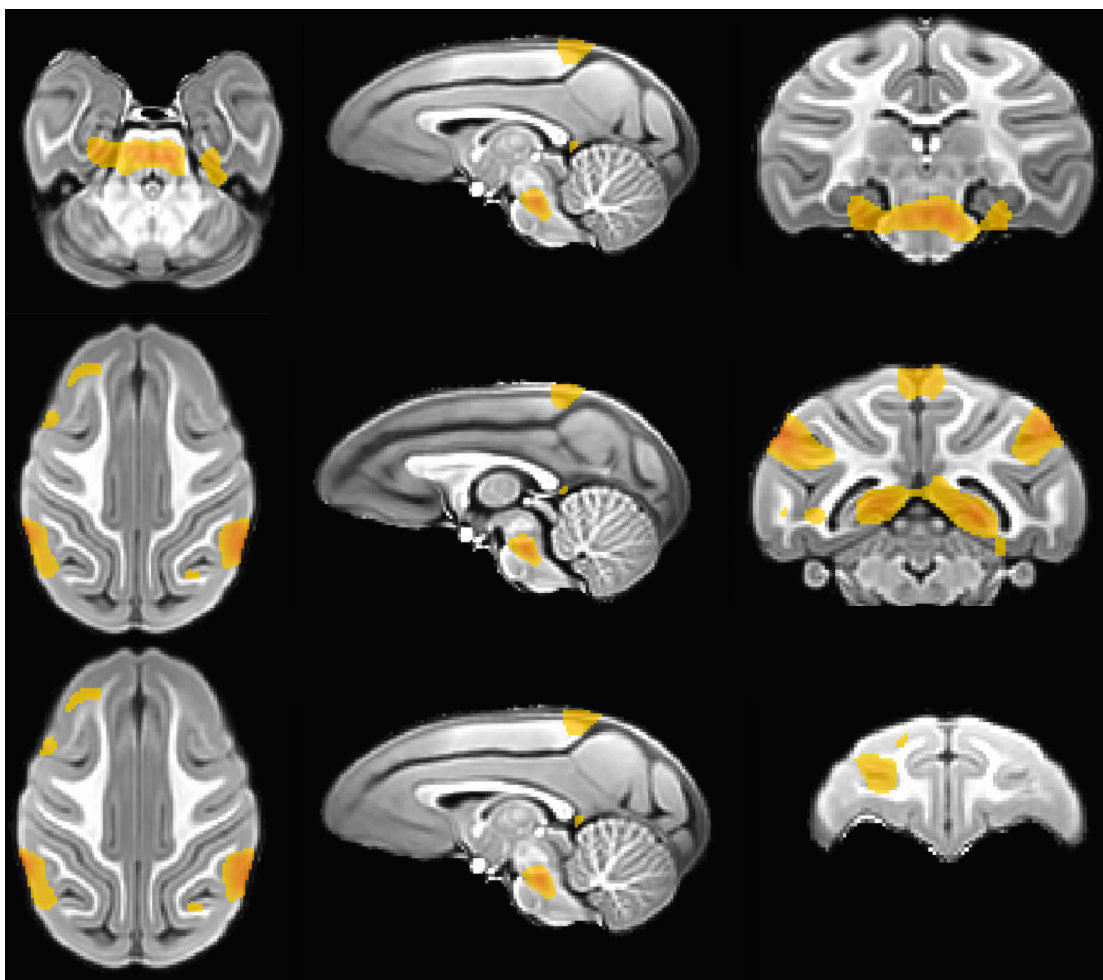
VO **Other Vocals:** Vocalizations other than bark, girn, shriek, and coo. *(frequency)*

VV **Coo:** Vocalization made by rounding and pursing the lips with an increase then decrease in frequency and intensity. *(frequency)*
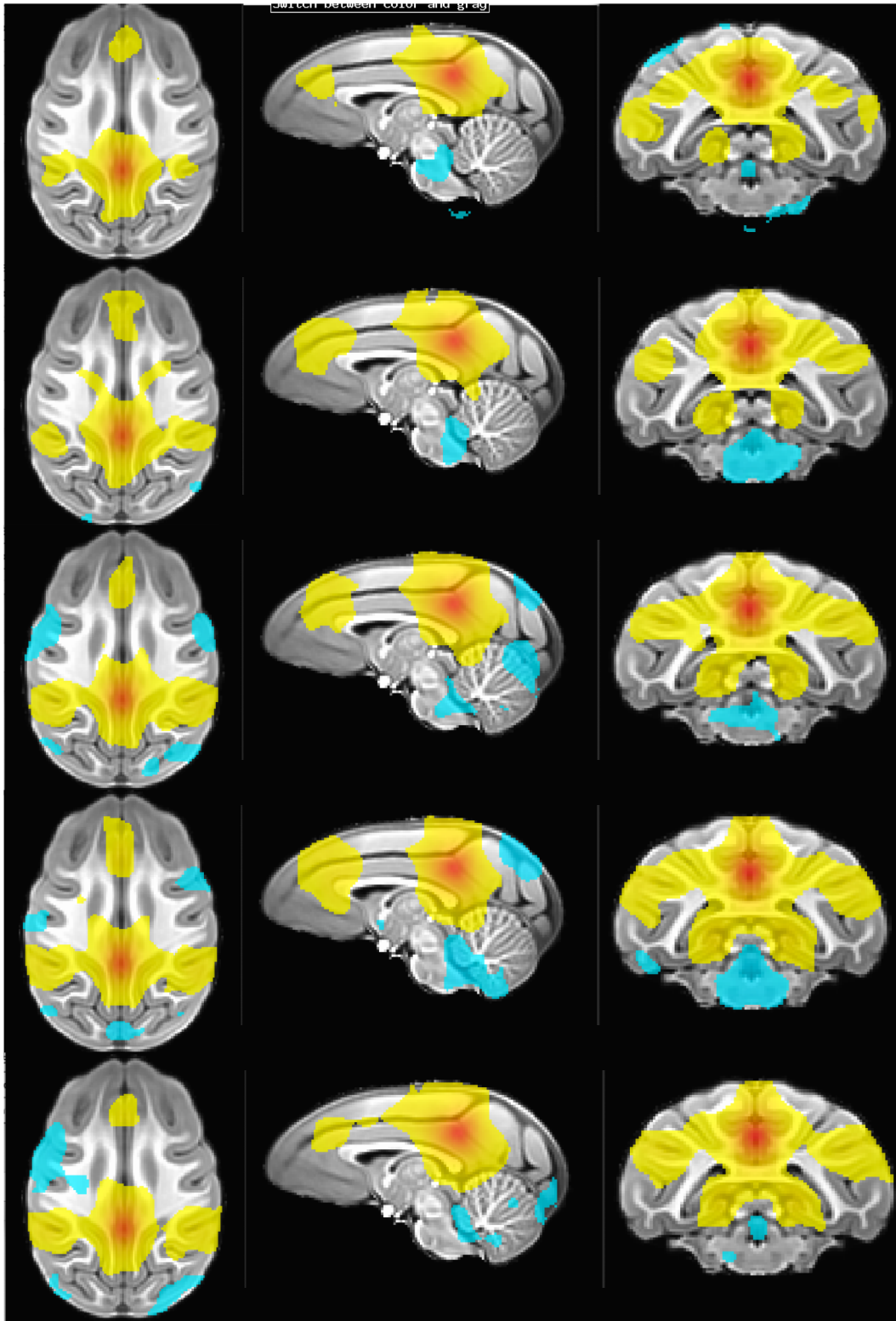
Appendix A.2- Visualization Default Model Network
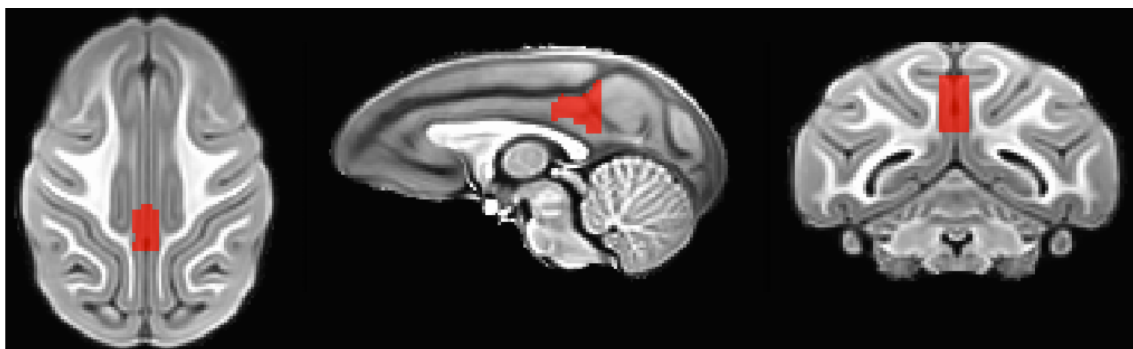
Posterior Cingulate Seed used for visualization of default mode network

Regions with age-related PC functional connectivity differences, p<0.005 uncorrected, controlling for sex and gestation length. Clusters do not illustrate directionality, only regions showing significant age-related changes.

T1 (top image), T2, T3, T4, T5 (bottom image) – main-effect posterior cingulate functional connectivity maps, threshold at p<0.005, uncorrected